Novel Curcumin-based Analogues as Potential VEGFR2 Inhibitors with Promising Metallic Loading Nanoparticles: Synthesis, Biological Evaluation, and Molecular Modelling Investigation

Asmaa S. A. Yassen[1,2,*], Sherief M. Abdel-Wahab[3,*], Khaled M. Darwish[4,2], Mohamed S. Nafie[5, 6], Reda F. A. Abdelhameed [7, 8], Gharieb S. El-Sayyad [9, 10], Ahmed I. El-Batal[10], Khadiga M. Attia[3], Hosam A. Elshihawy[1], Ranza A. Elrayess[1]

[1]Pharmaceutical Organic Chemistry Department, Faculty of Pharmacy, Suez Canal University, Ismailia 41522, Egypt. (Asmaa_yaseeen@pharm.suez.edu.eg), (hossameldeen_ahmed@pharm.suez.edu.eg), (ranza.el-rayes@pharm.suez.edu.eg)

[2]Department of Medicinal Chemistry, Faculty of Pharmacy, Galala University, New Galala 43713, Egypt.

[3]Pharmaceutical Organic Chemistry Department, College of Pharmaceutical Sciences and Drug Manufacturing, Misr University for Science and Technology, Giza, Egypt. (sherief.abdalwahab@must.edu.eg) (Khadeja.attia@must.edu.eg)

[4]Medicinal Chemistry Department, Faculty of Pharmacy, Suez Canal University, Ismailia 41522, Egypt. (khaled_darwish@pharm.suez.edu.eg)

[5]Department of Chemistry, College of Sciences, University of Sharjah (P.O. 27272), Sharjah, United Arab Emirates. (Mohamed.ElSayed@sharjah.ac.ae)

[6]Department of Chemistry, Faculty of Science, Suez Canal University, Ismailia 41522, Egypt. (Mohamed_nafie@science.suez.edu.eg)

[7]Department of Pharmacognosy, Faculty of Pharmacy, Galala University, New Galala City, Suez 43713, Egypt. (reda.fouad@gu.edu.eg)

[8]Pharmacognosy Department, Faculty of Pharmacy, Suez Canal University, Ismailia 41522, Egypt.

[9]Microbiology and Immunology Department, Faculty of Pharmacy, Galala University, New Galala City, Suez 43713, Egypt. (Gharieb.Elsayyad@gu.edu.eg)

[10]Drug Radiation Research Department, National Center for Radiation Research and Technology (NCRRT), Egyptian Atomic Energy Authority (EAEA), Cairo, Egypt. (aelbatal2000@gmail.com)

***Corresponding authors**:

Asmaa S. A. Yassen: Pharmaceutical Organic Chemistry Department, Faculty of Pharmacy, Suez Canal University, Ismailia 41522, Egypt; Email: asmaa_yaseeen@pharm.suez.edu.eg

Sherief M. Abdel-Wahab: Pharmaceutical Organic Chemistry Department, College of Pharmaceutical Sciences and Drug Manufacturing, Misr University for Science and Technology, Giza, Egypt; Email: sherief.abdalwahab@must.edu.eg

2. Materials and Methods

2.1. Chemistry

2.1.1. Instrument

Melting points were measured with Gallenkamp melting point apparatus and were uncorrected. The structure of the target compounds was confirmed by IR (Pye-Unicam SP-3-300 infrared spectrophotometer, KBr disks), ^{1}H NMR (400 MHz, Varian Mercury VX-300 and Bruker Avance III NMR spectrometer) and ^{13}C NMR (100 MHz, BRUKERNMR spectrometer, BRUKER, Manufacturing & Engineering Inc., Anaheim, CA, USA). The abbreviations used are as follows: s, singlet; d, doublet; m, multiplet. The mass spectra (EI-MS) were recorded on a Shimadzu GCMSQP-1000EX mass spectrometer at 70 eV. UV fluorescent silica gel Merck 60 F254plates were used to monitor the reactions and were visualized using a UV lamp.

2.1.2. Chemicals and Reagents

Aniline, 4-methoxy aniline, 4-chloro aniline, triethyl amine, chloroacetyl chloride, piperidine 4- one hydrochloride, 2-furaldehyde, benzaldehyde, 4-chloro benzaldehyde, 4-methoxy benzaldehyde, 3,4-dimethoxy benzaldehyde, 3,4,5 trimethoxy benzaldehyde, were purchased from Aldrich (USA). Solvents and other reagents were of pure grade and used without further purification.

3. Results and Discussion

3.3. Molecular Modeling Investigation

Table **S1.** MM/GBSA binding energies and per-residue energy contributions for the hotspot VEGFR2 amino acids based on FastDRH server analysis.

Ligand	MM_GBSA	Per-residue MM/GBSA energy contributions
4b	-47.68	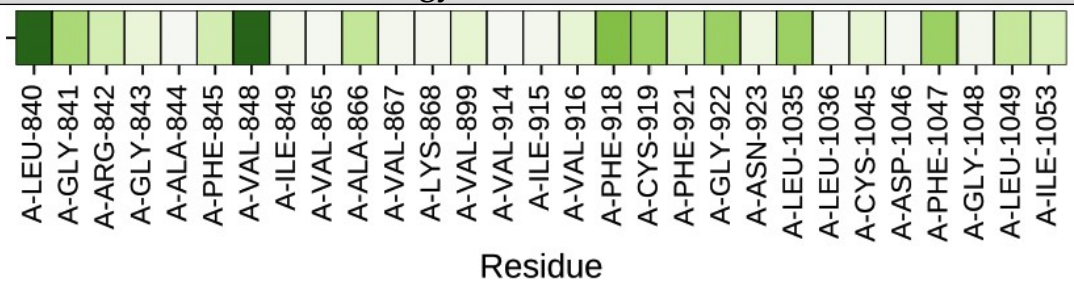
4d	-55.92	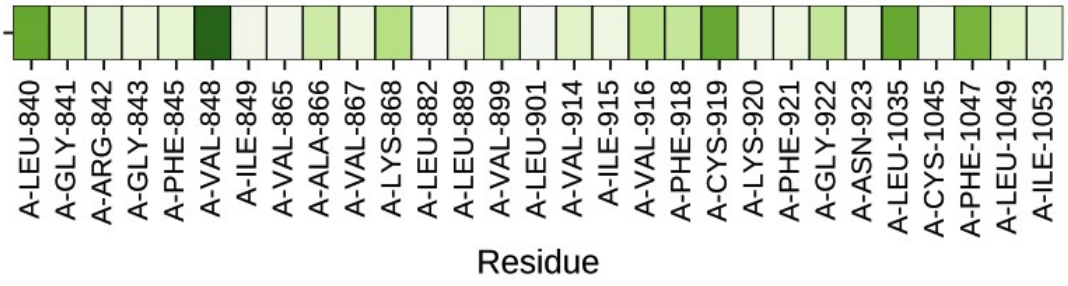
4e	-58.06	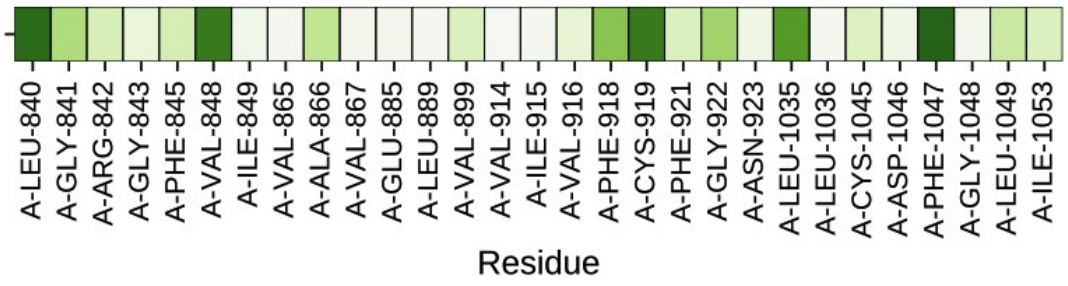
4f	-54.27	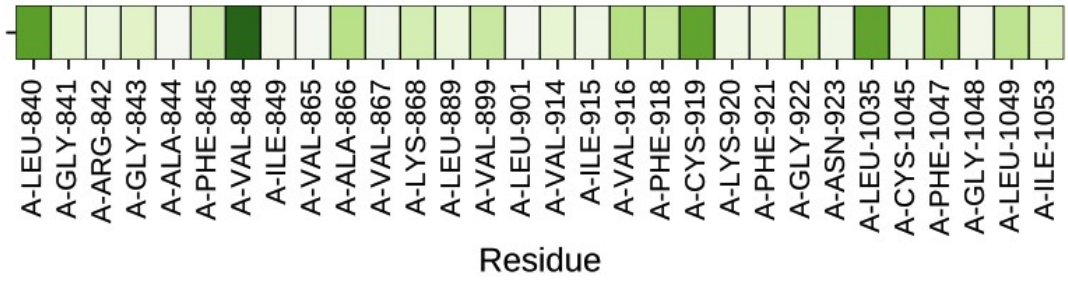

Sorafenib	**-63.15**	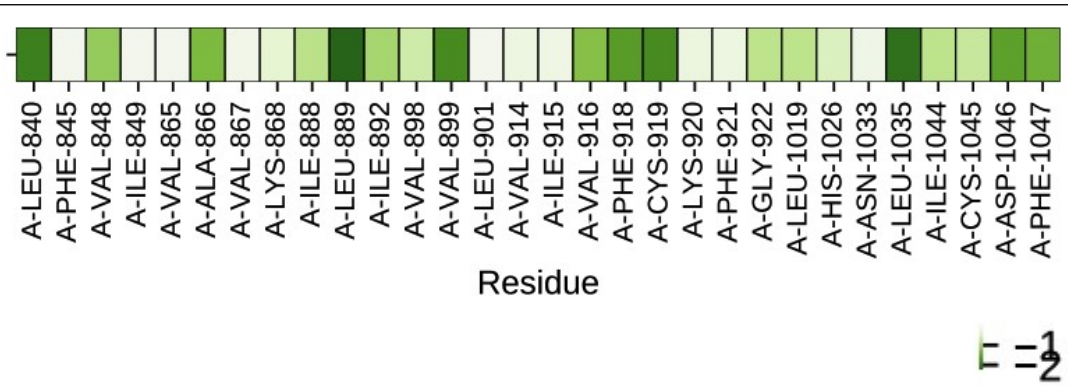

Table S2. Toxicity model report of compound 4e using ProTox 3.0 webserver

ProTox-3.0 - Prediction of TOXicity of chemicals				
Classification	**Target**	**Shorthand**	**Prediction**	**Probability**
Organ toxicity	Hepatotoxicity	dili	Inactive	0.72
Organ toxicity	Nephrotoxicity	nephro	Inactive	0.66
Organ toxicity	Cardiotoxicity	cardio	Inactive	0.78
Toxicity end points	Carcinogenicity	carcino	Inactive	0.61
Toxicity end points	Immunotoxicity	immuno	Inactive	0.85
Toxicity end points	Mutagenicity	mutagen	Inactive	0.68
Toxicity end points	Cytotoxicity	cyto	Inactive	0.65
Toxicity end points	Nutritional toxicity	nutri	Inactive	0.54
Tox21-Nuclear receptor signalling pathways	Aryl hydrocarbon Receptor (AhR)	nr_ahr	Inactive	0.81
Tox21-Nuclear receptor signalling pathways	Androgen Receptor (AR)	nr_ar	Inactive	0.95
Tox21-Nuclear receptor signalling pathways	Androgen Receptor Ligand Binding Domain (AR-LBD)	nr_ar_lbd	Inactive	0.95
Tox21-Nuclear receptor signalling pathways	Aromatase	nr_aromatase	Inactive	0.93
Tox21-Nuclear receptor signalling pathways	Estrogen Receptor Alpha (ER)	nr_er	Inactive	0.88
Tox21-Nuclear receptor signalling pathways	Estrogen Receptor Ligand Binding Domain (ER-LBD)	nr_er_lbd	Inactive	0.96
Tox21-Nuclear receptor signalling pathways	Peroxisome Proliferator Activated Receptor Gamma (PPAR-Gamma)	nr_ppar_gamma	Inactive	0.96
Tox21-Stress response pathways	Nuclear factor (erythroid-derived 2)-like 2/antioxidant responsive element (nrf2/ARE)	sr_are	Inactive	0.83
Tox21-Stress response pathways	Heat shock factor response element (HSE)	sr_hse	Inactive	0.83
Tox21-Stress response pathways	Mitochondrial Membrane Potential (MMP)	sr_mmp	Inactive	0.77
Tox21-Stress response pathways	Phosphoprotein (Tumor Supressor) p53	sr_p53	Inactive	0.82
Tox21-Stress response pathways	ATPase family AAA domain-containing protein 5 (ATAD5)	sr_atad5	Inactive	0.96
Molecular Initiating Events	Thyroid hormone receptor alpha (THRα)	mie_thr_alpha	Inactive	0.89
Molecular Initiating Events	Thyroid hormone receptor beta (THRβ)	mie_thr_beta	Inactive	0.66
Molecular Initiating Events	Transtyretrin (TTR)	mie_ttr	Inactive	0.87
Molecular Initiating Events	Ryanodine receptor (RYR)	mie_ryr	Inactive	0.92
Molecular Initiating Events	GABA receptor (GABAR)	mie_gabar	Inactive	0.79
Molecular Initiating Events	Glutamate N-methyl-D-aspartate receptor (NMDAR)	mie_nmdar	Inactive	0.91
Molecular Initiating Events	alpha-amino-3-hydroxy-5-methyl-4-isoxazolepropionate receptor (AMPAR)	mie_ampar	Inactive	0.99
Molecular Initiating Events	Kainate receptor (KAR)	mie_kar	Inactive	1
Molecular Initiating Events	Achetylcholinesterase (AChE)	mie_ache	Inactive	0.52
Molecular Initiating Events	Constitutive androstane receptor (CAR)	mie_car	Inactive	0.99
Molecular Initiating Events	Pregnane X receptor (PXR)	mie_pxr	Inactive	0.52
Molecular Initiating Events	NADH-quinone oxidoreductase (NADHOX)	mie_nadhox	Inactive	0.95
Molecular Initiating Events	Na+/I- symporter (NIS)	mie_nis	Inactive	0.79
Metabolism	Cytochrome CYP1A2	CYP1A2	Inactive	0.84
Metabolism	Cytochrome CYP2C19	CYP2C19	Inactive	0.73
Metabolism	Cytochrome CYP3A4	CYP3A4	Inactive	0.62
Metabolism	Cytochrome CYP2E1	CYP2E1	Inactive	0.99

Toxicity targets

Possible binding to toxicity targets is shown below. For more information on the targets, please click on the individual abbreviations.

AA2AR	ADRB2	ANDR	AOFA	CRFR1	DRD3	ESR1	ESR2	GCR	HRH1	NR1I2	OPRK	OPRM	PDE4D	PGH1	PRGR

List of Supplementary Figures

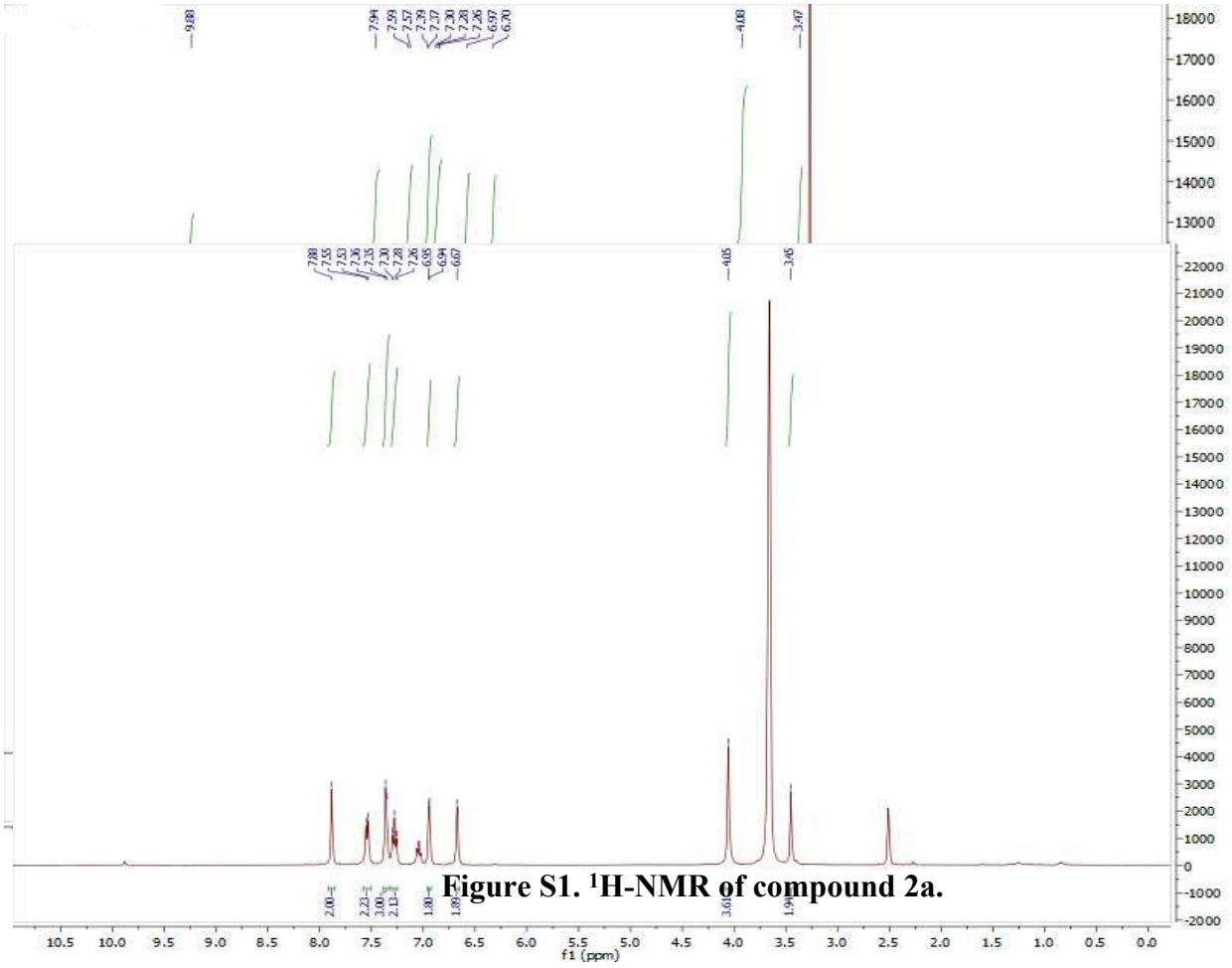

Figure S1. ^{1}H-NMR of compound 2a.

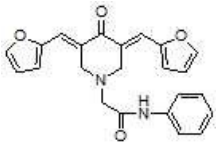

Figure S2. ^{1}H-NMR of compound 2a with D_2O.

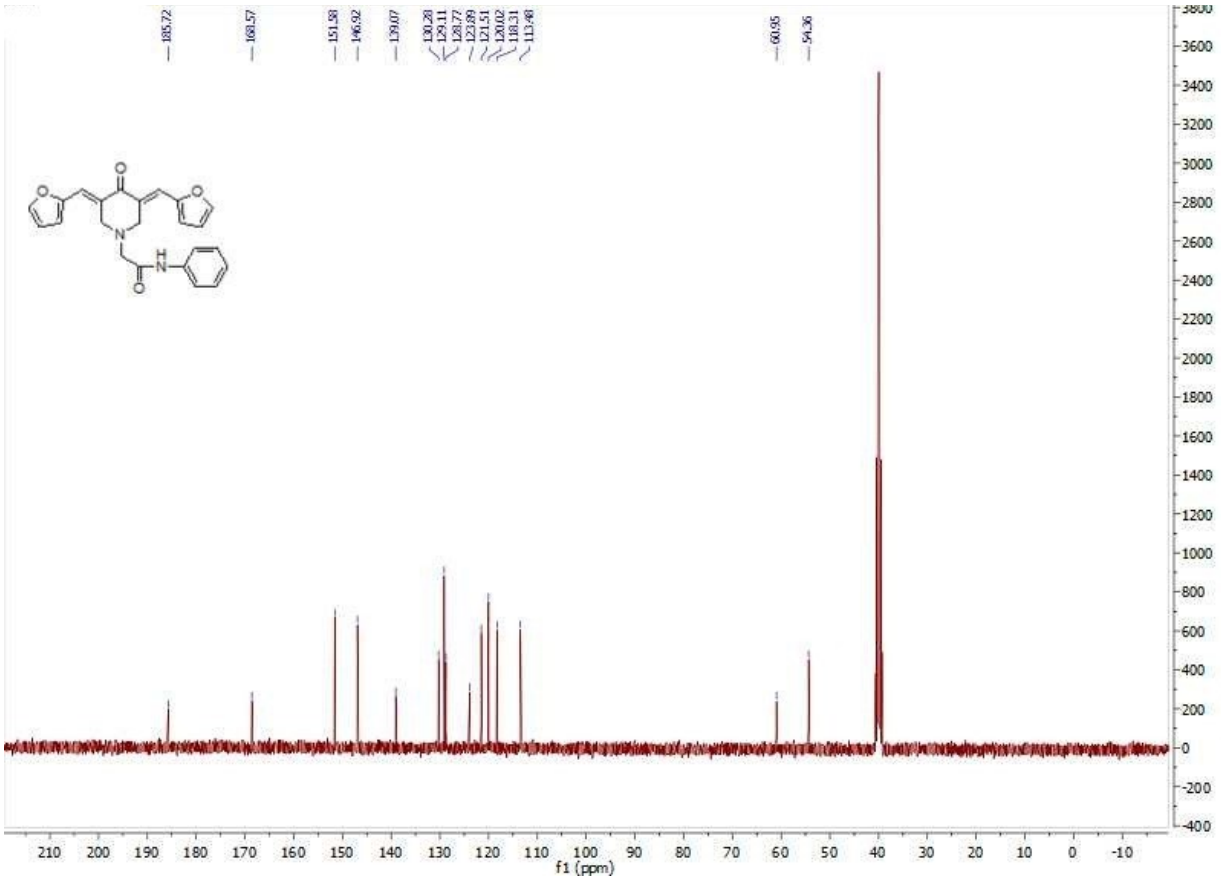

Figure S3. ^{13}C-NMR of compound 2a.

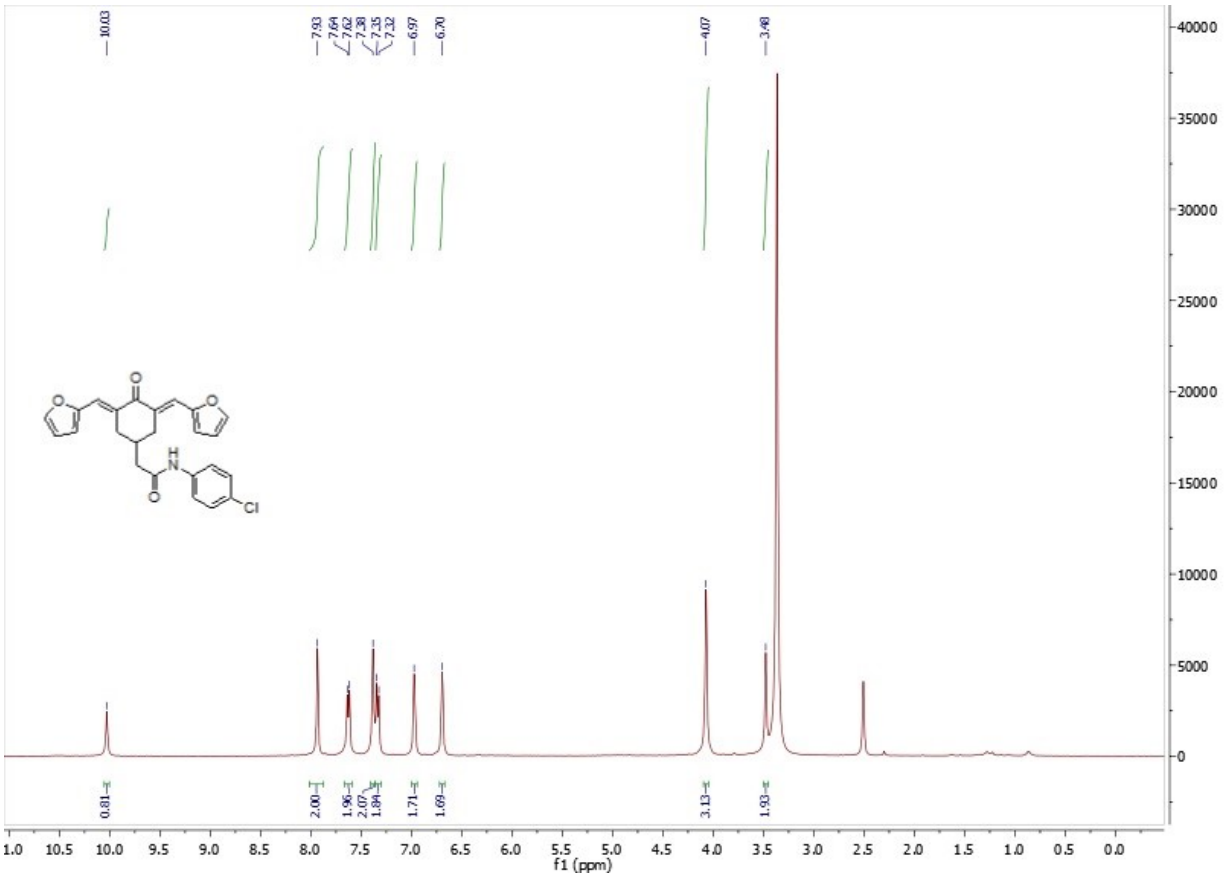

Figure S4. ^{1}H-NMR of compound 2b.

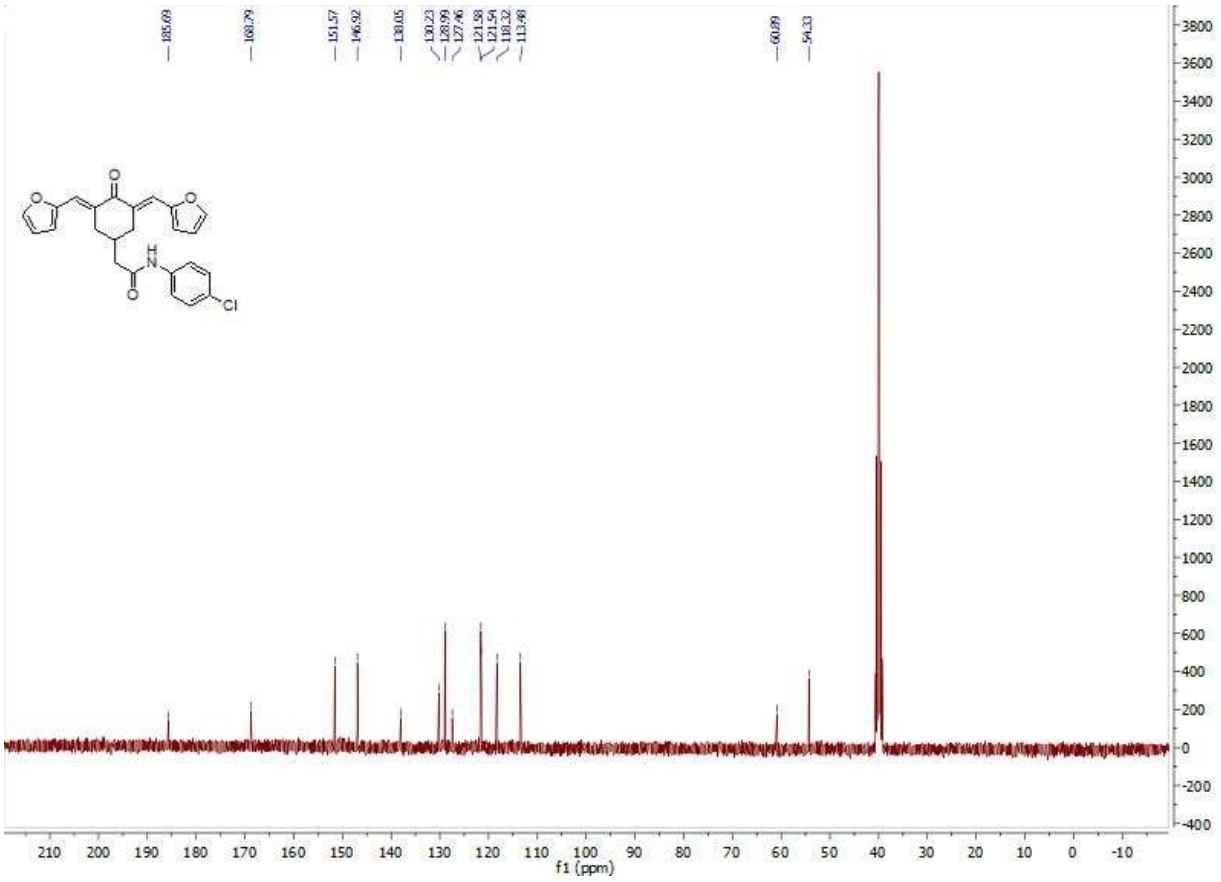

Figure S5. ^{13}C-NMR of compound 2b.

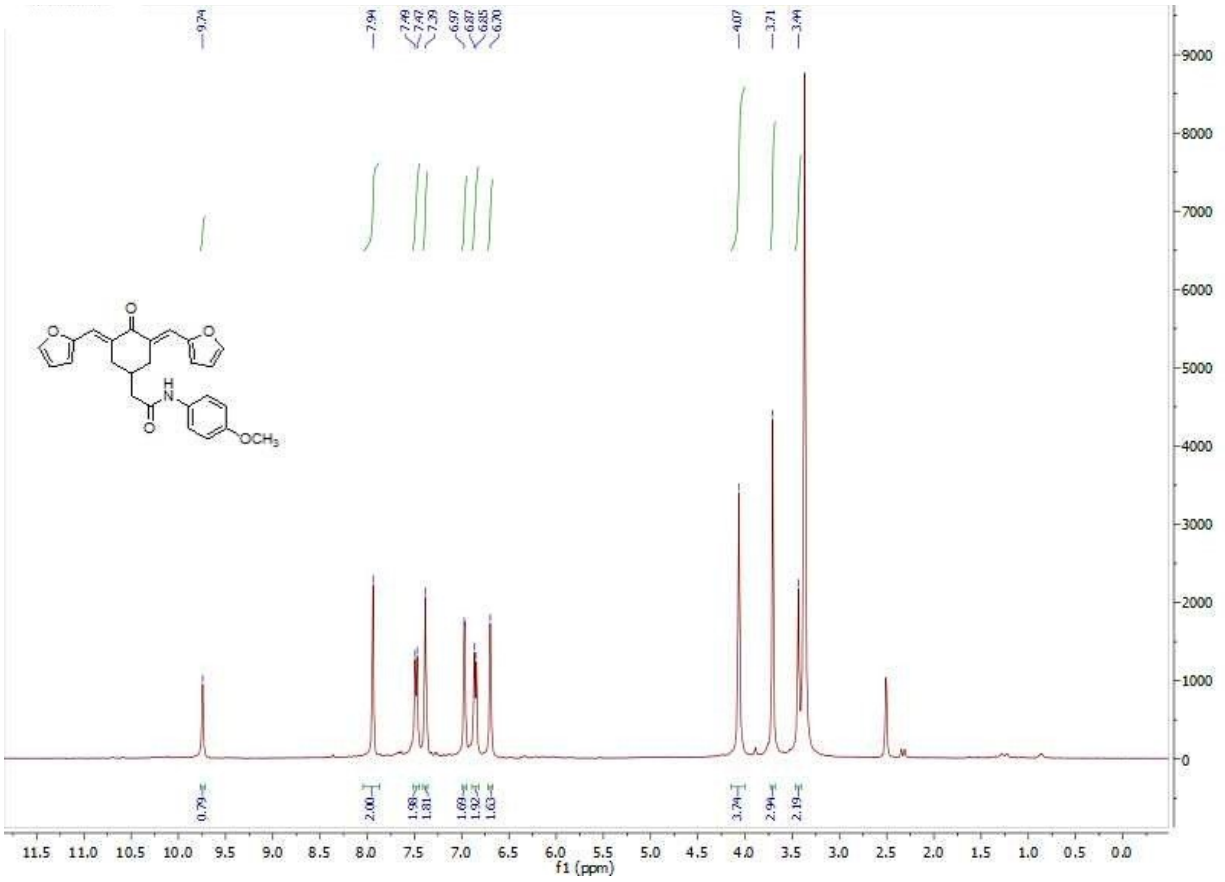

Figure S6. ^{1}H-NMR of compound 2c.

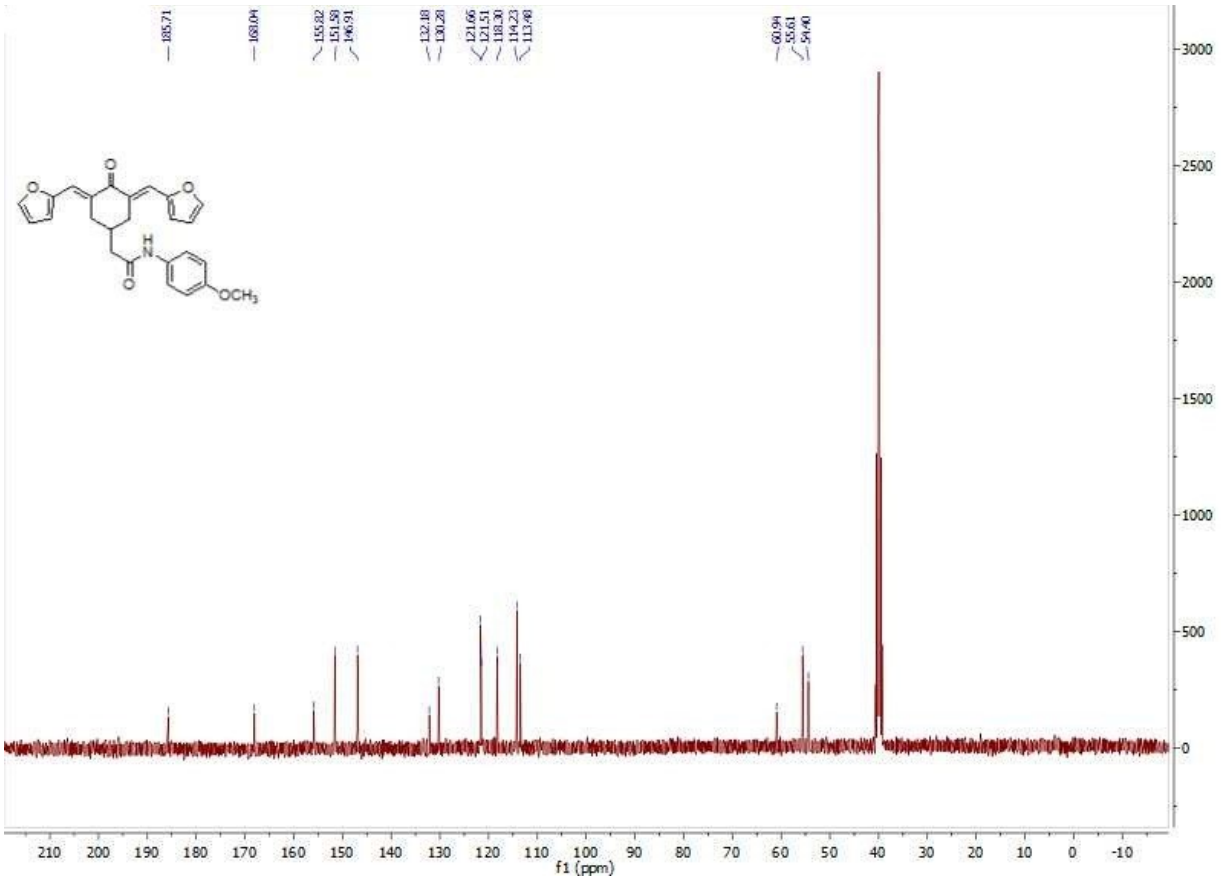

Figure S7. ^{13}C-NMR of compound 2c.

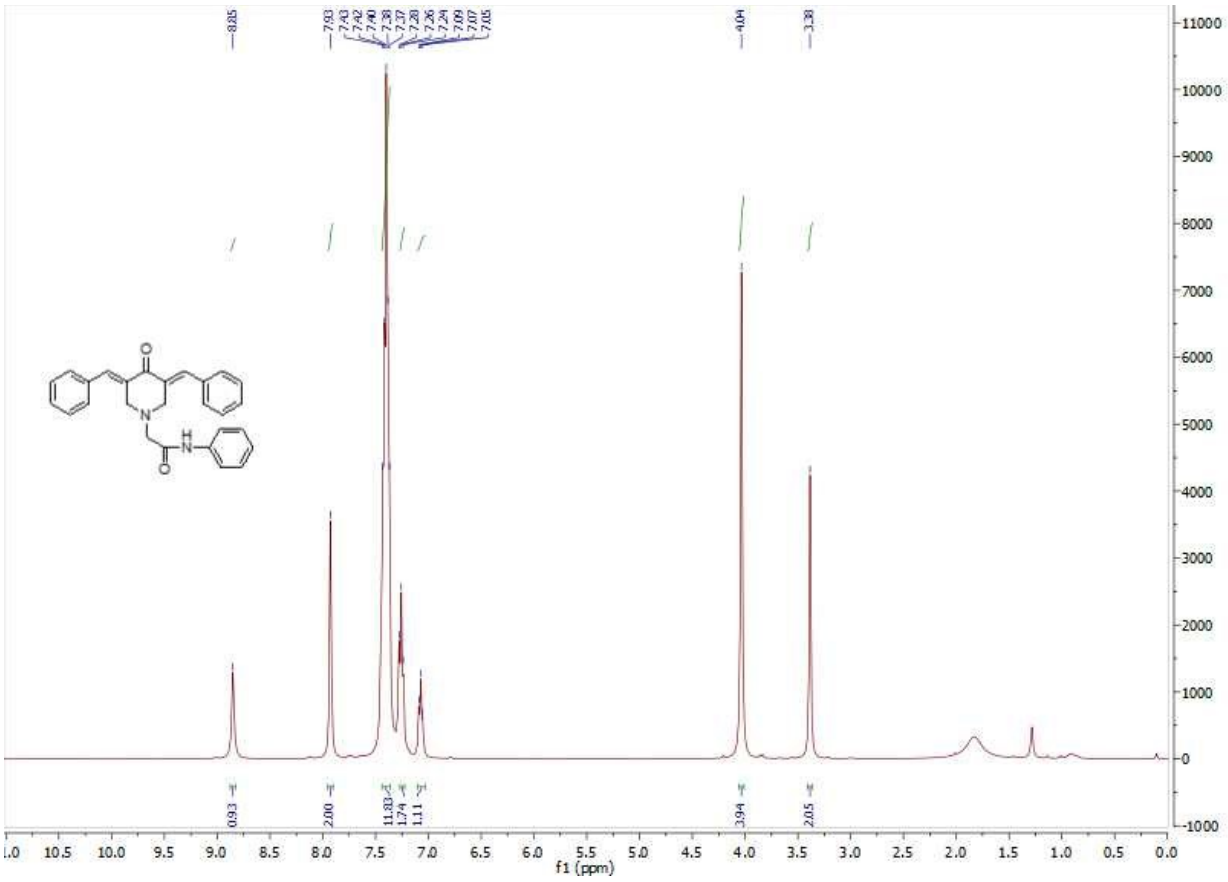

Figure S8. ^{1}H-NMR of compound 4a.

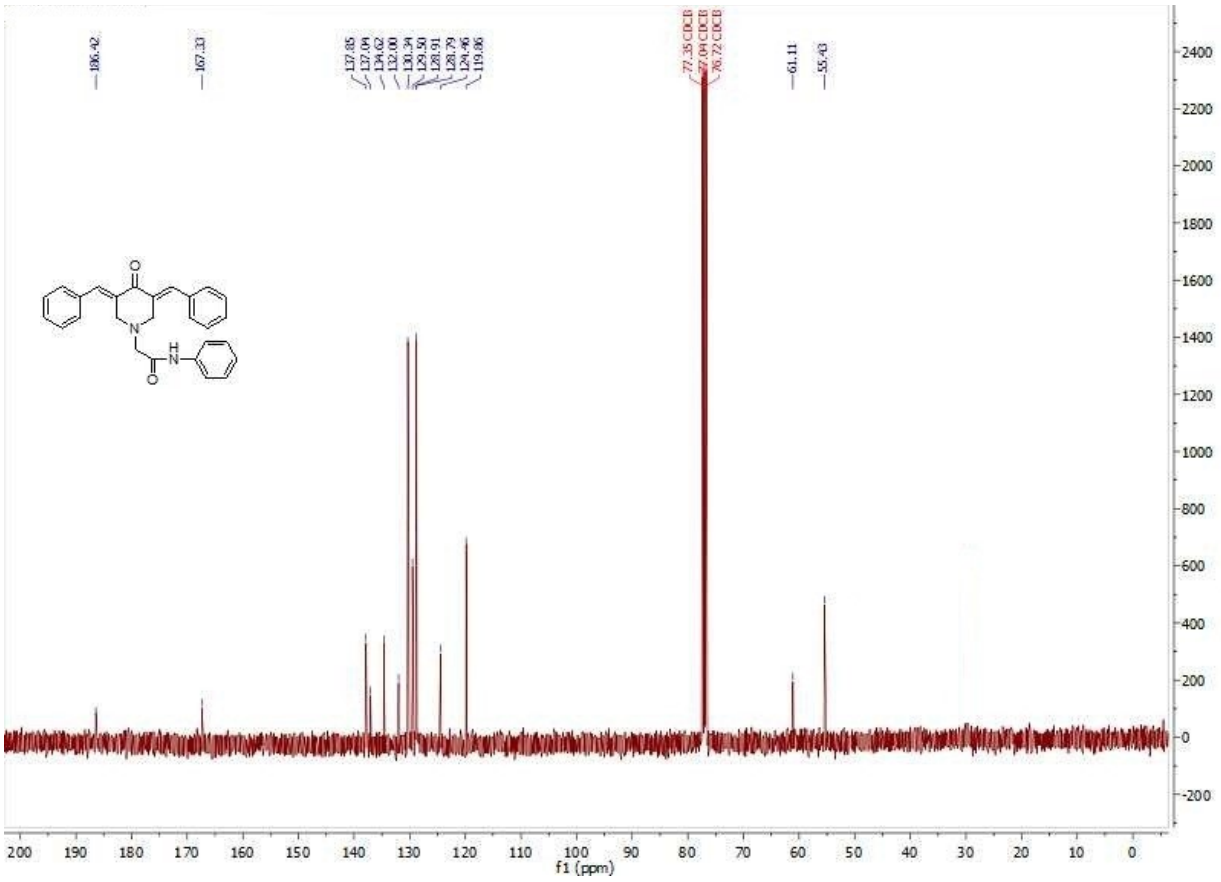

Figure S9. ^{13}C-NMR of compound 4a.

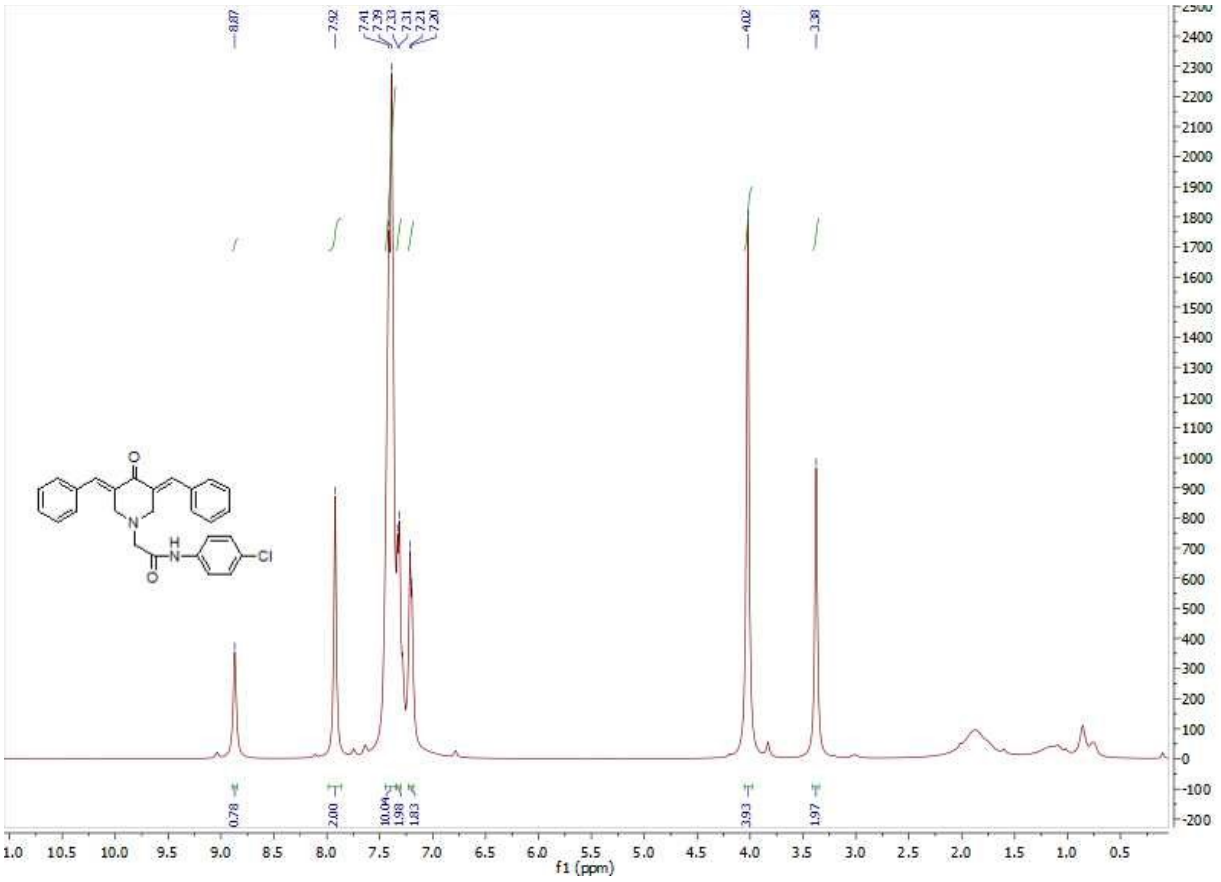

Figure S10. ^{1}H-NMR of compound 4b.

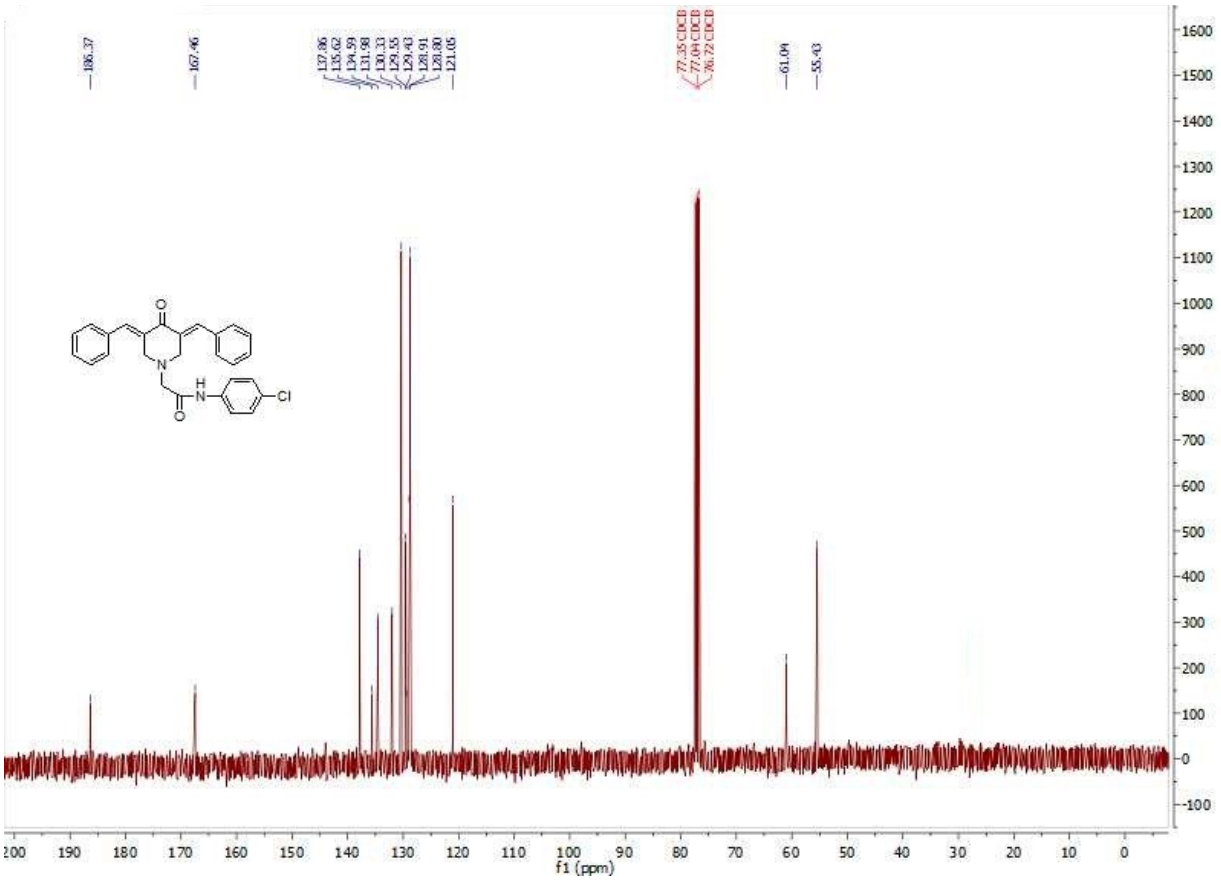

Figure S11. ^{13}C-NMR of compound 4b.

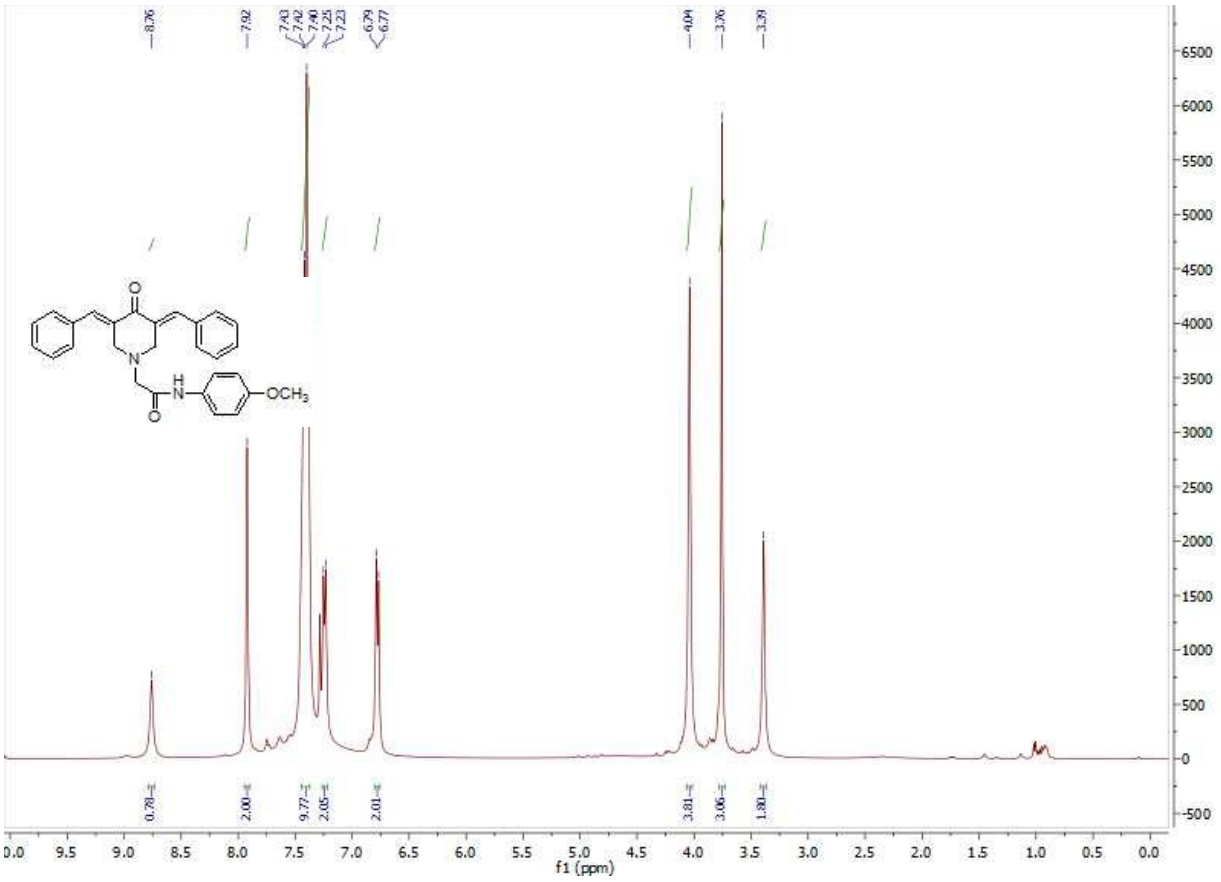

Figure S12. ^{1}H-NMR of compound 4c.

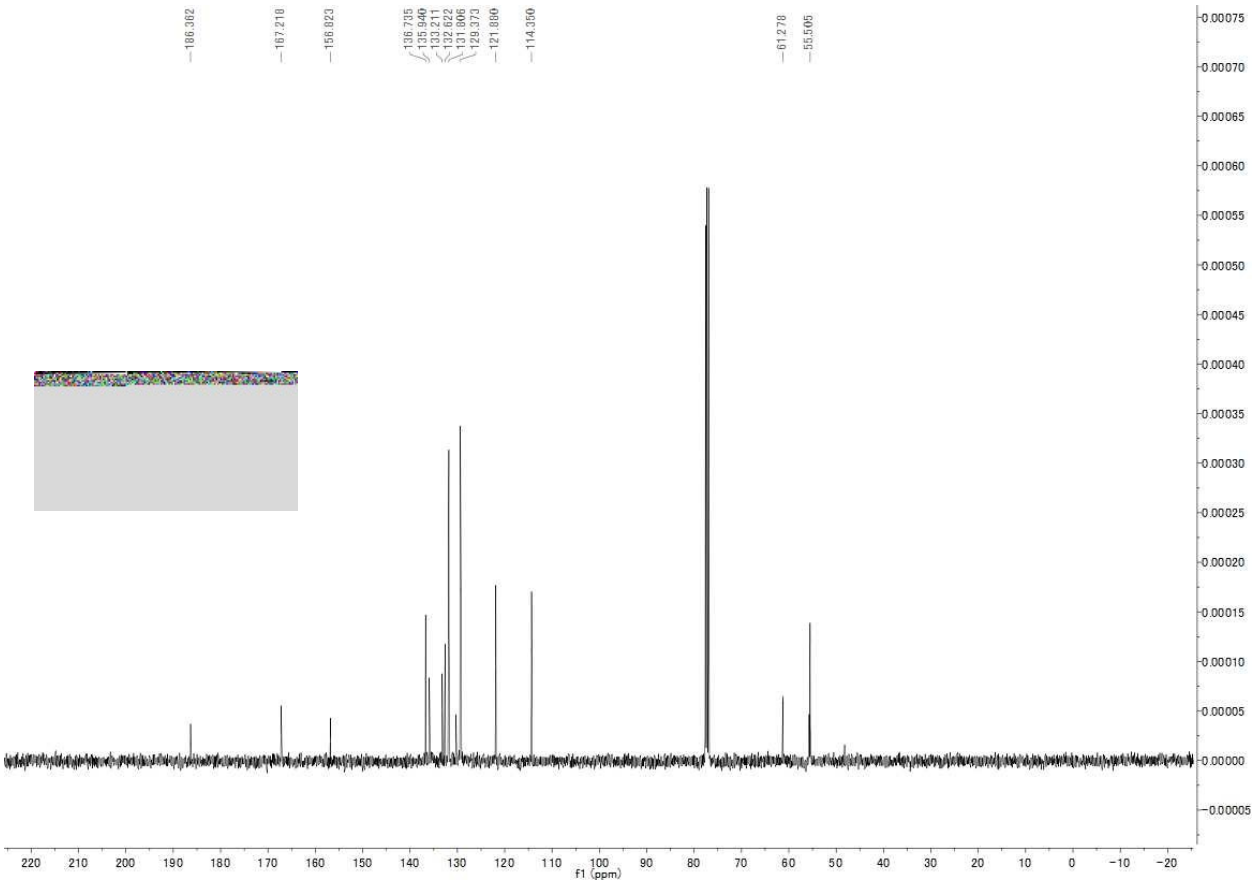

Figure S13. ^{13}CNMR of compound 4c.

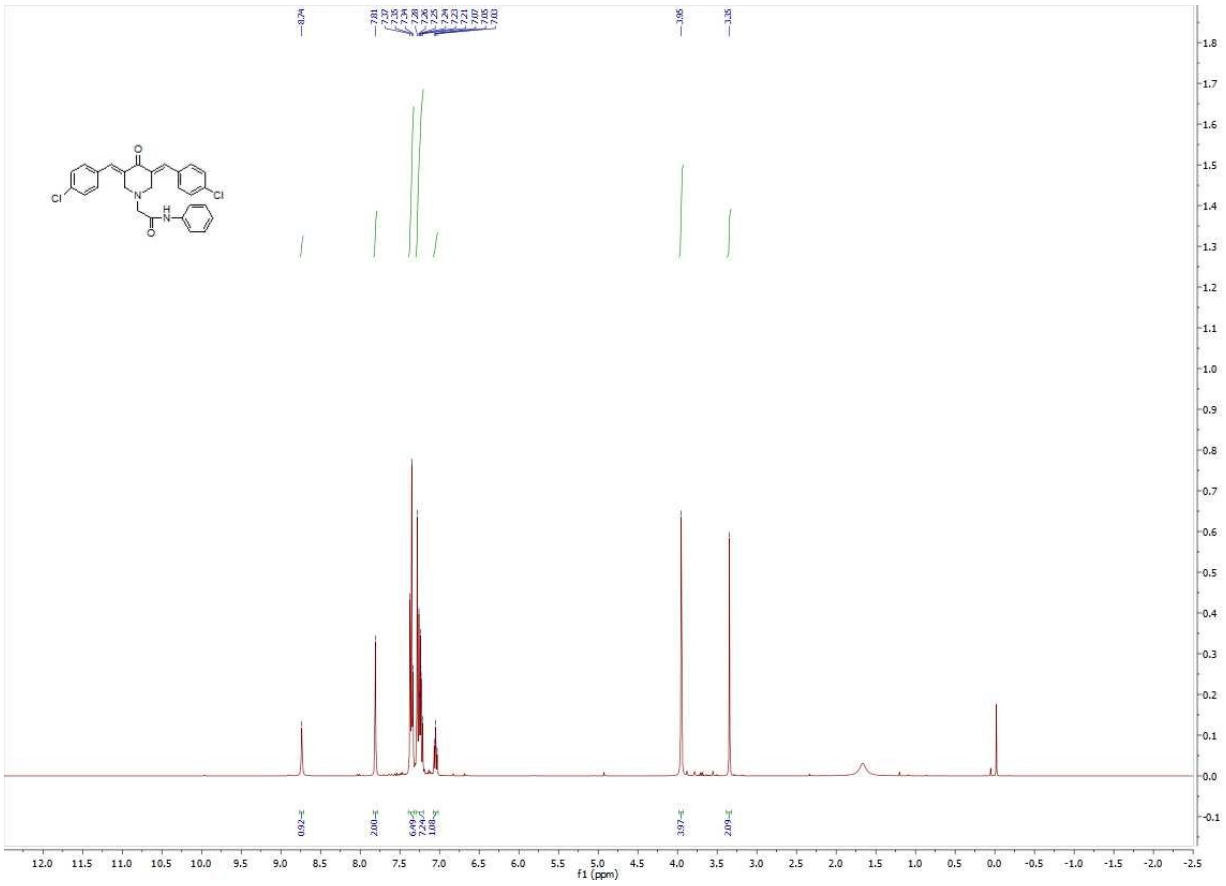

Figure S14. ^{1}H-NMR of compound 4d.

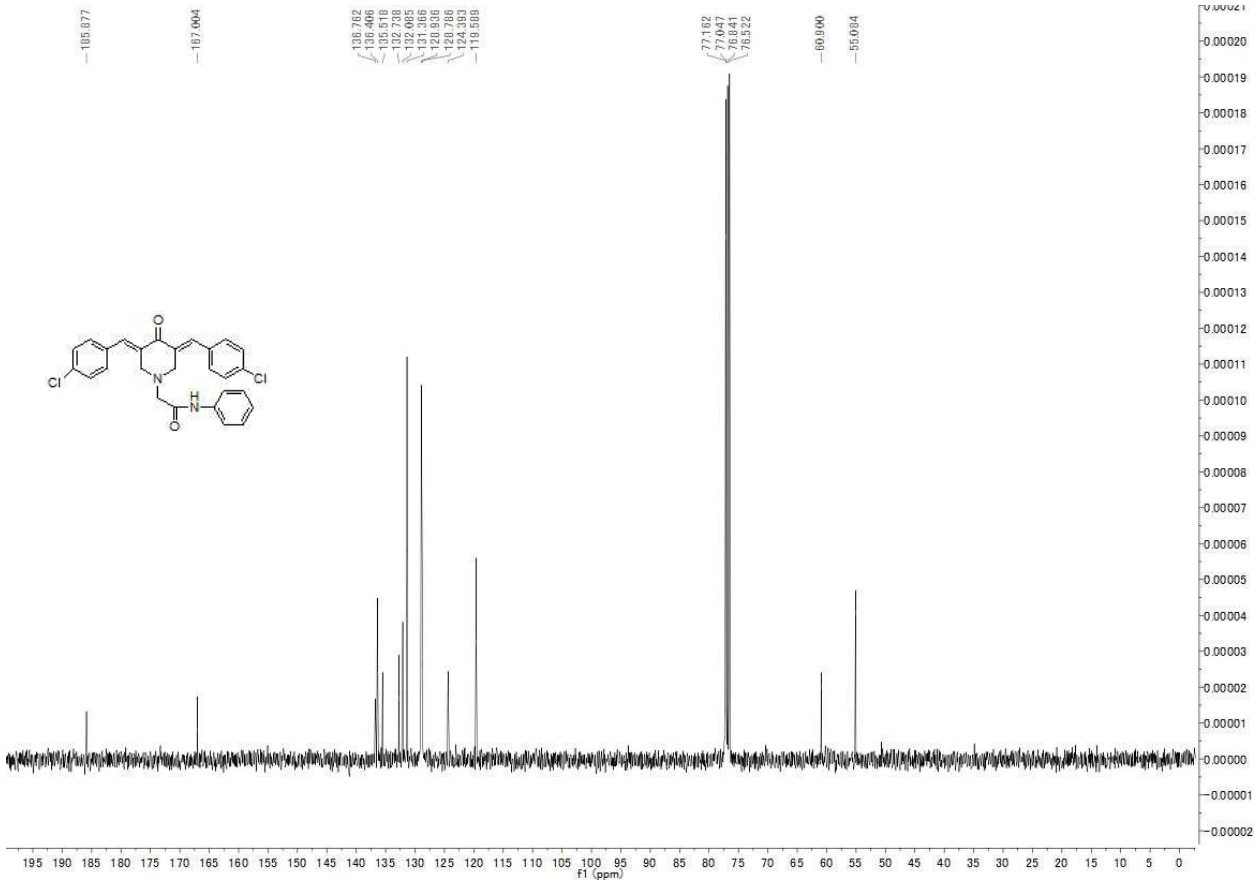

Figure S15. ^{13}C-NMR of compound 4d.

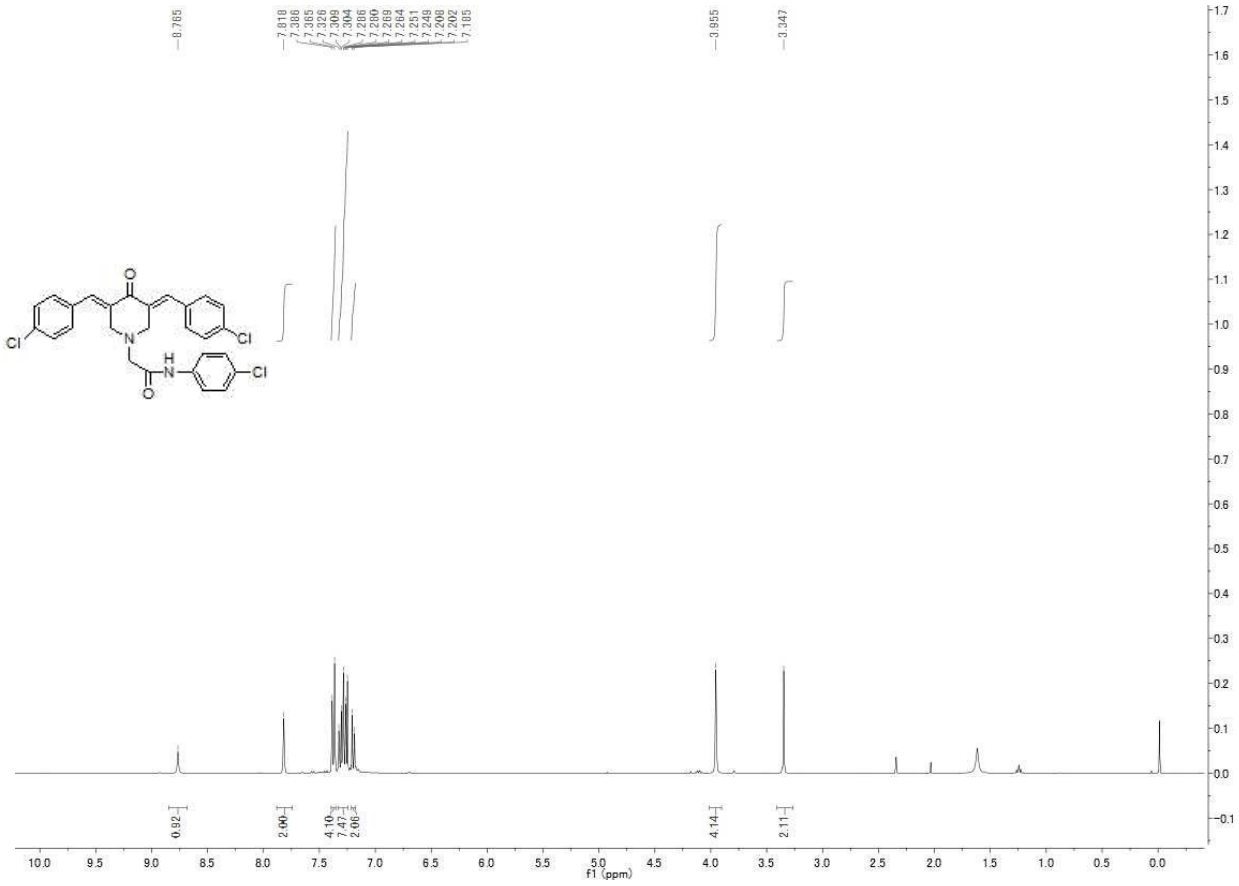

Figure S16. ^{1}H-NMR of compound 4e.

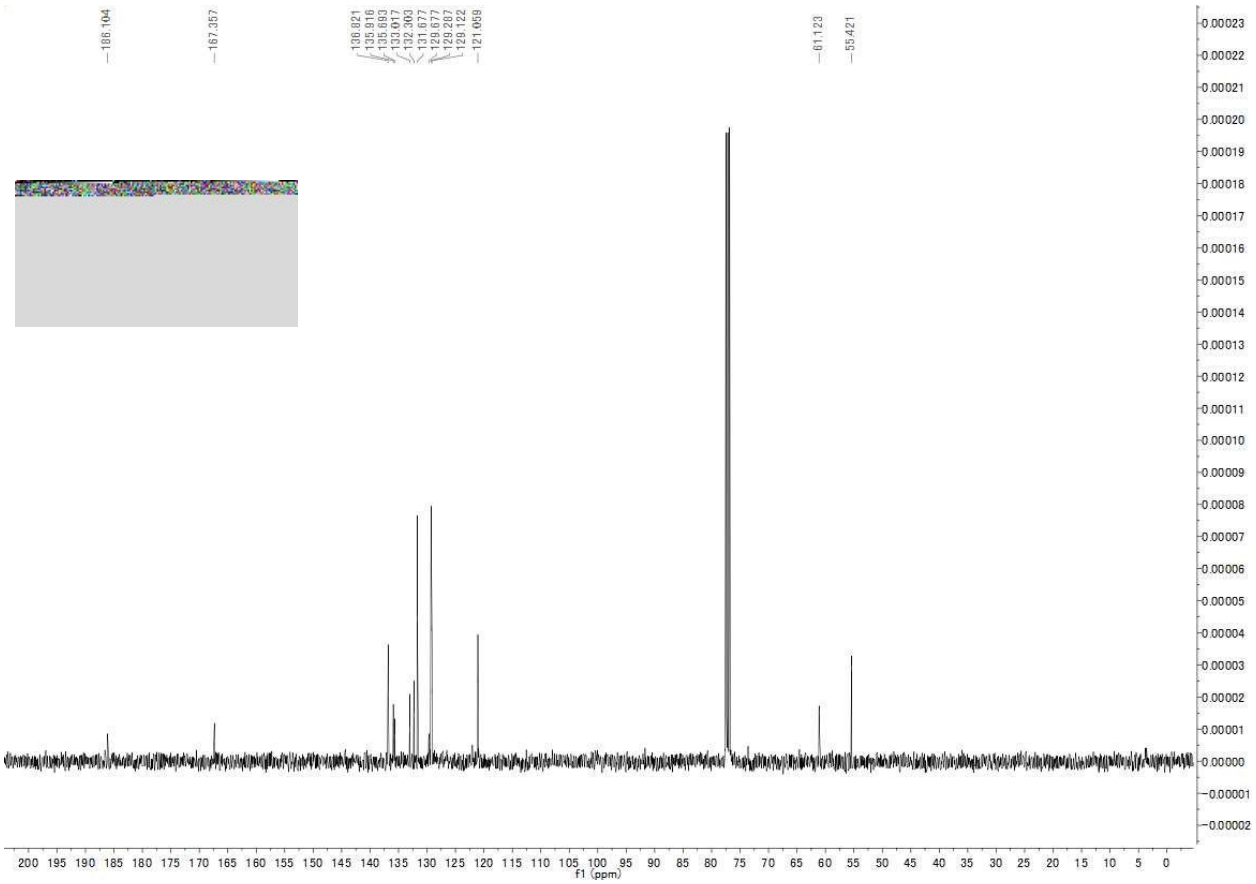

Figure S17. ^{13}C-NMR of compound 4e.

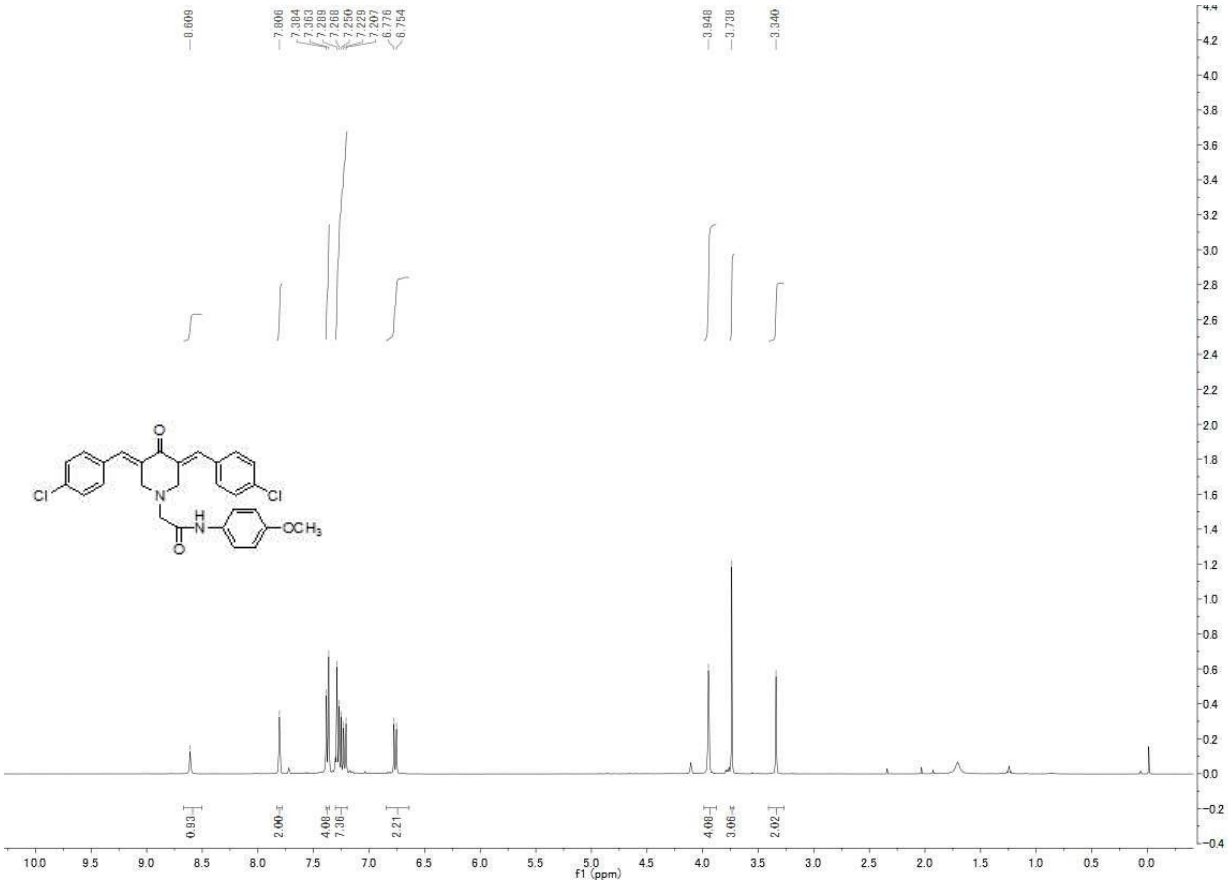

Figure S18. ^{1}H-NMR of compound 4f.

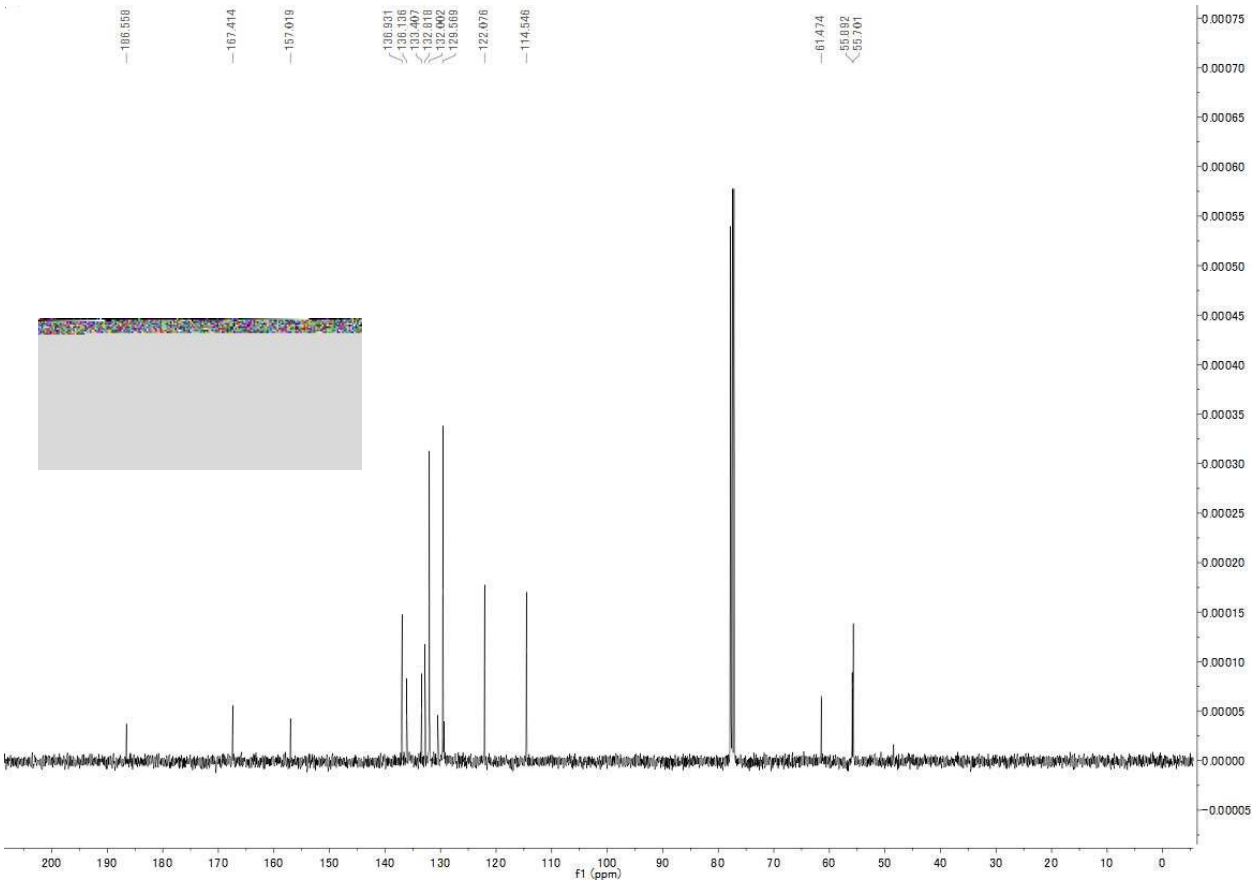

Figure S19. ^{13}C-NMR of compound 4f.

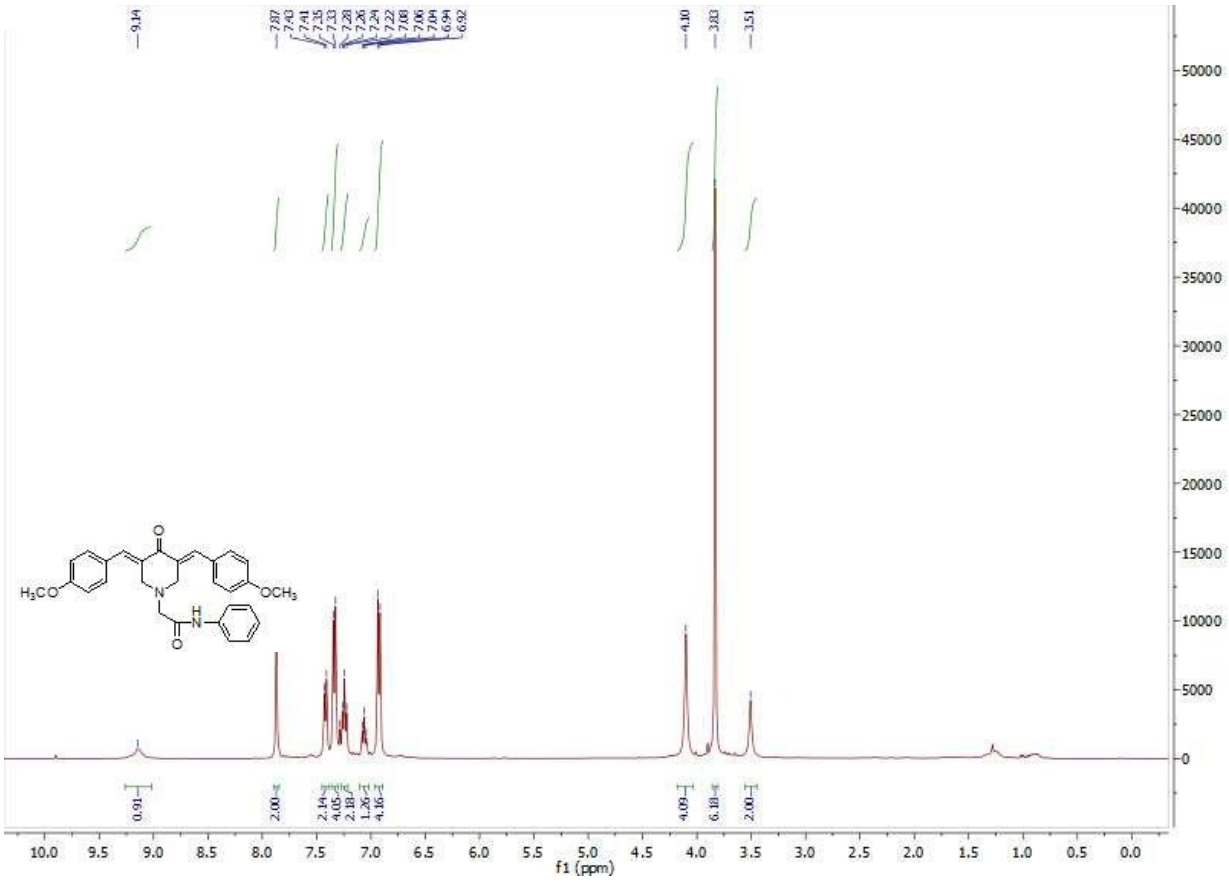

Figure S20. ^{1}H-NMR of compound 4g.

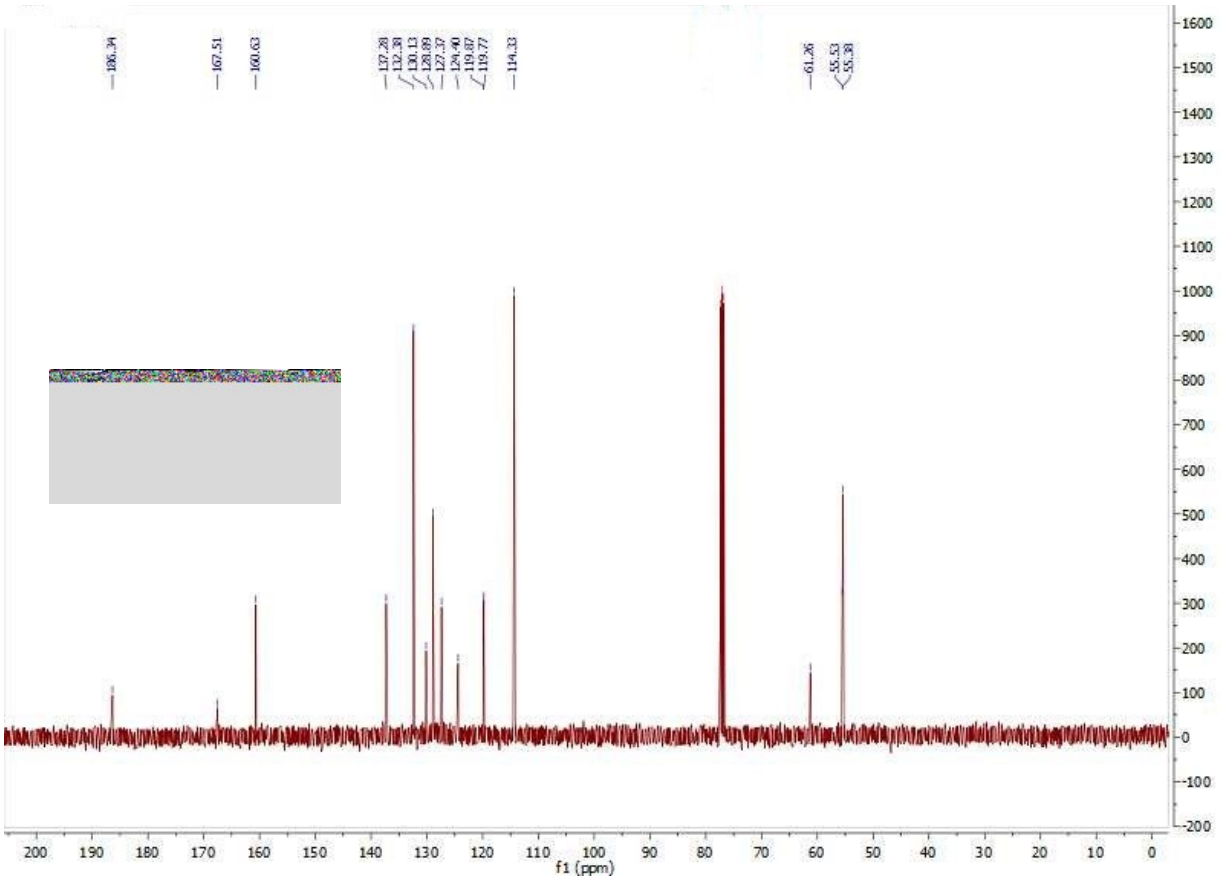

Figure S21. ^{13}C-NMR of compound 4g.

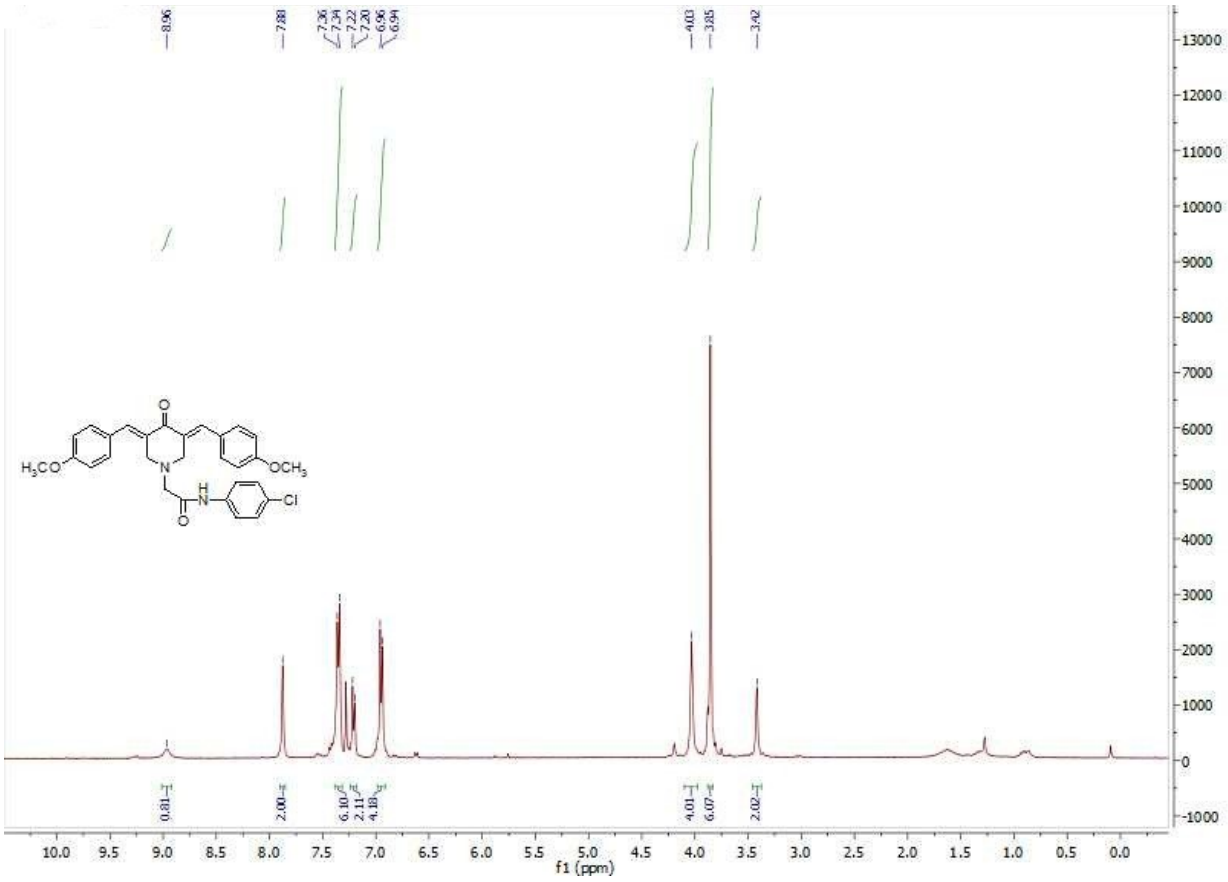

Figure S22. ^{1}H-NMR of compound 4h.

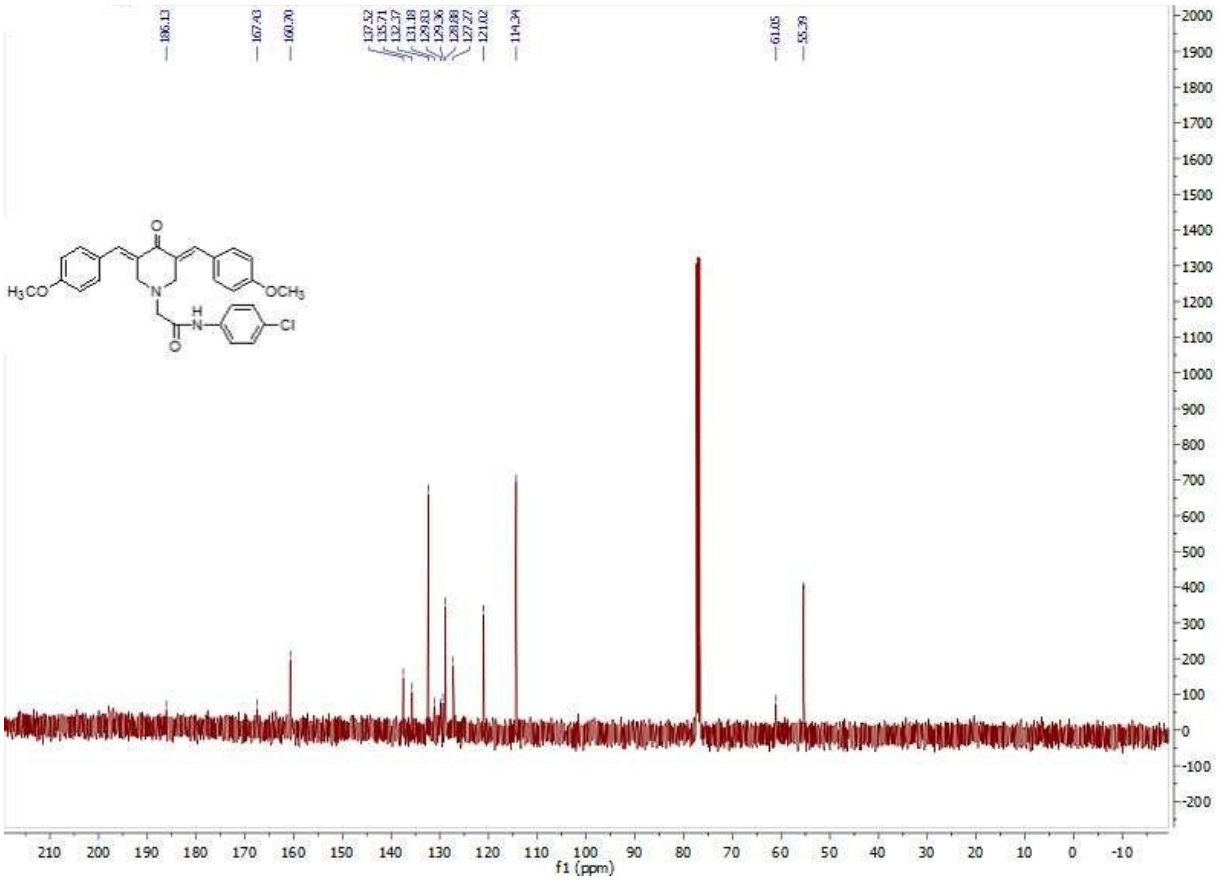

Figure S23. ^{13}C-NMR of compound 4h.

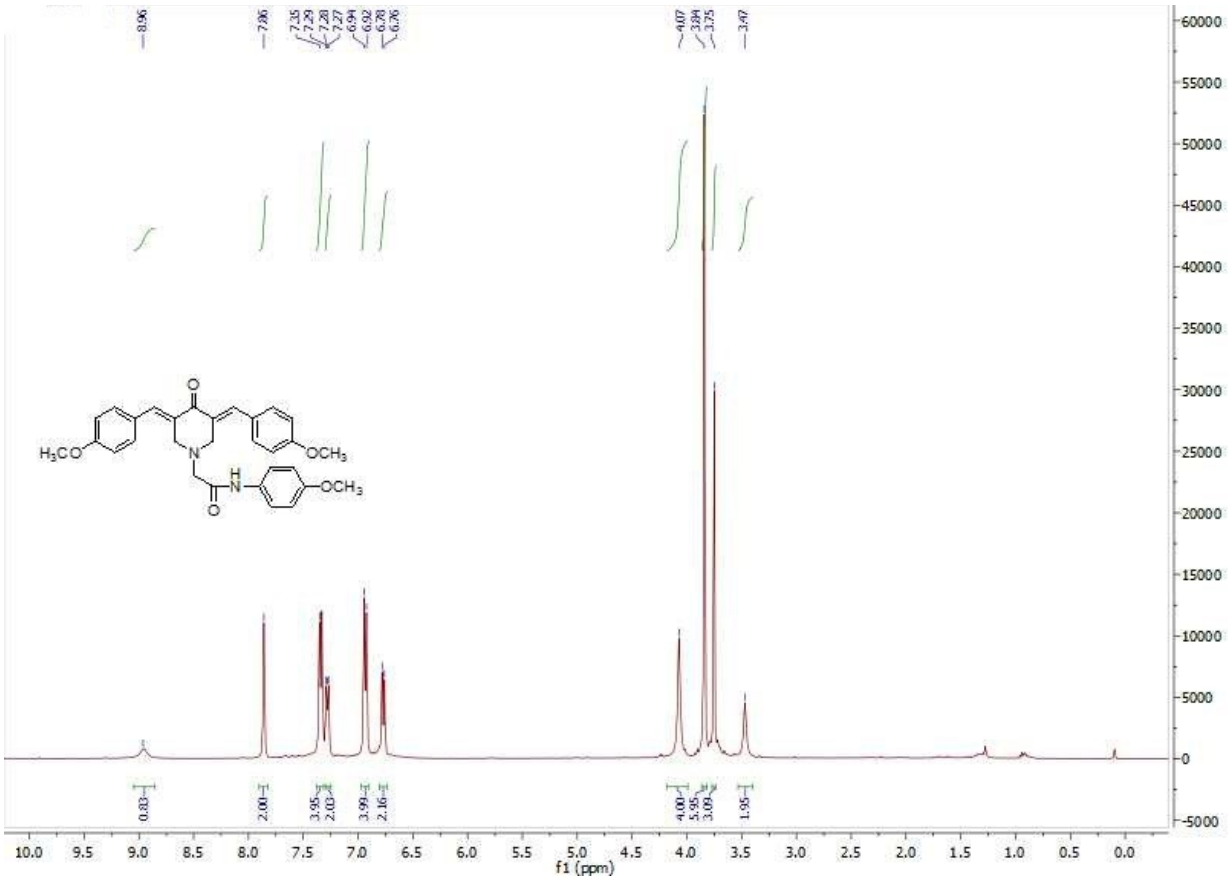

Figure S24. ^{1}H-NMR of compound 4i.

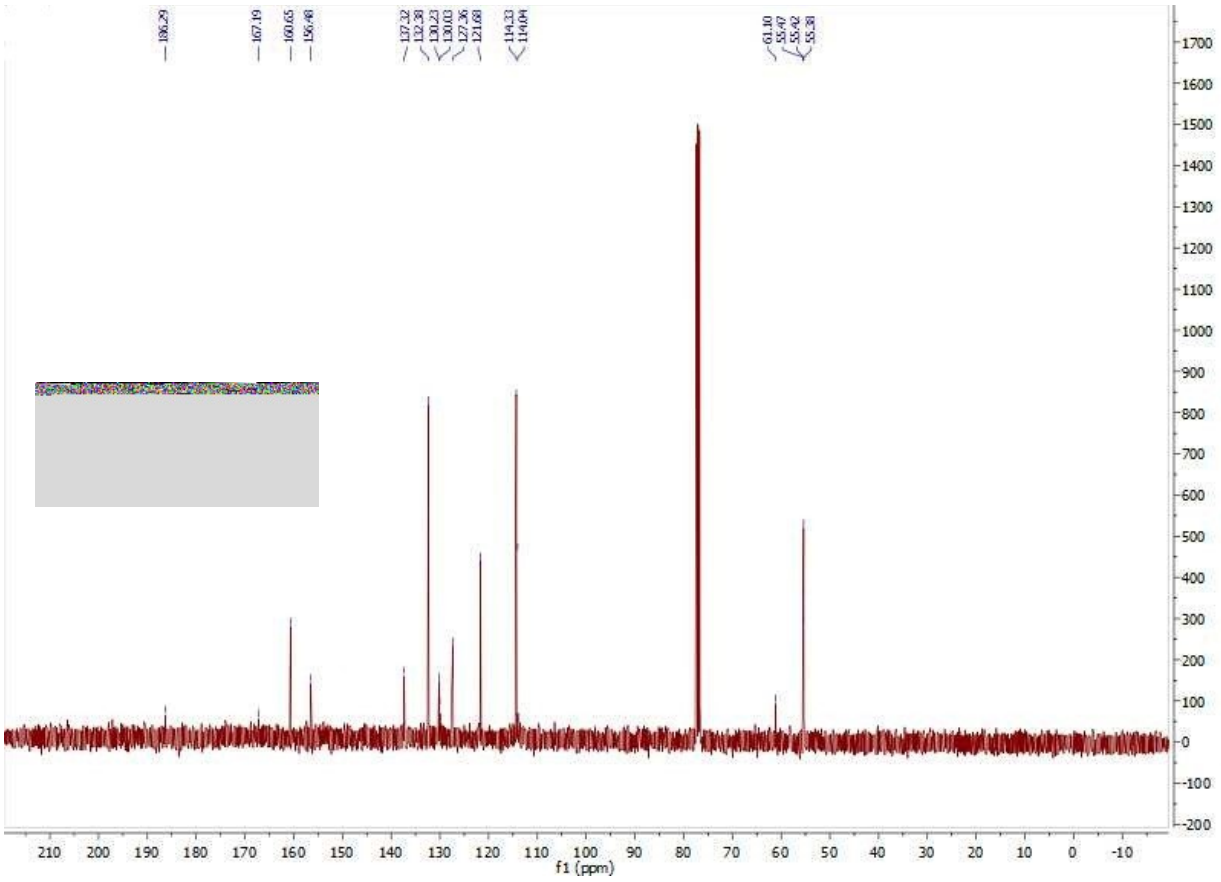

Figure S25. ^{13}C-NMR of compound 4i.

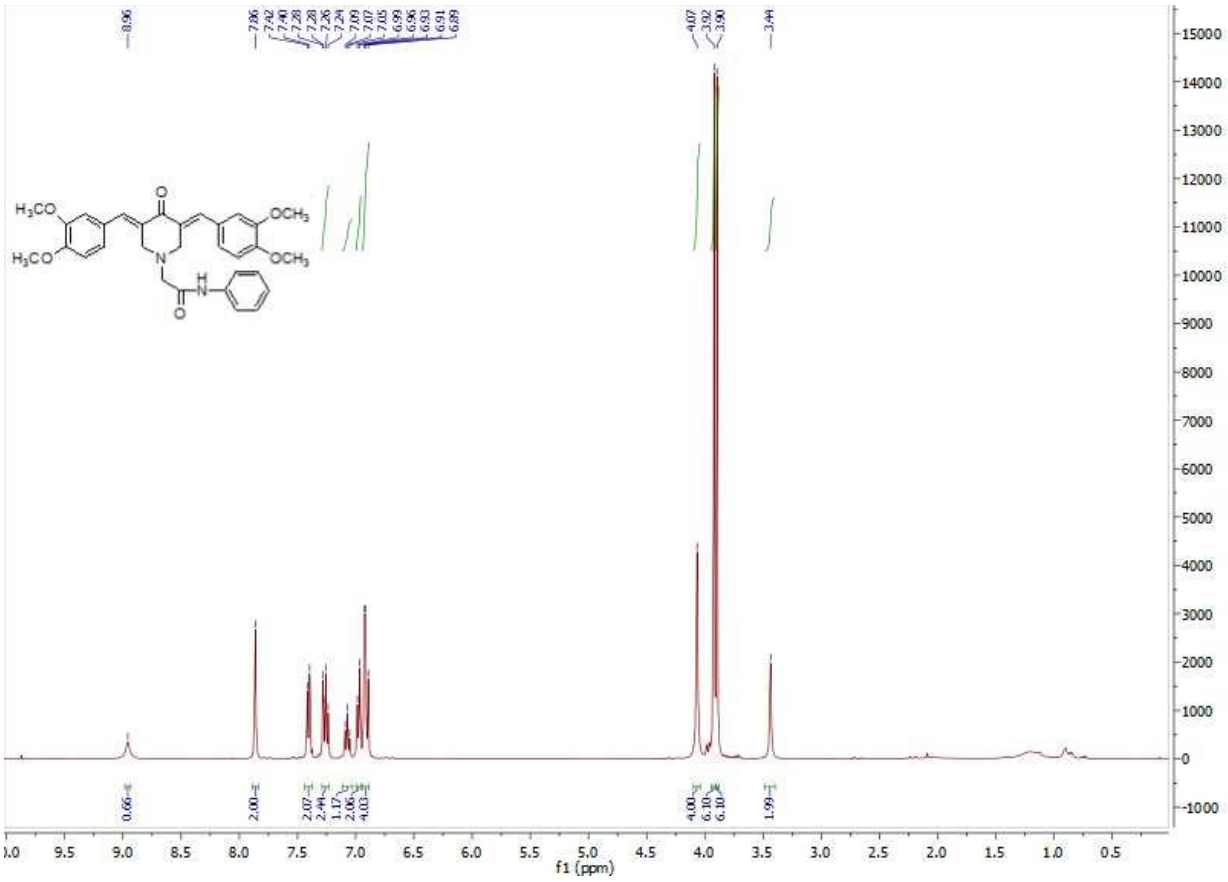

FigureS26. ^{1}H-NMR of compound 4j.

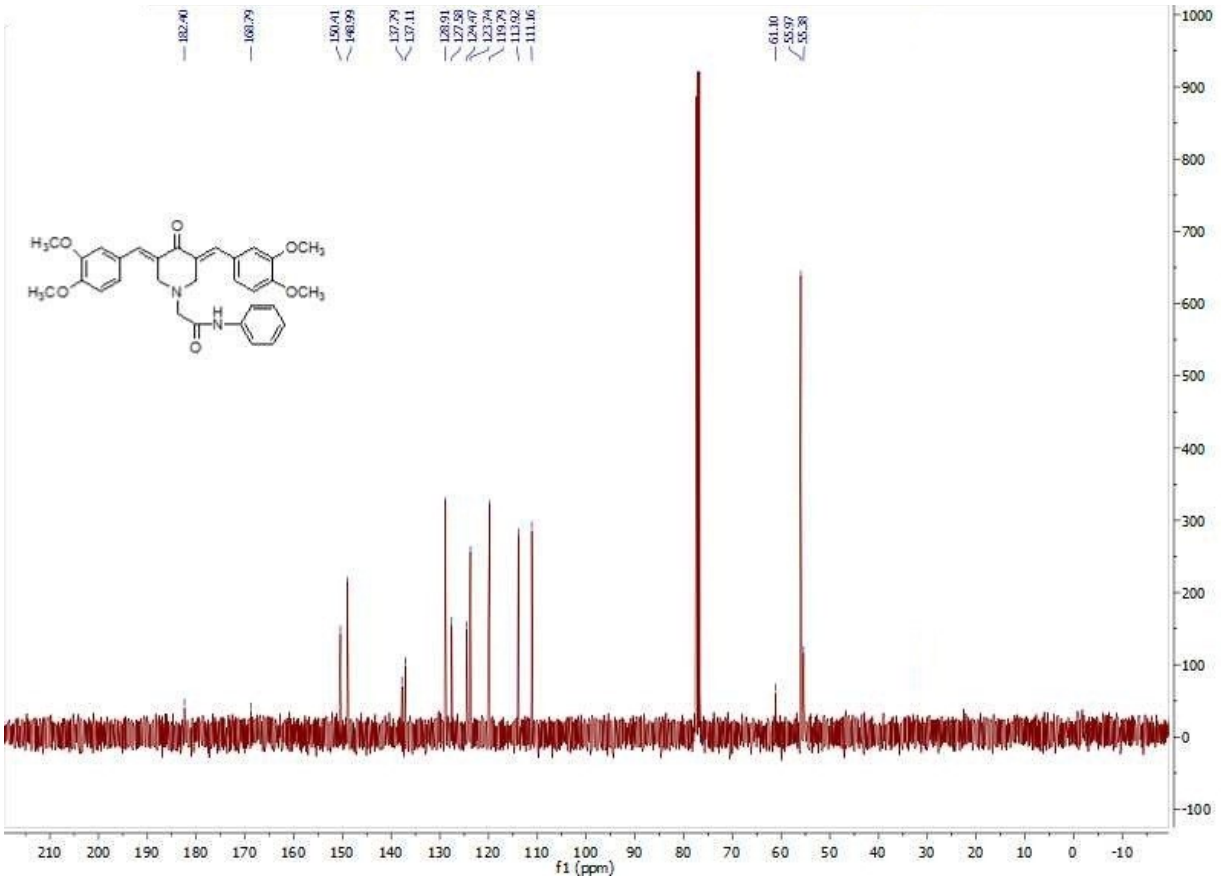

FigureS27. ^{13}C-NMR of compound 4j.

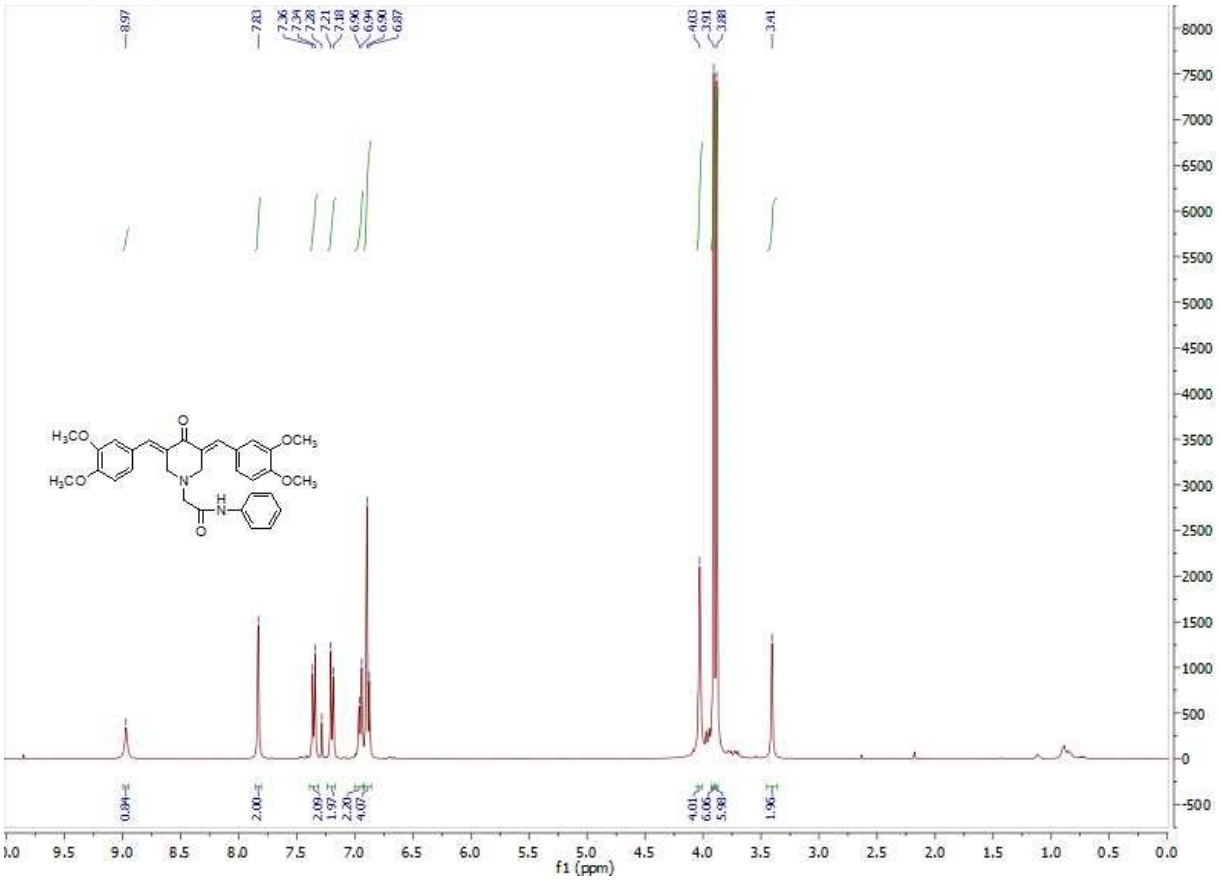

Figure S28. ^{1}H-NMR of compound 4k.

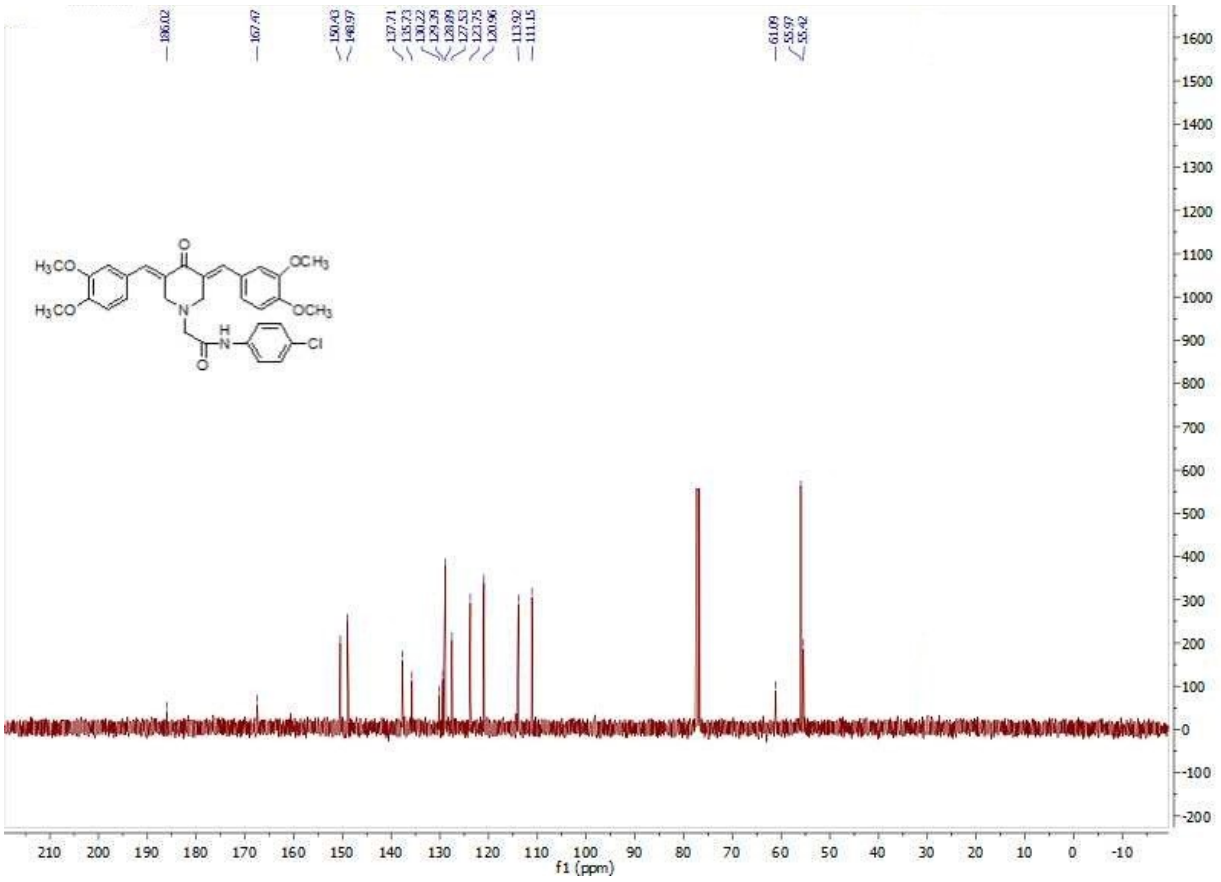

Figure S29. ^{13}C-NMR of compound 4k.

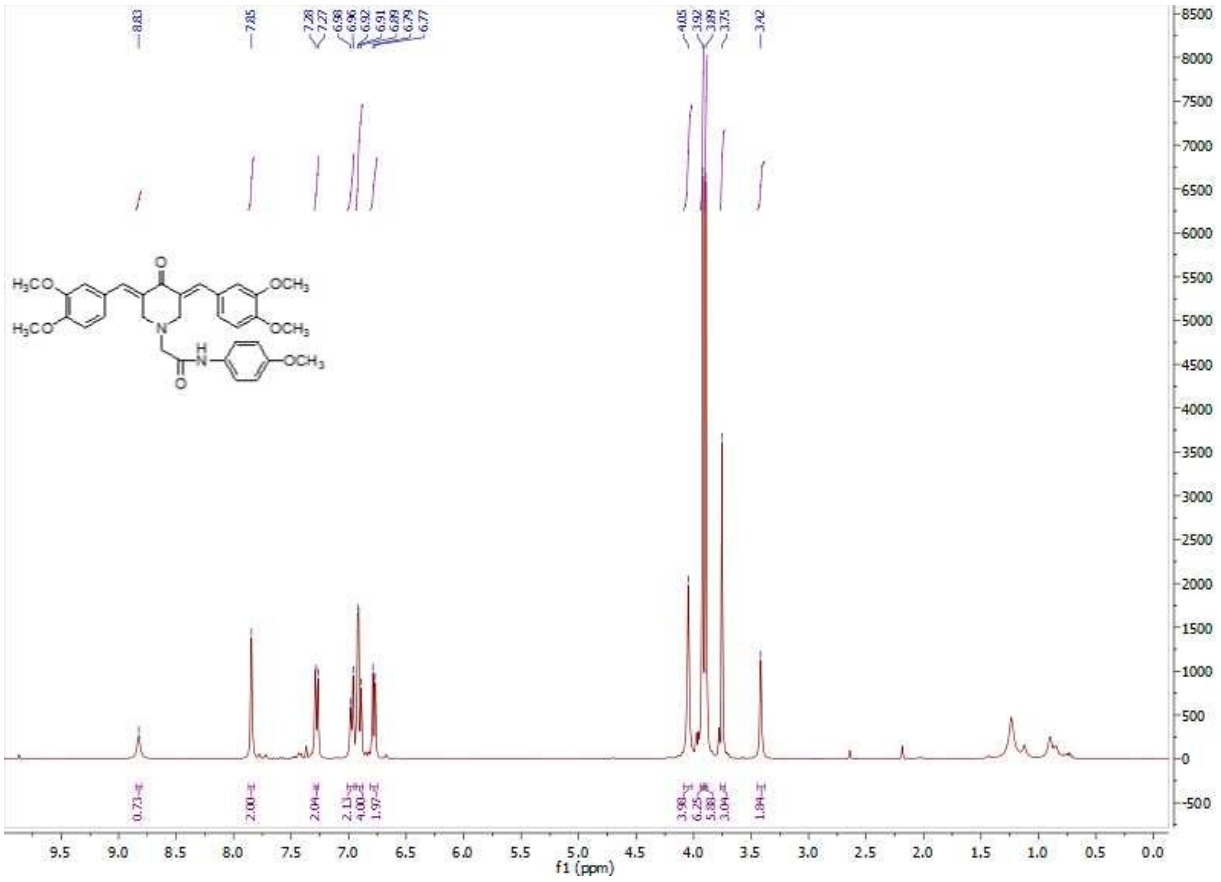

Figure S30. ^{1}H-NMR of compound 4l.

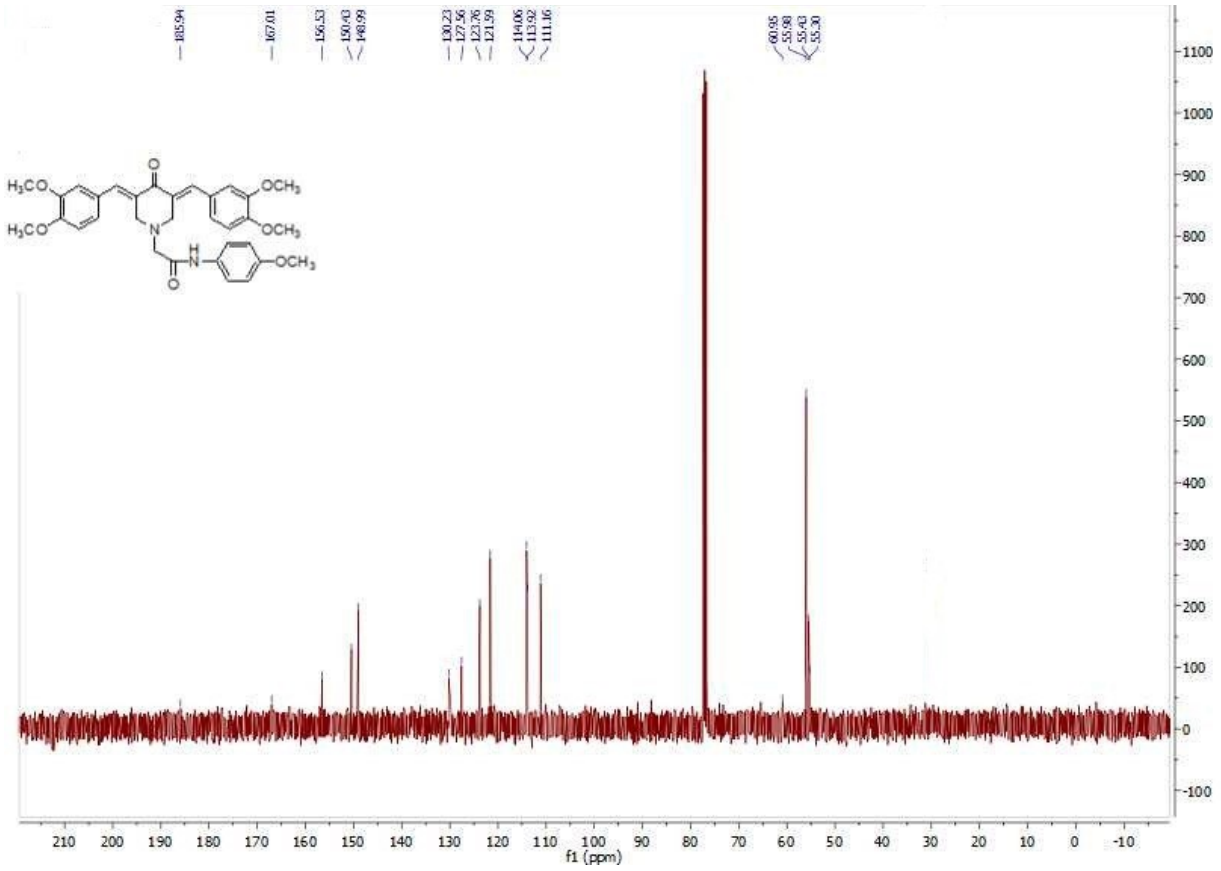

Figure S31. ^{13}C-NMR of compound 4l.

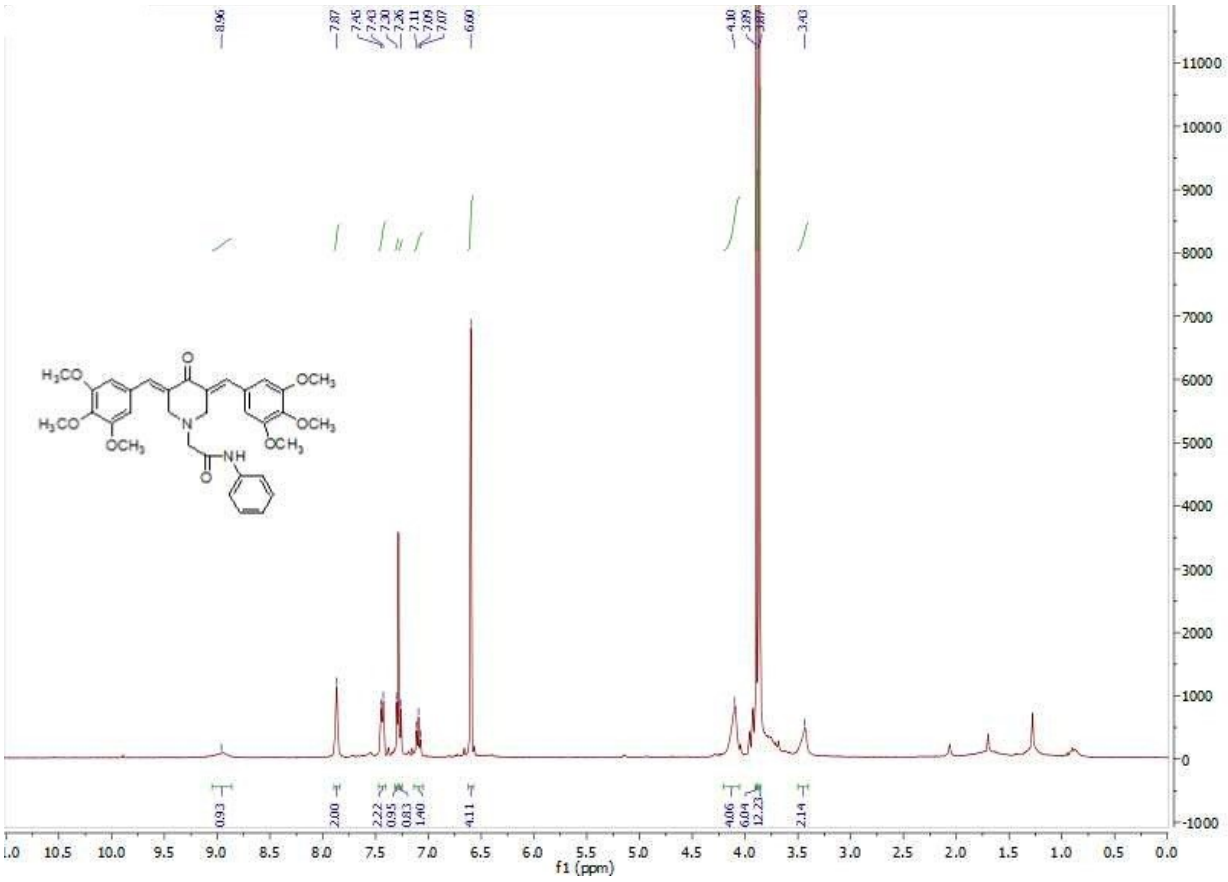

Figure S32. ^{1}H-NMR of compound 4m.

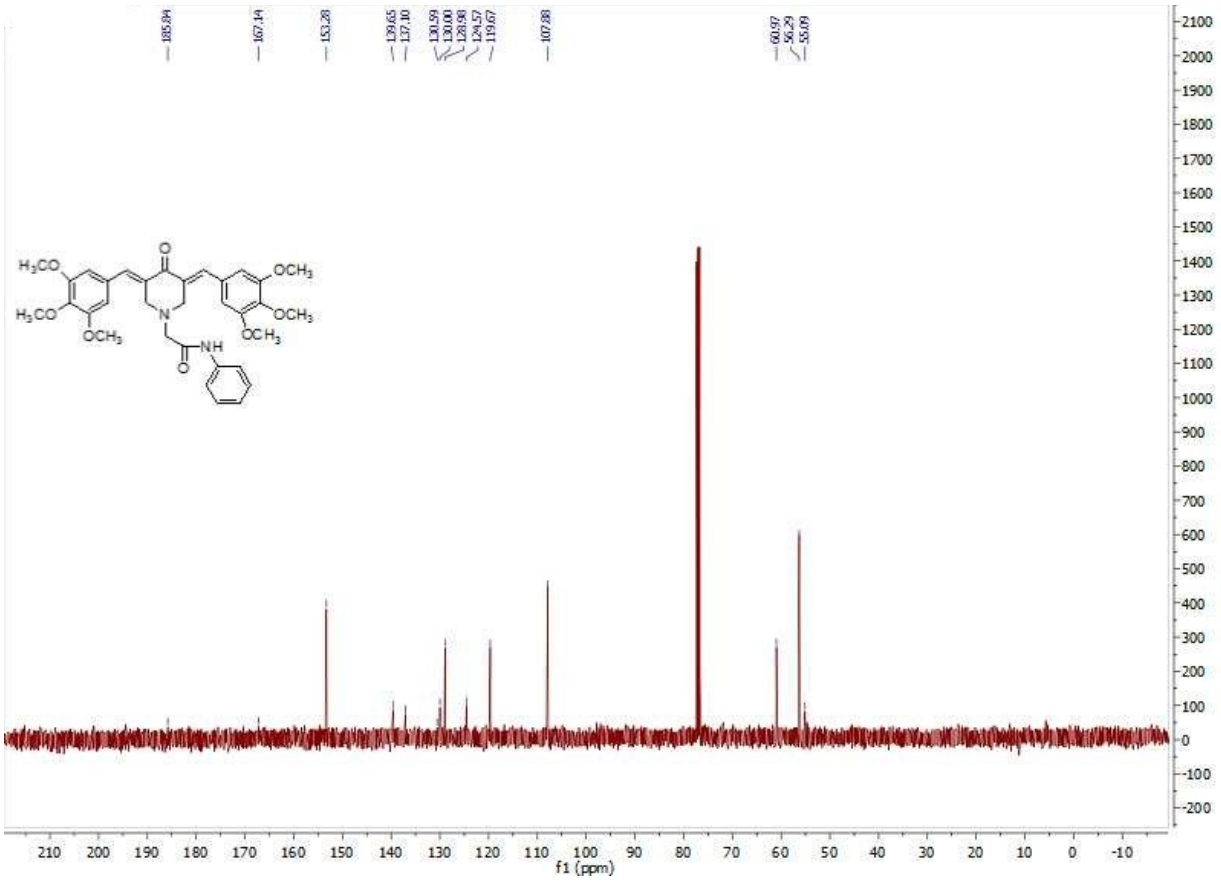

Figure S33. ^{13}C-NMR of compound 4m.

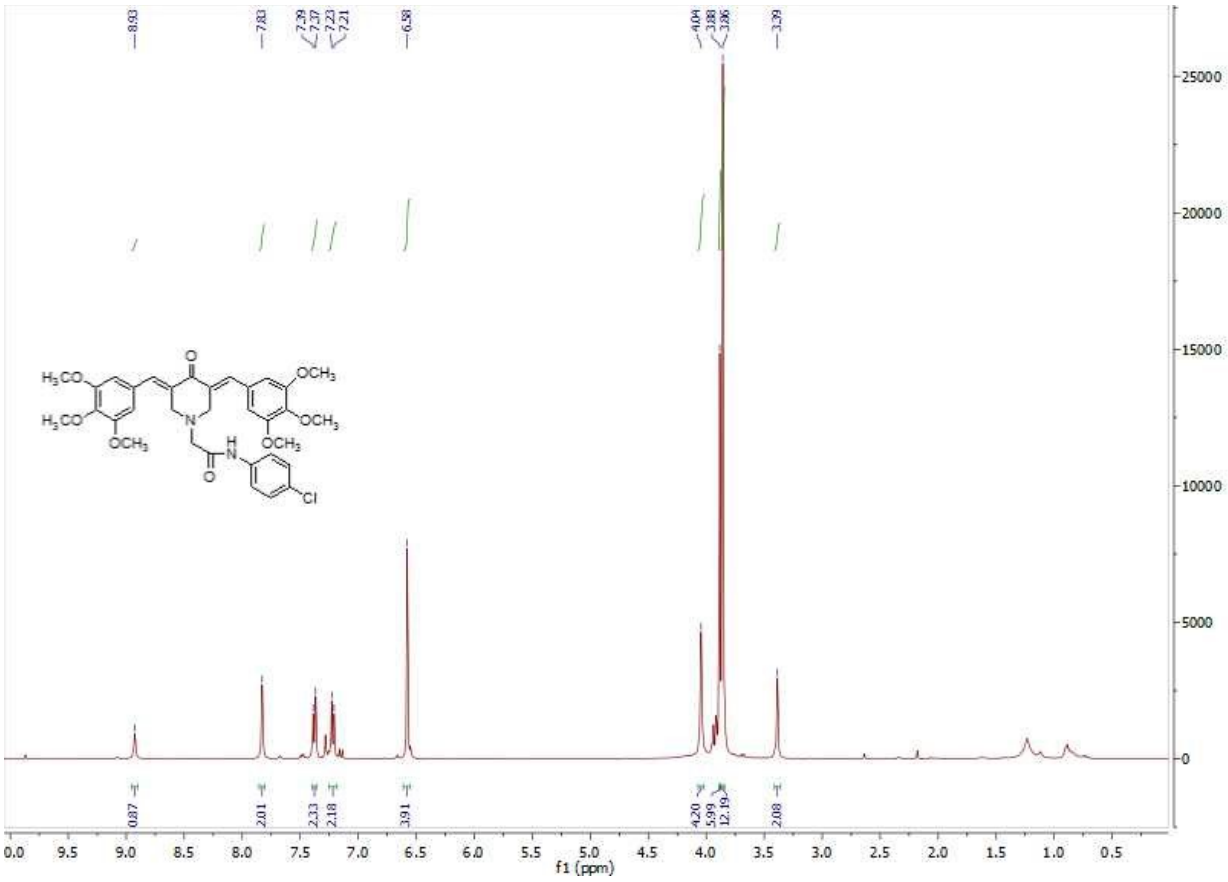

Figure S34. ^{1}H-NMR of compound 4n.

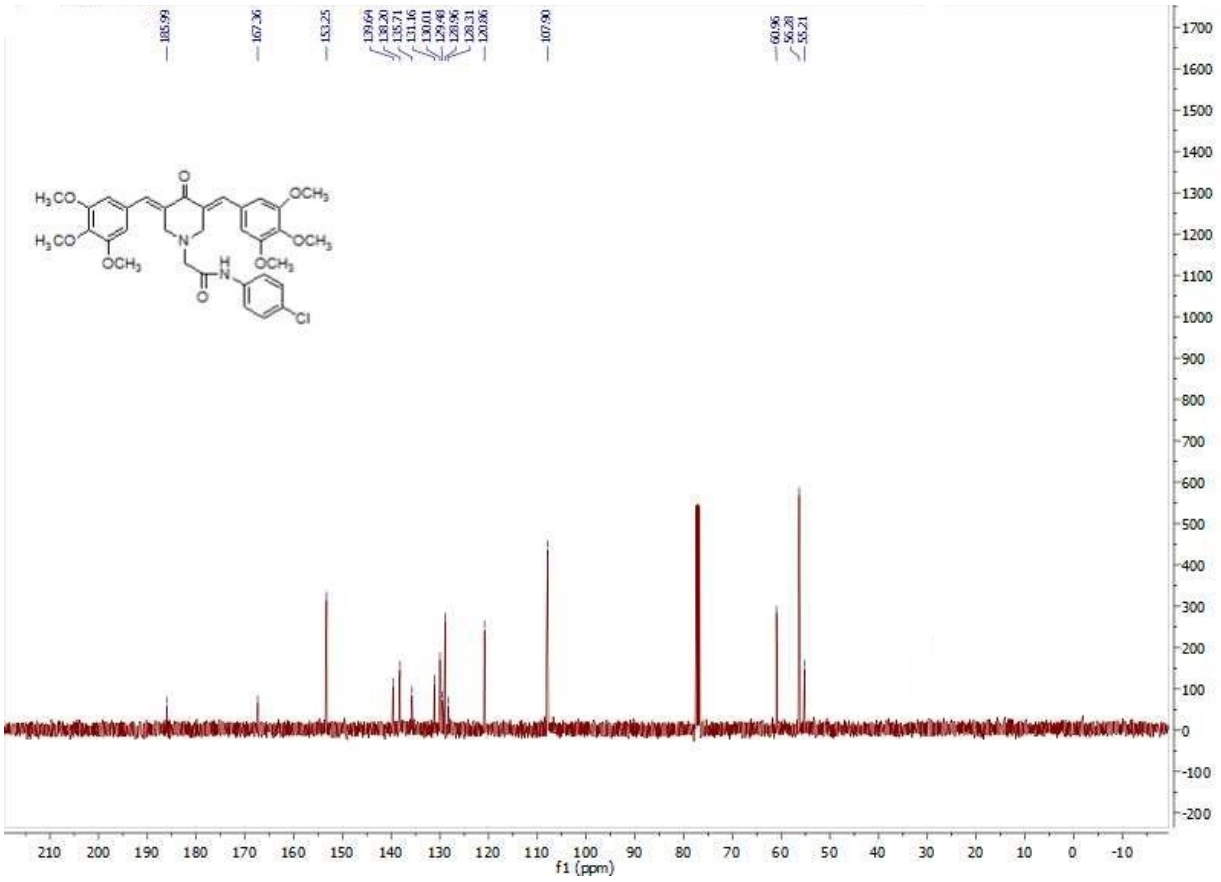

Figure S35. ^{13}C-NMR of compound 4n.

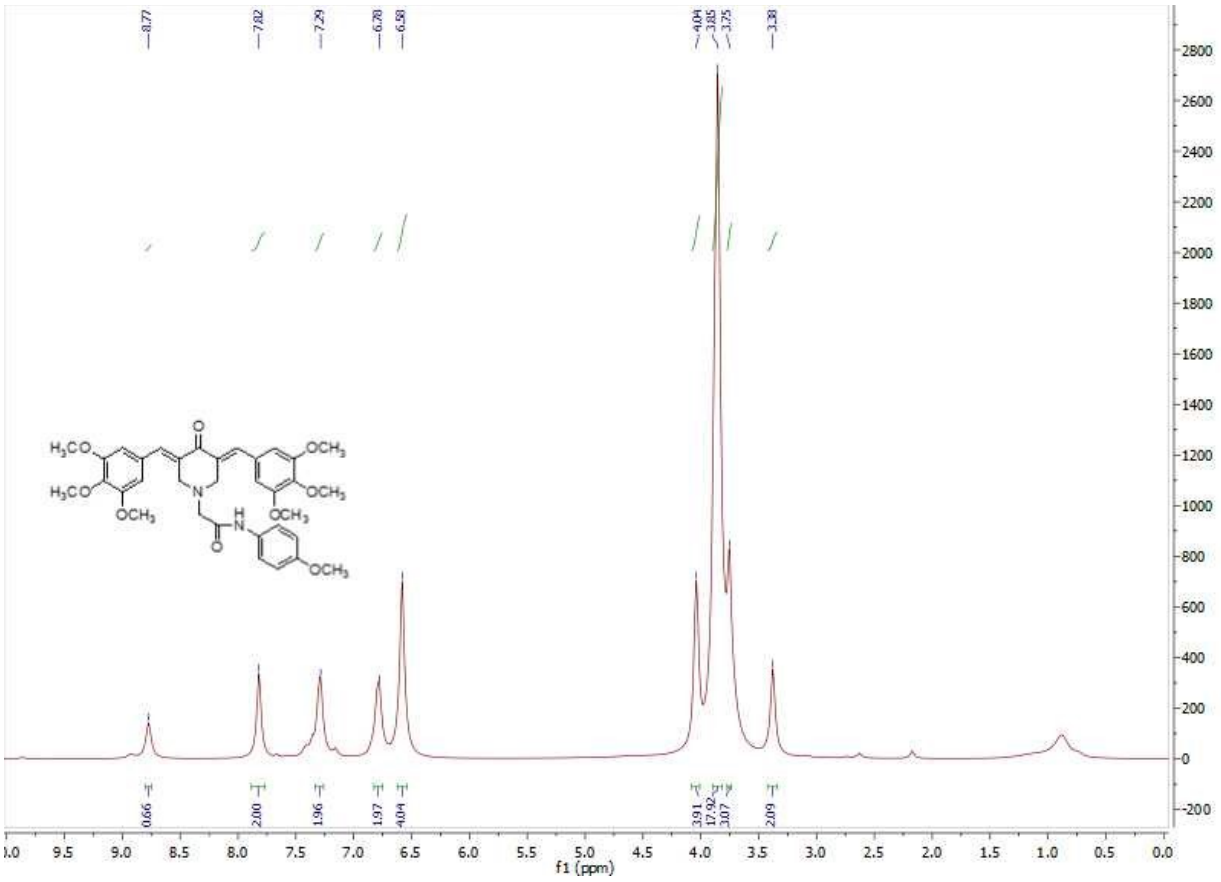

Figure S36. ^{1}H-NMR of compound 4o.

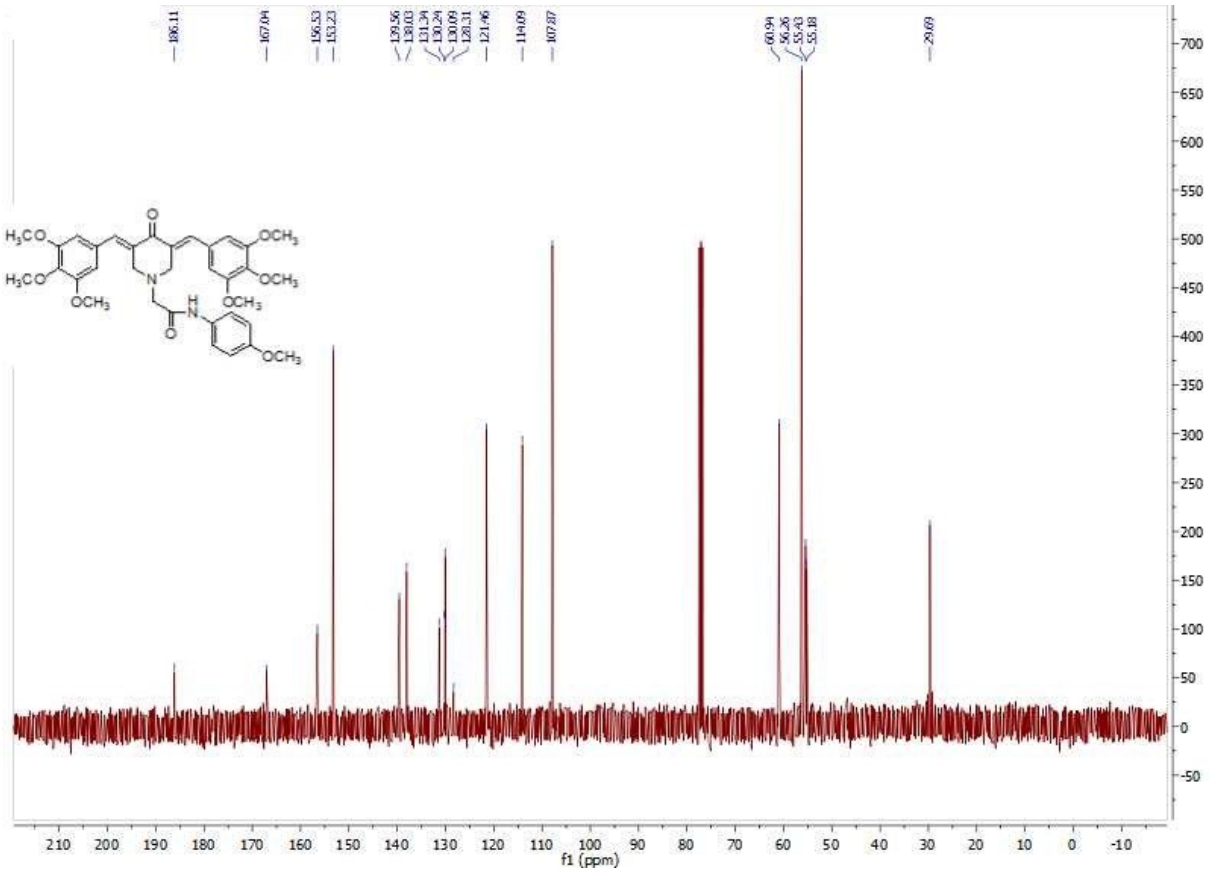

Figure S37. ^{1}H-NMR of compound 4o.

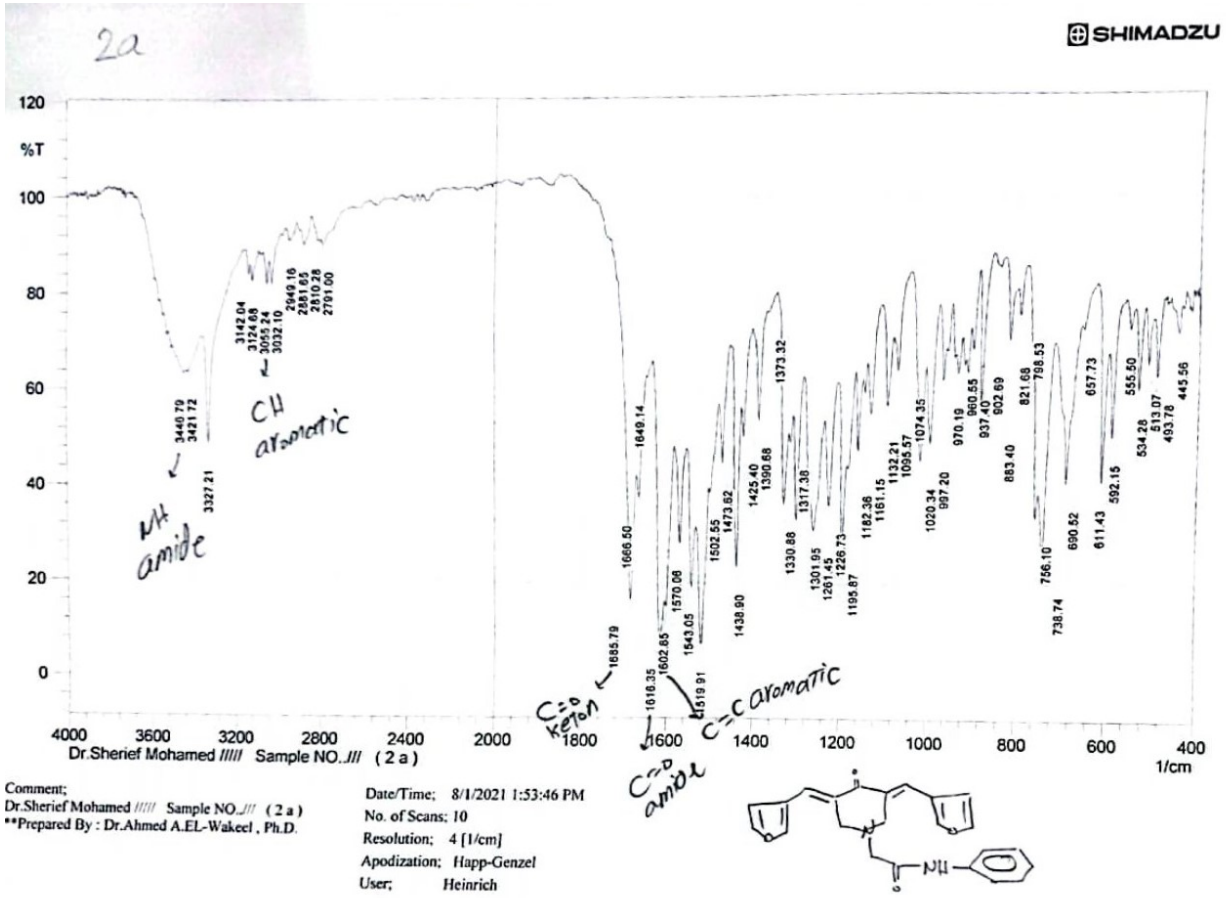

Figure S38. IR spectrum of compound 2a

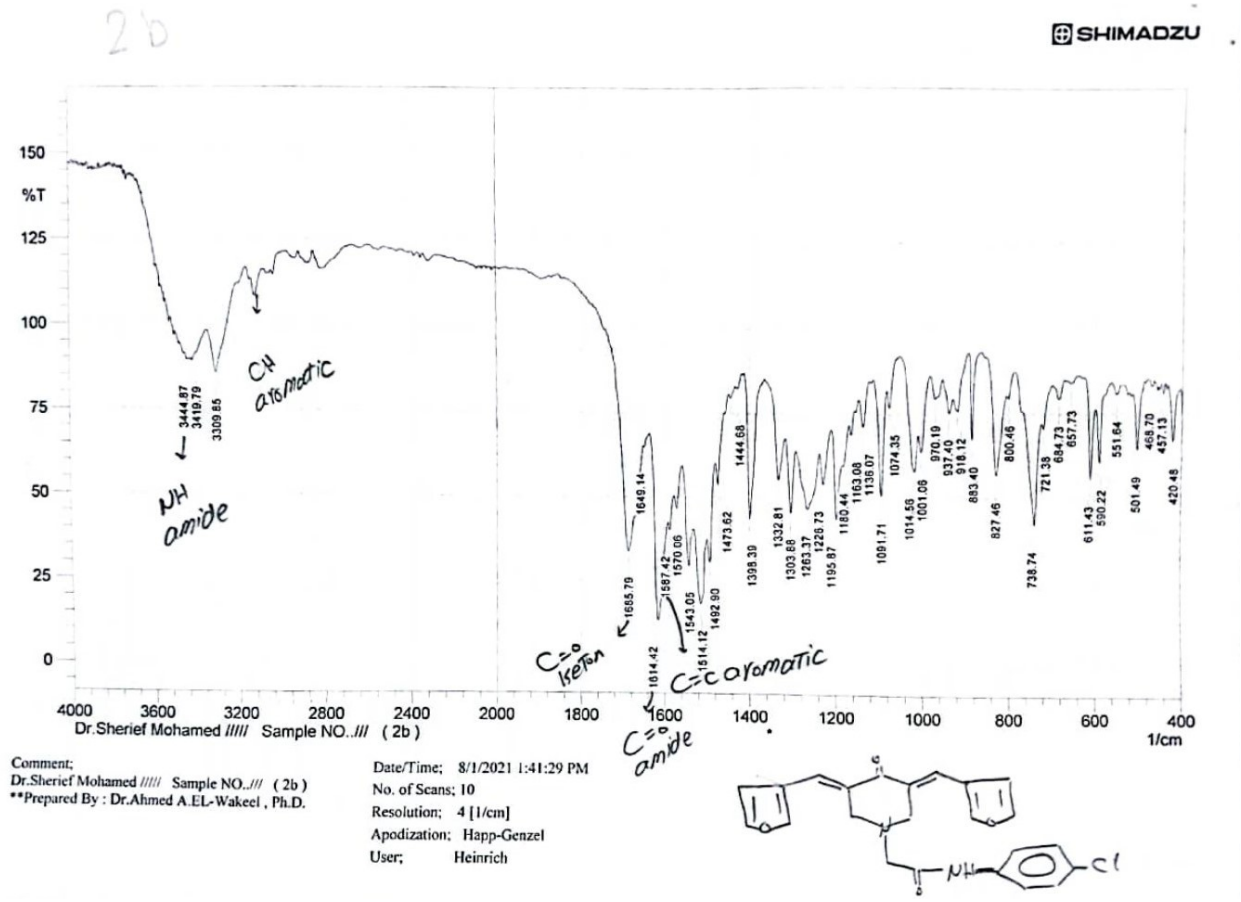

Figure S39. IR spectrum of compound 2b

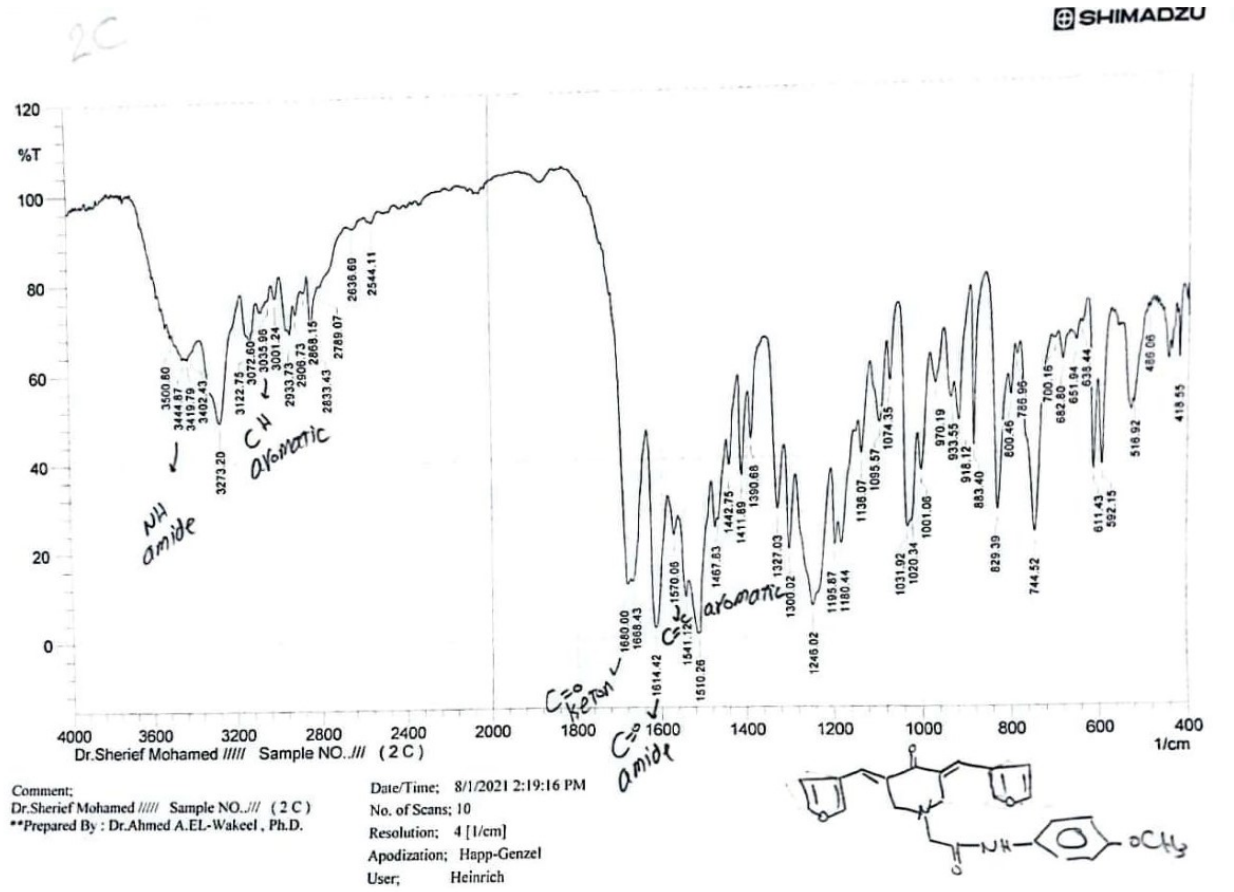

Figure S40. IR spectrum of compound 2C

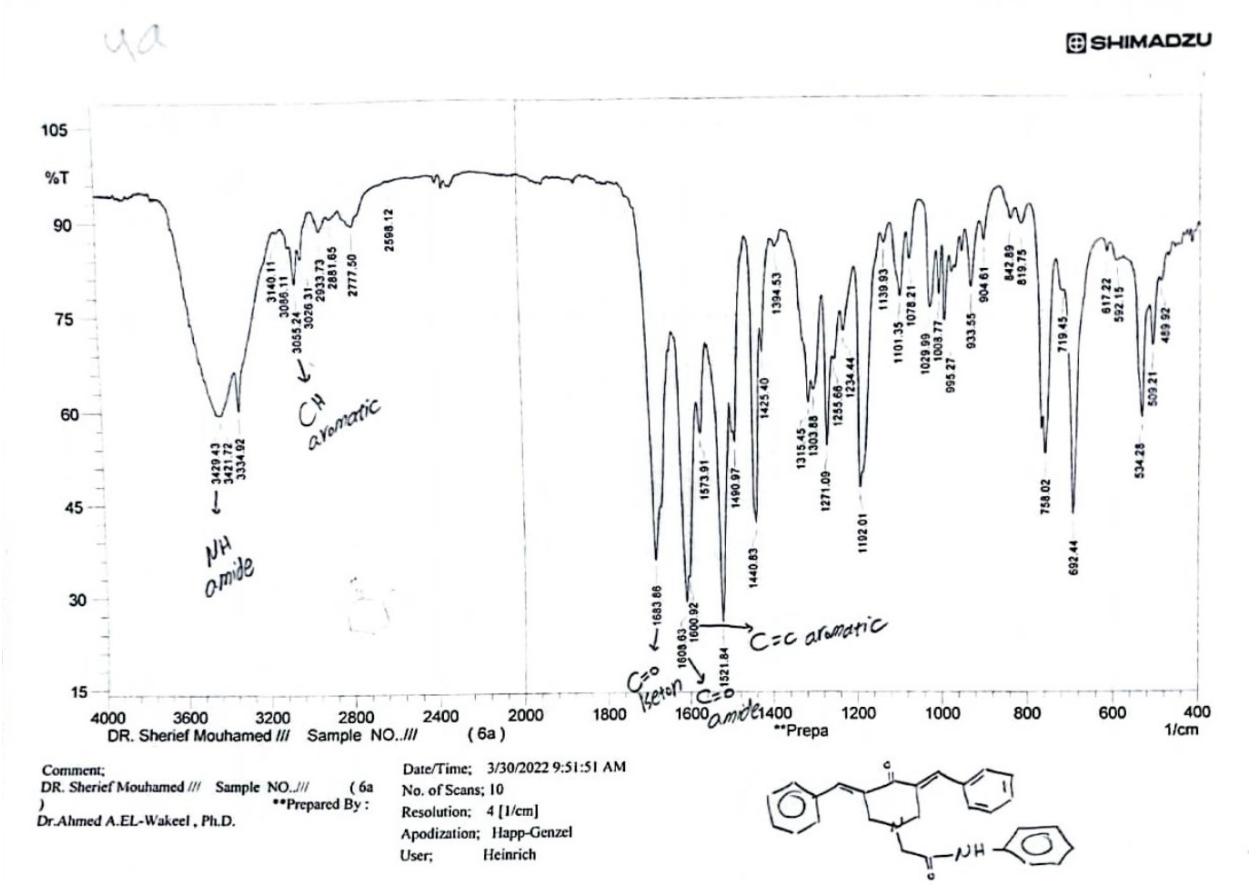

Figure S41. IR spectrum of compound 4a

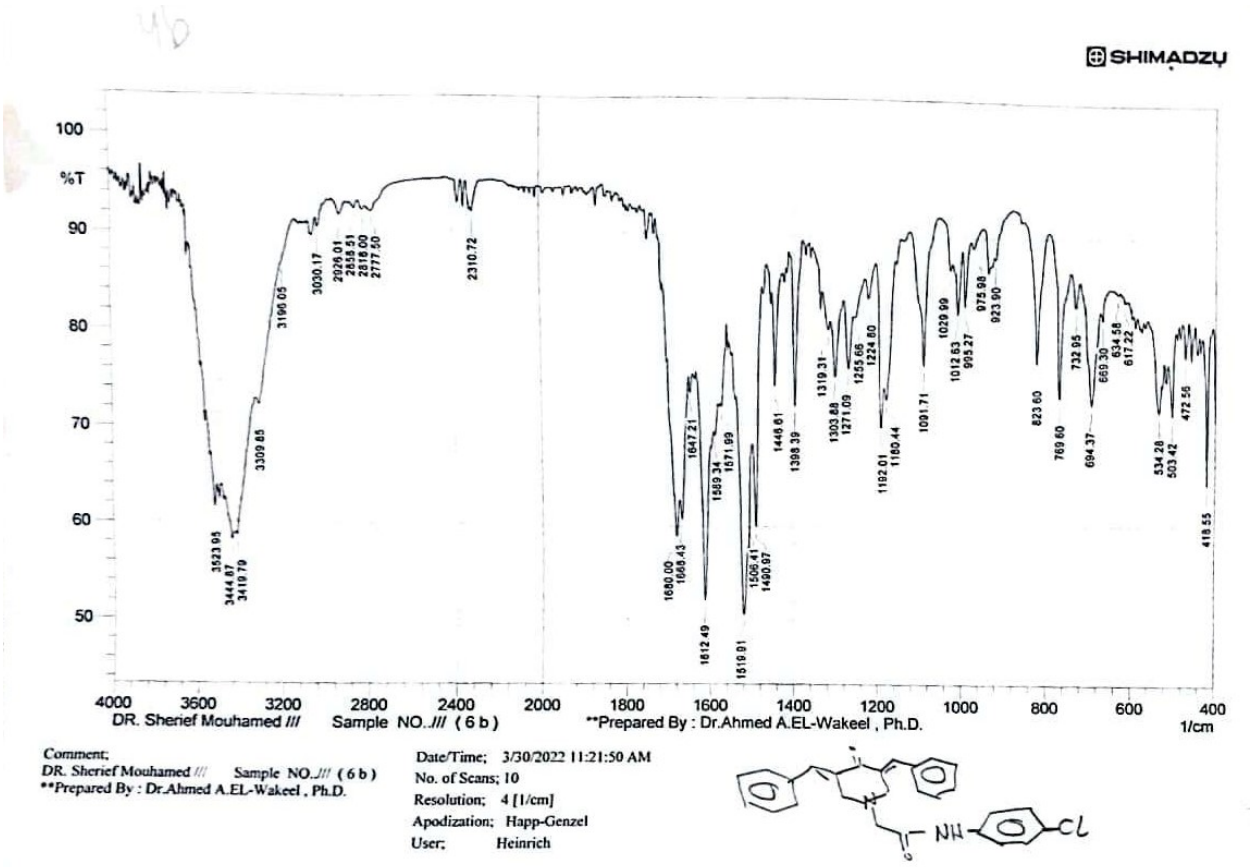

Figure S42. IR spectrum of compound 4b

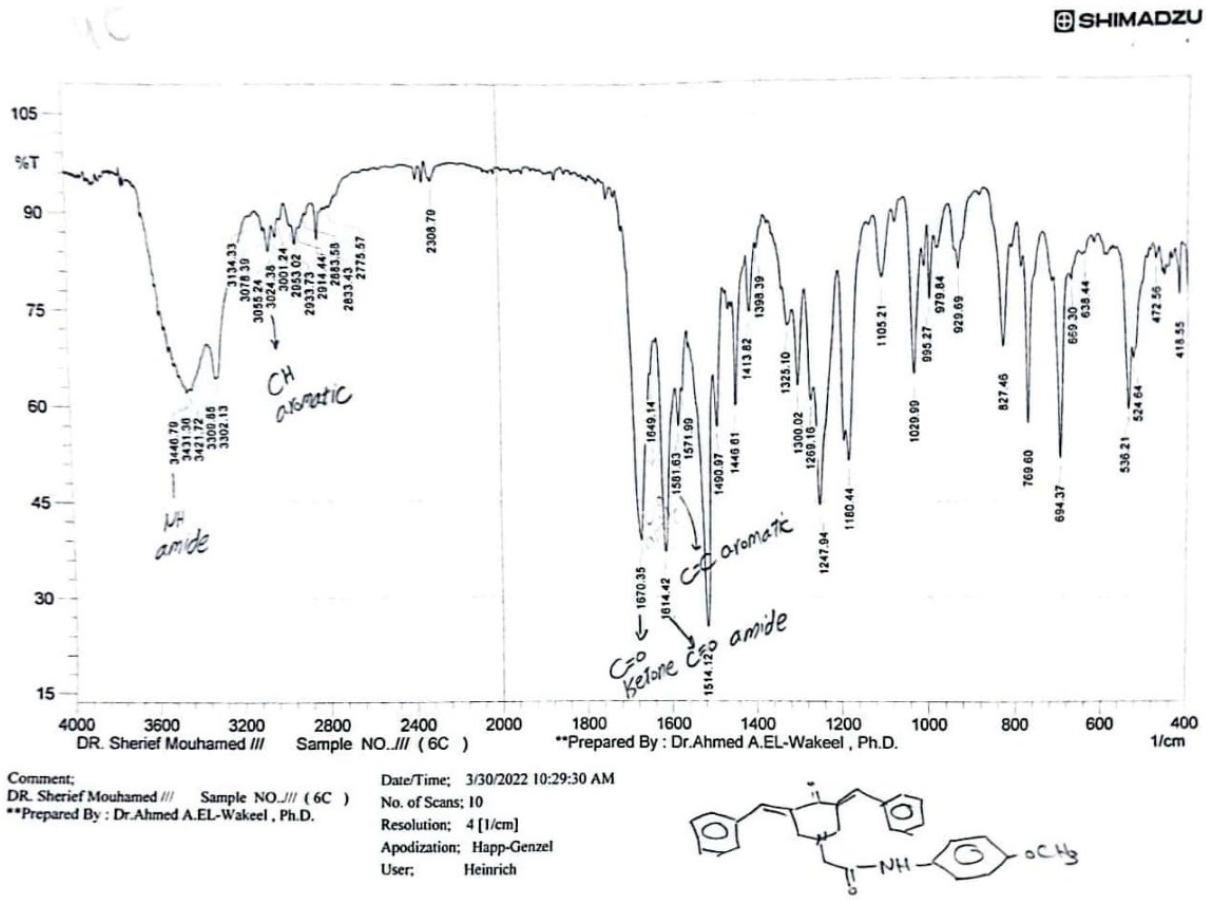

Figure S43. IR spectrum of compound 4C

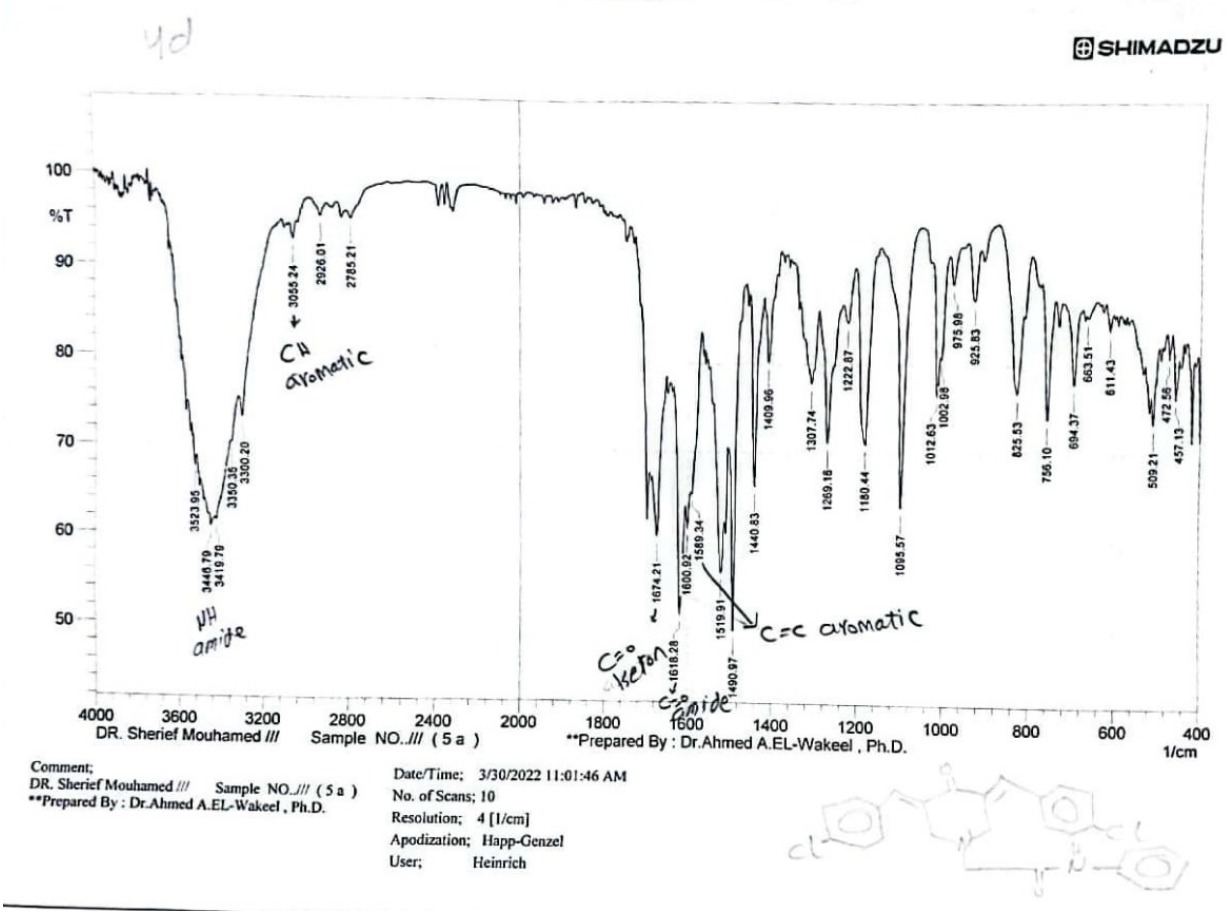

Figure S44. IR spectrum of compound 4d

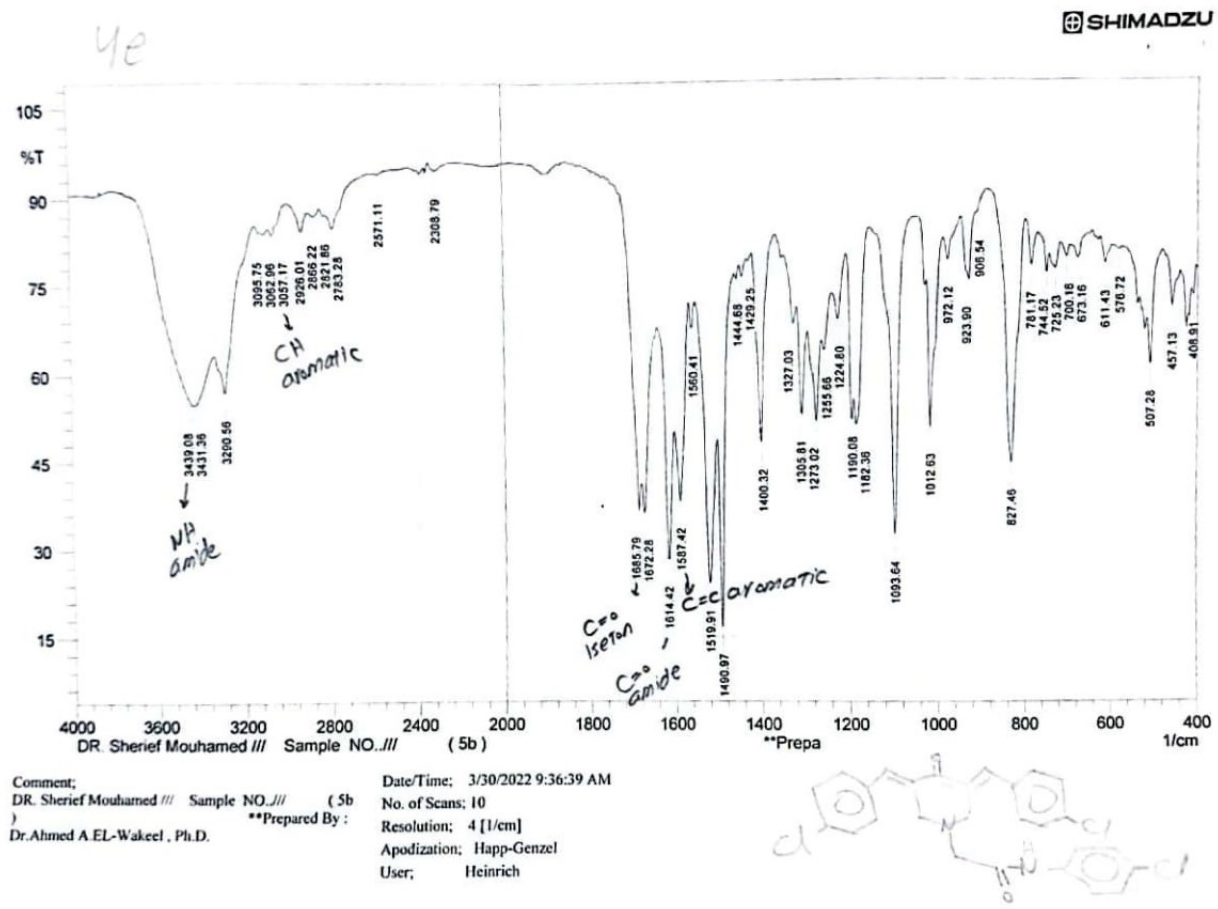

Figure S45. IR spectrum of compound 4e

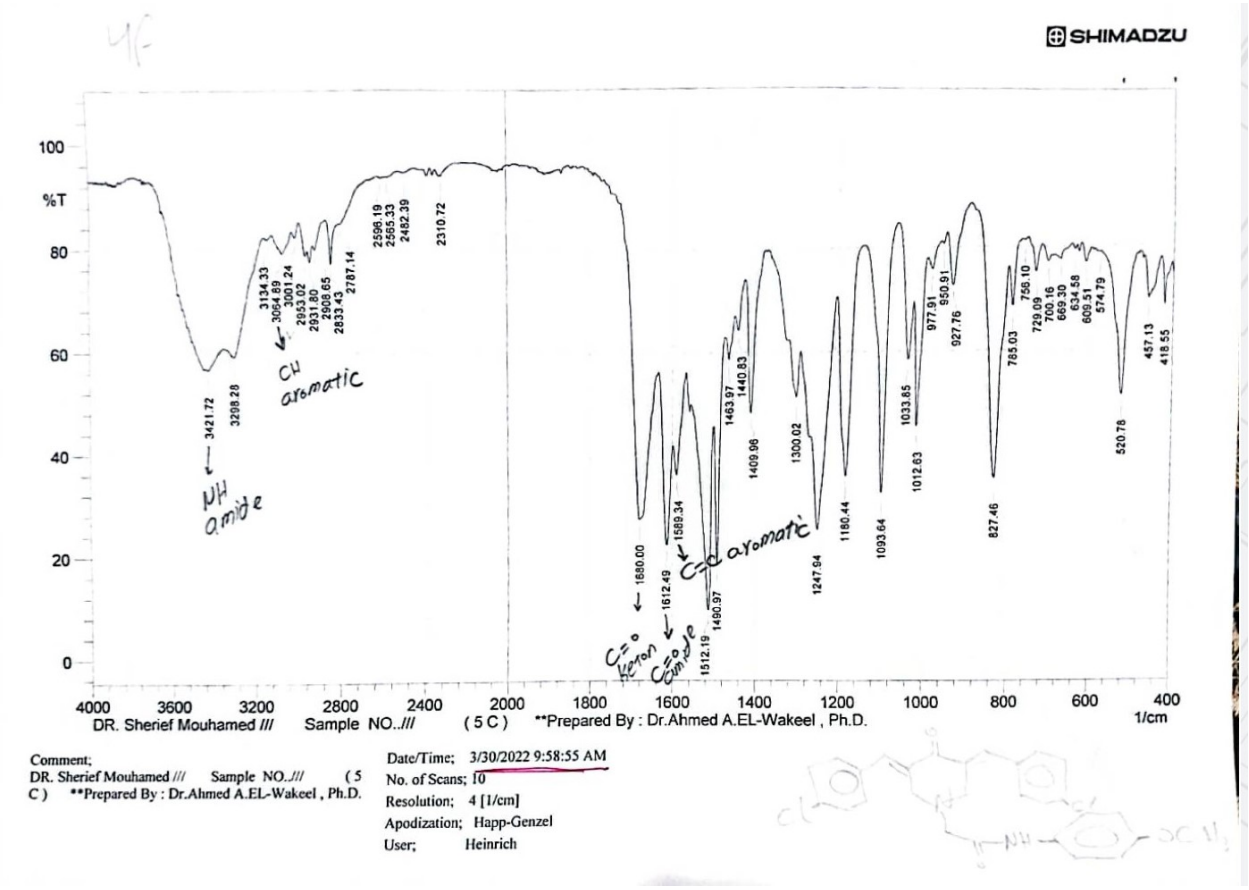

Figure S46. IR spectrum of compound 4f

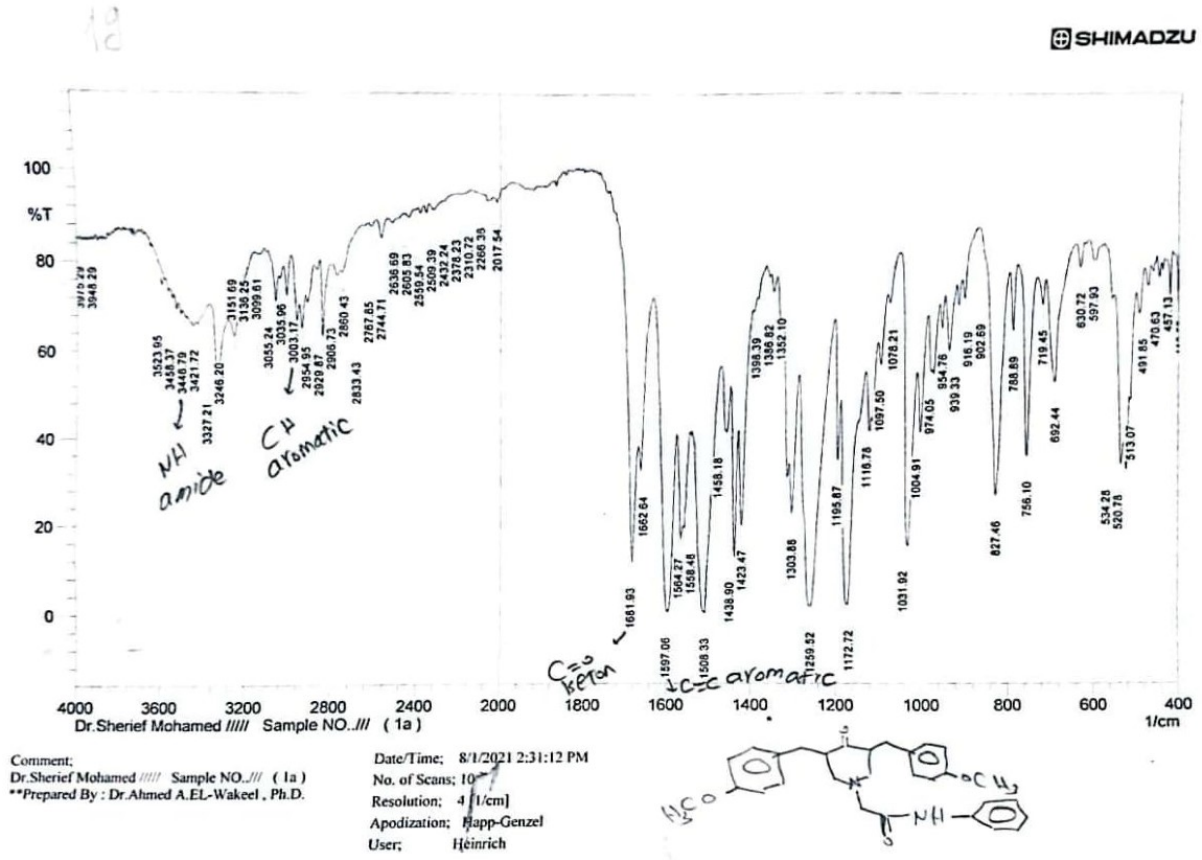

Figure S47. IR spectrum of compound 4g

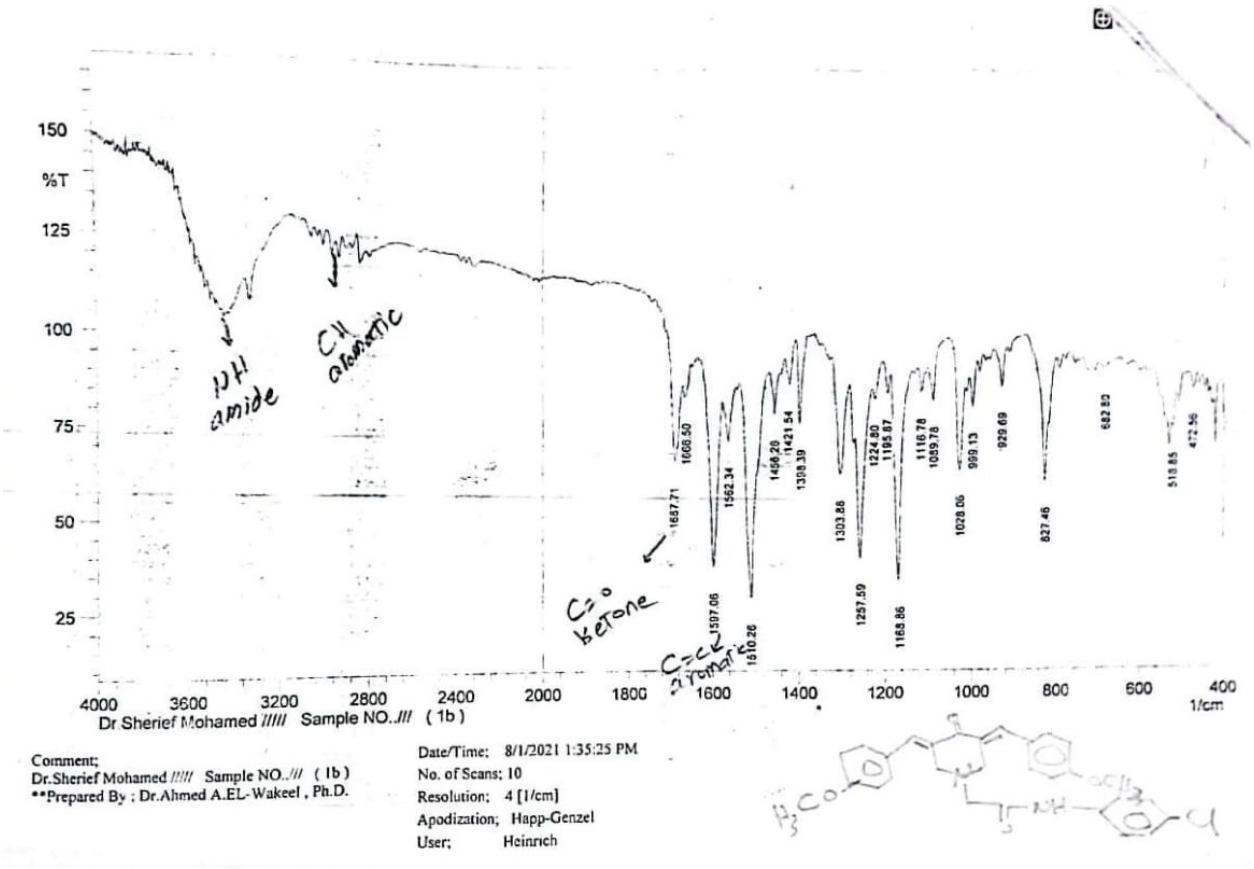

Figure S48. IR spectrum of compound 4h

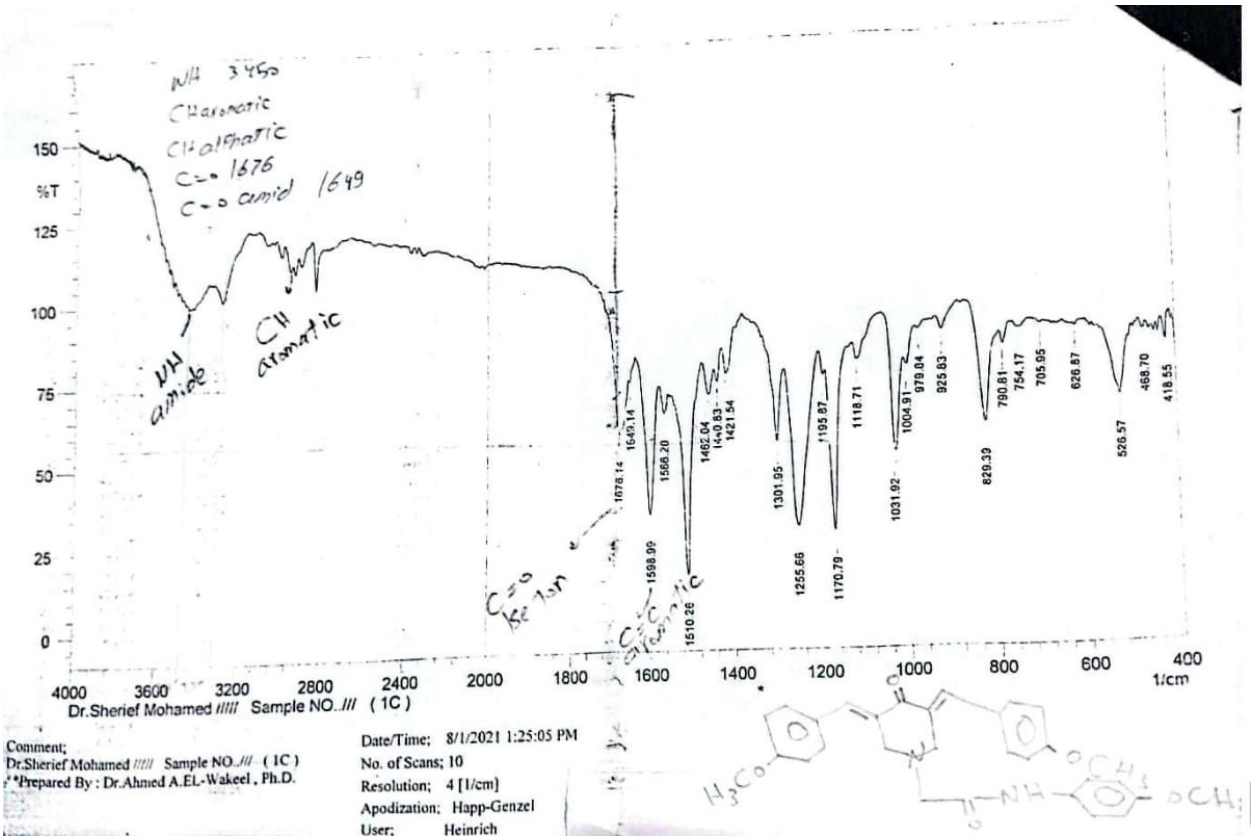

Figure S49. IR spectrum of compound 4i

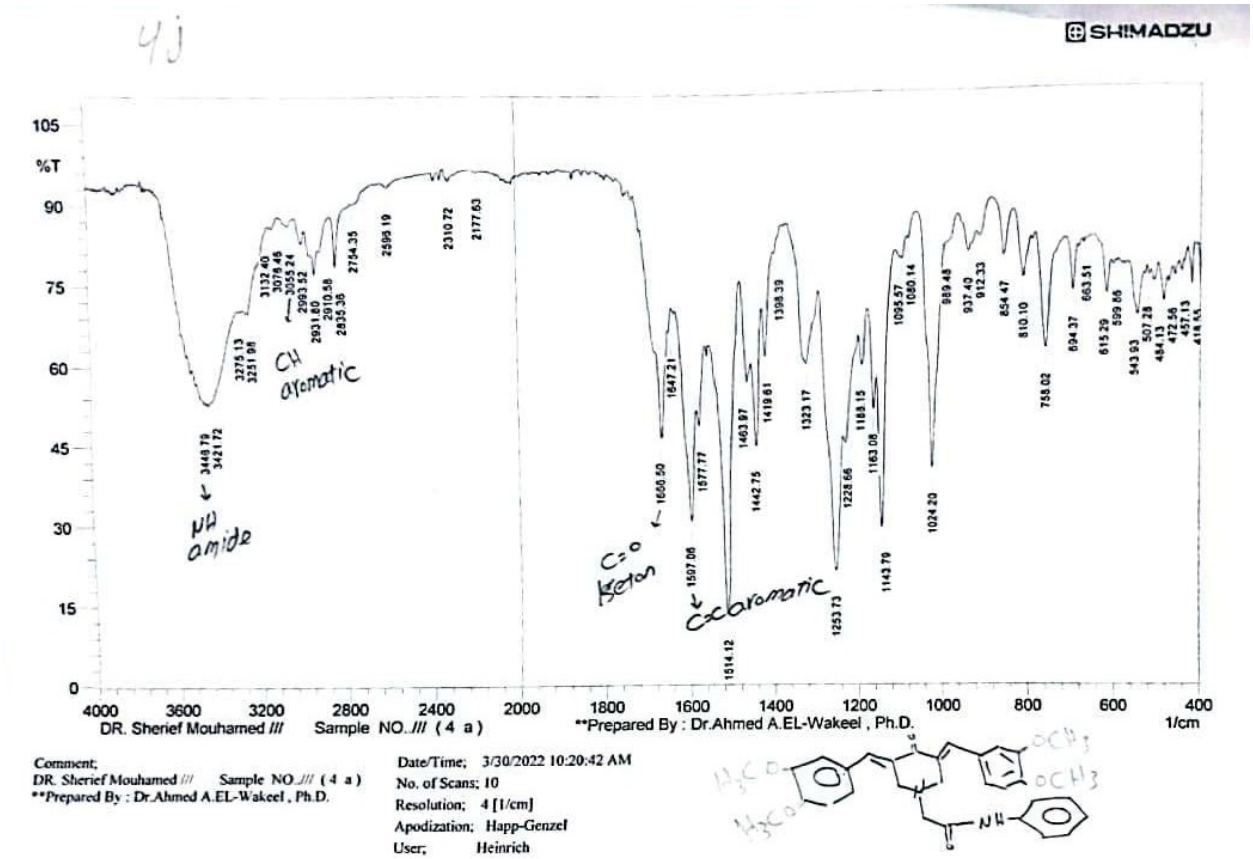

Figure S50. IR spectrum of compound 4j

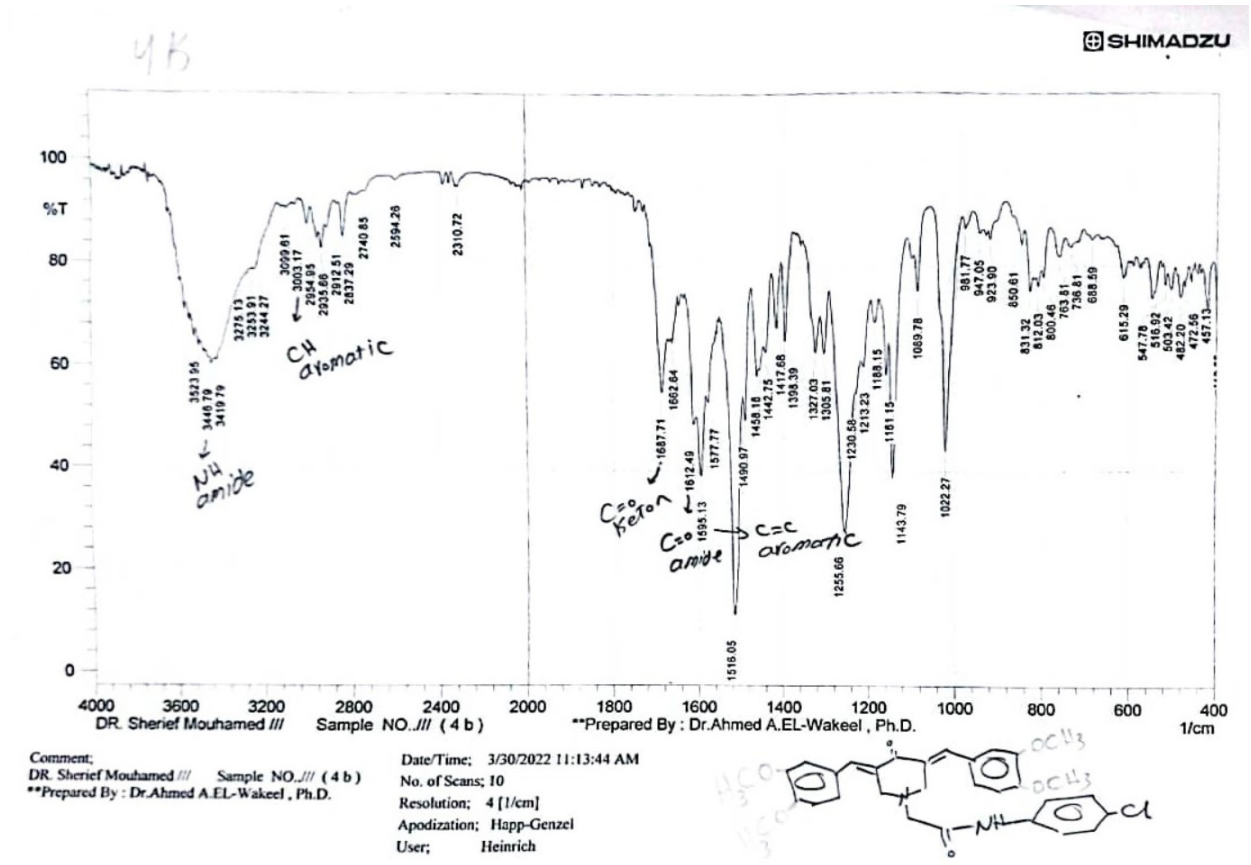

Figure S51. IR spectrum of compound 4k

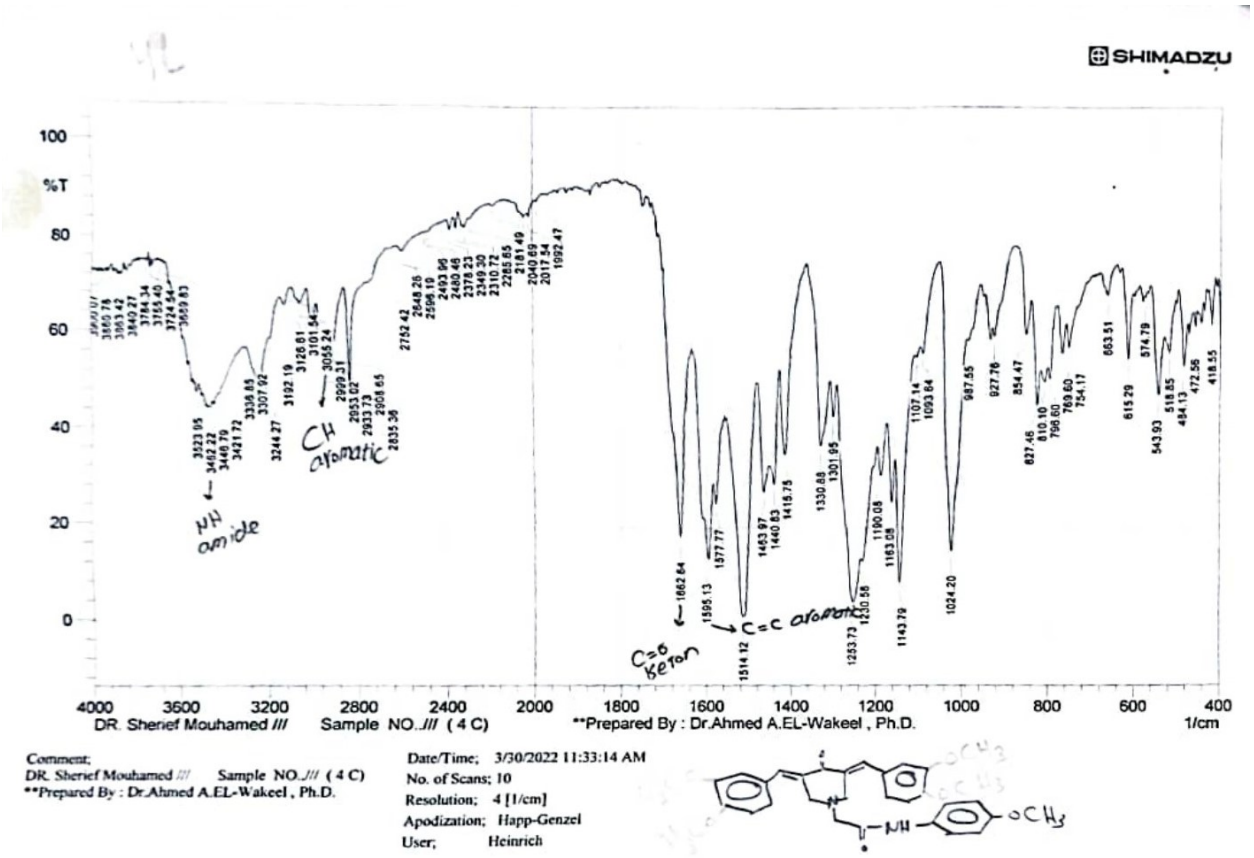

Figure S52. IR spectrum of compound 4L

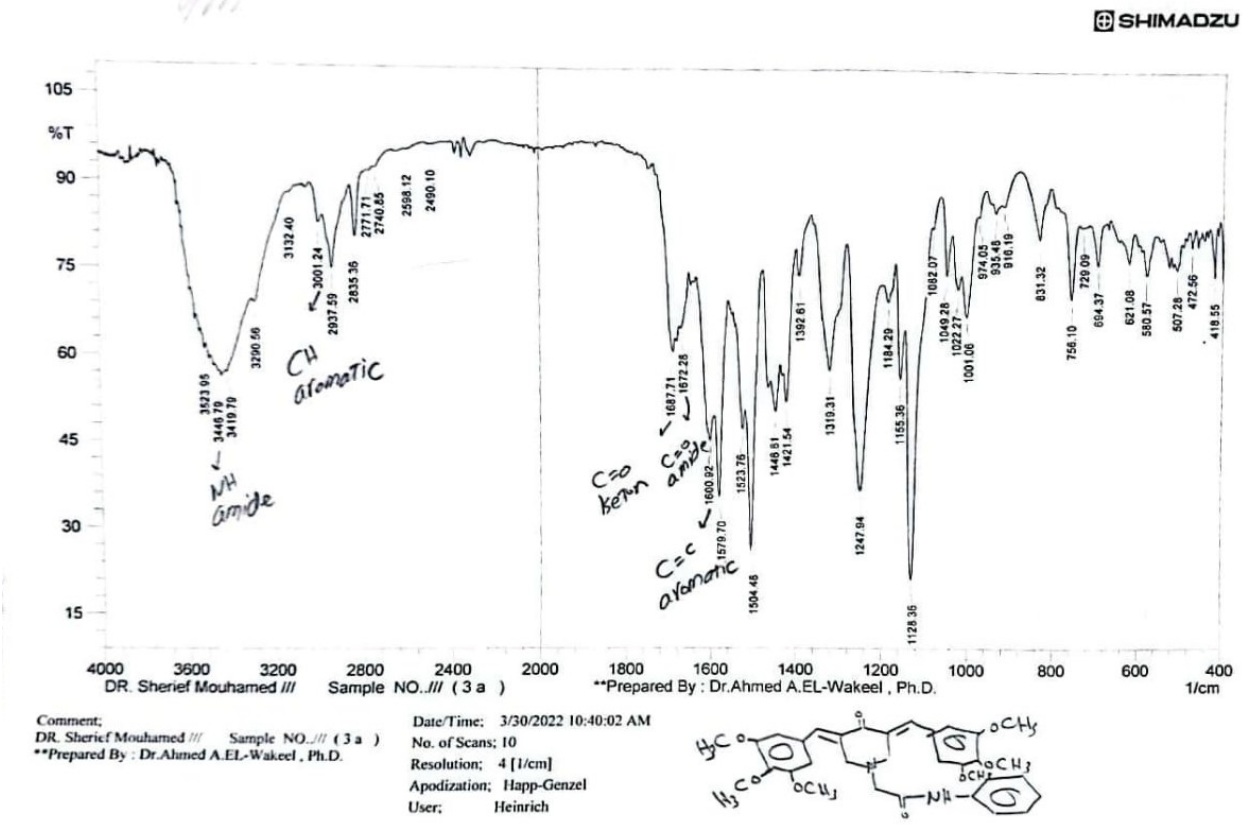

Figure S53. IR spectrum of compound 4m

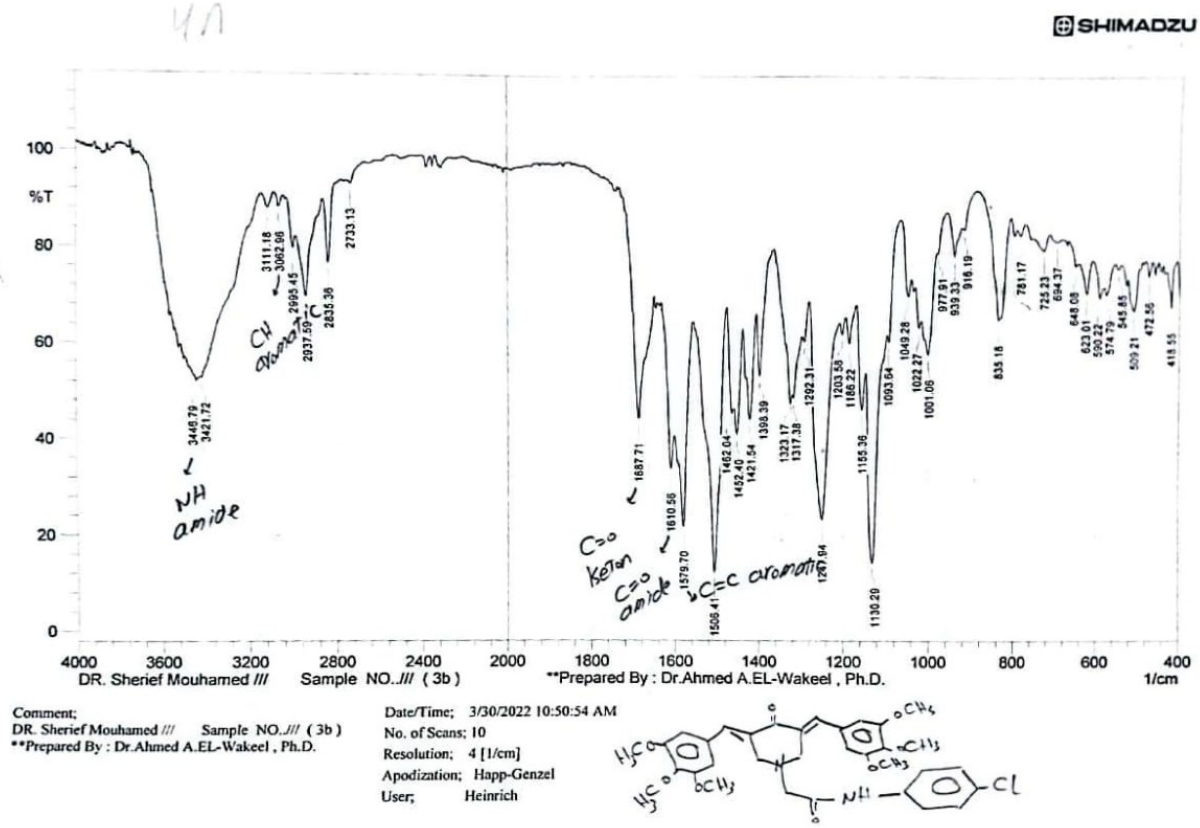

Figure S54. IR spectrum of compound 4n

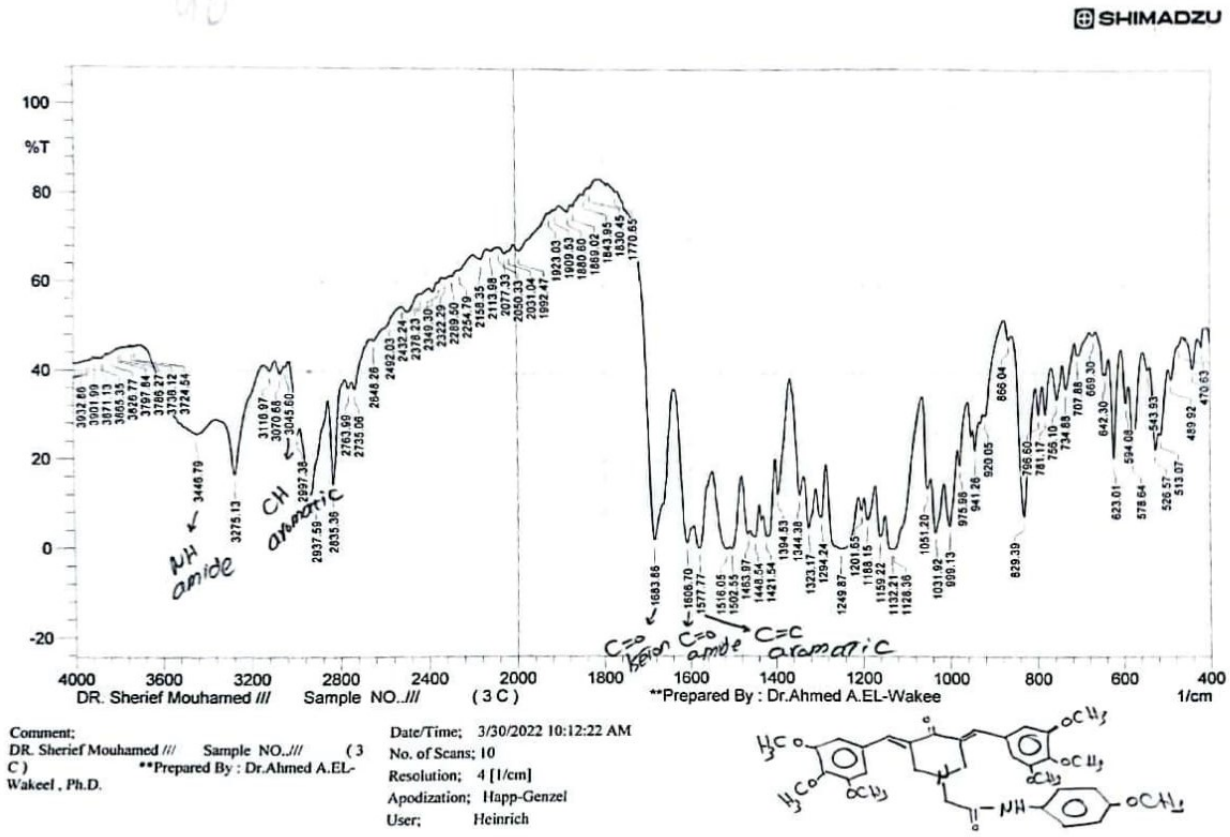

Figure S55. IR spectrum of compound 4o

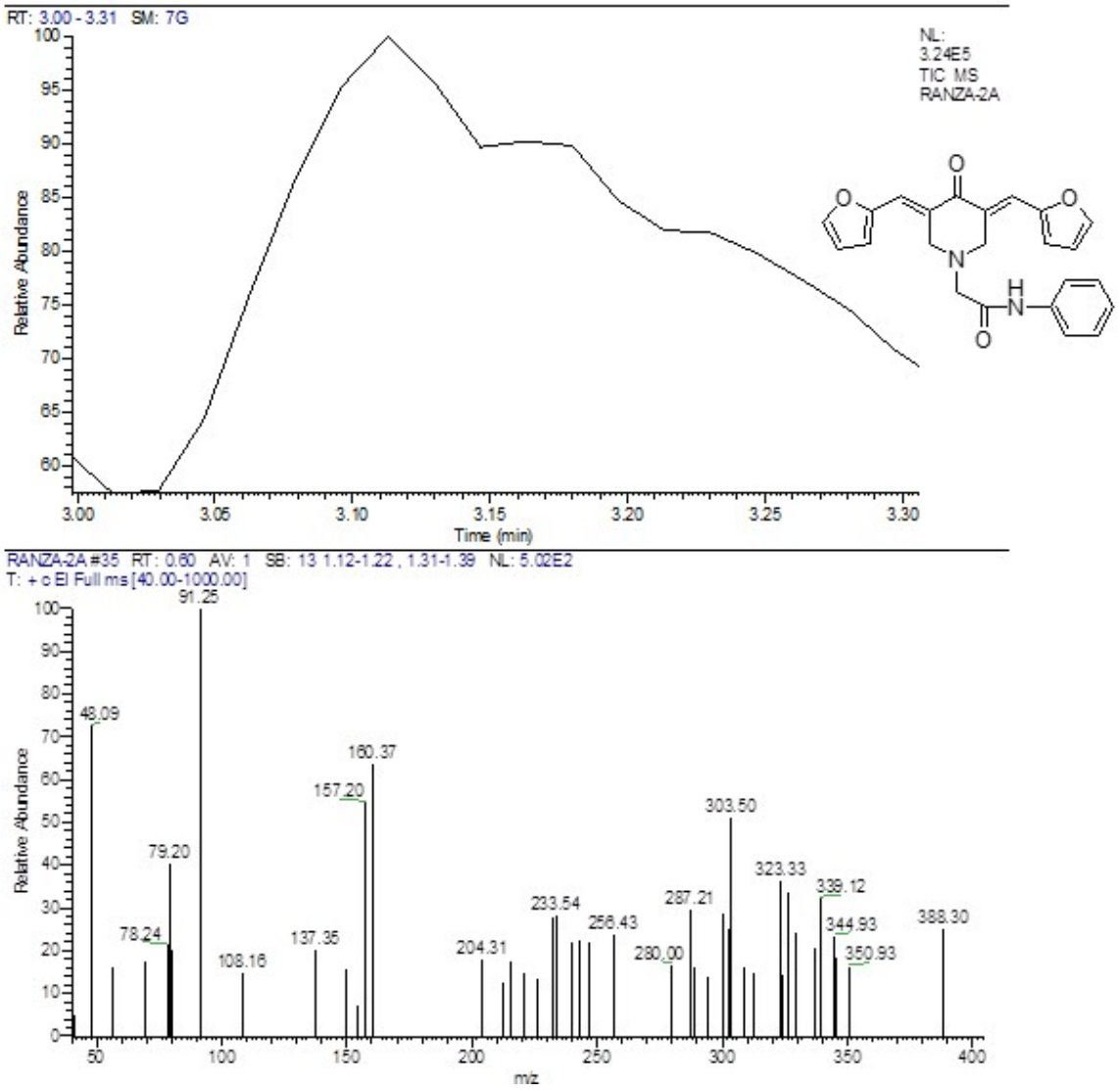

Figure S56. Mass spectrum of compound 2a

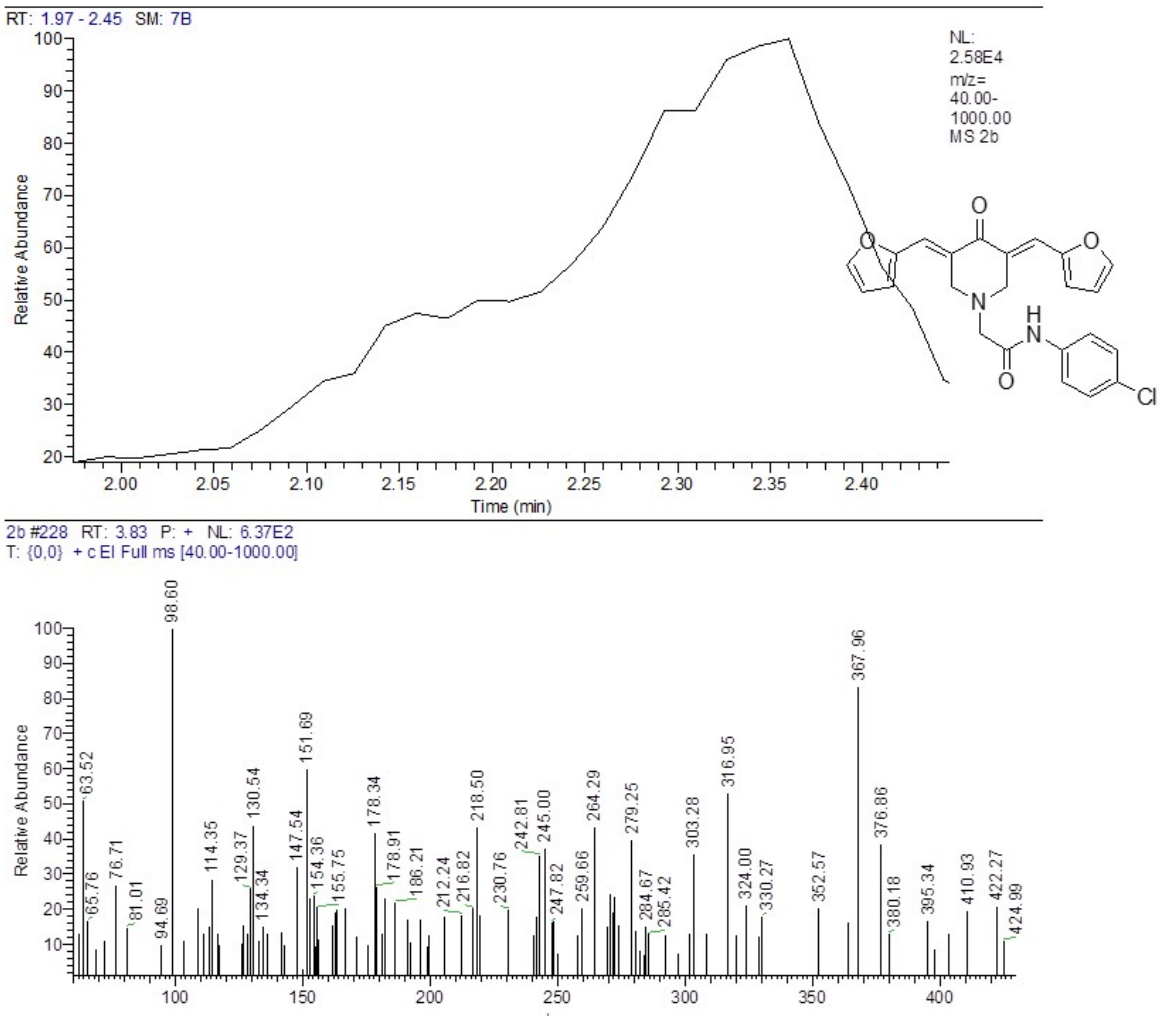

Figure S57. Mass spectrum of compound 2b

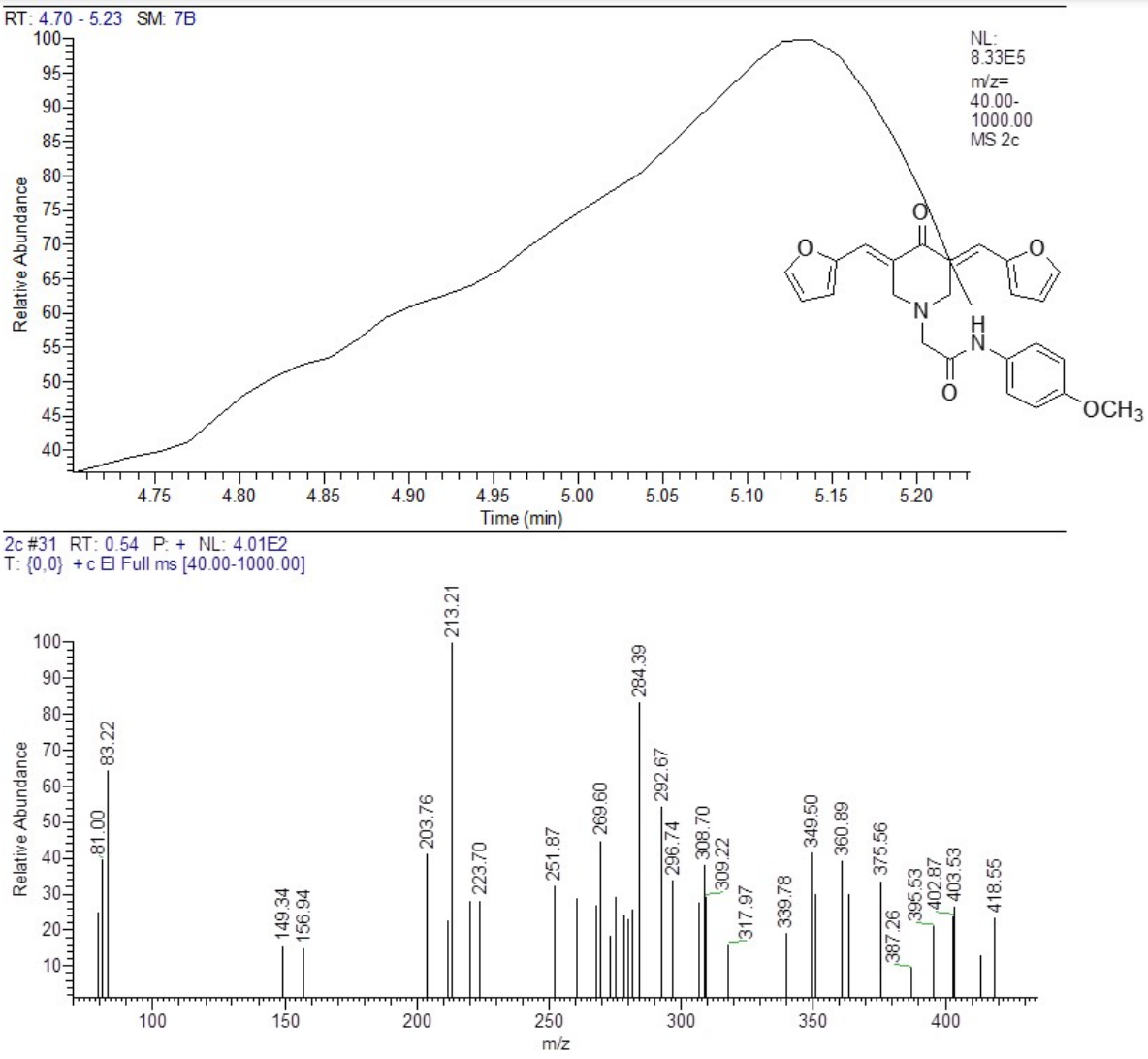

Figure S58. Mass spectrum of compound 2c

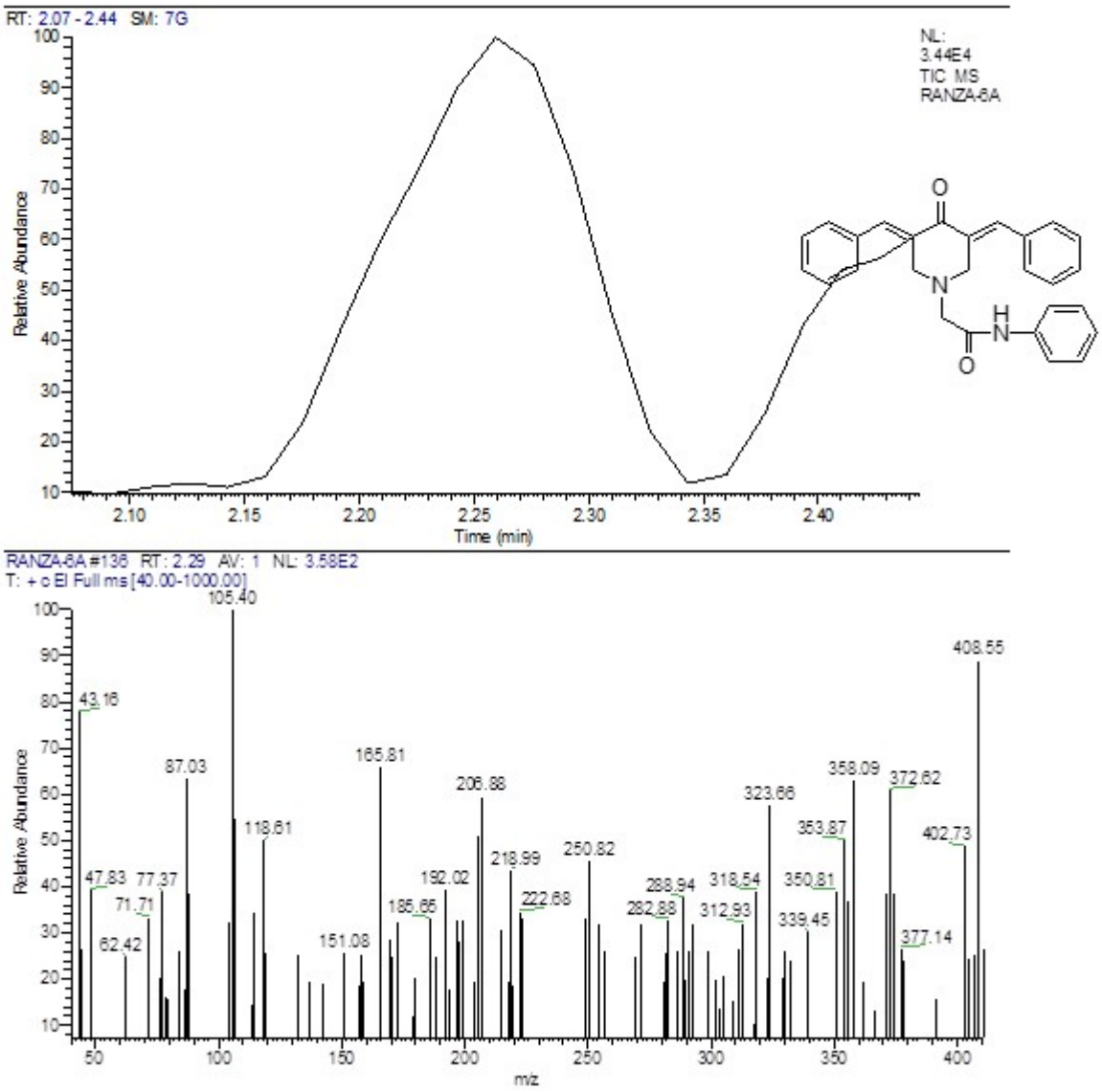

Figure S59. Mass spectrum of compound 4a

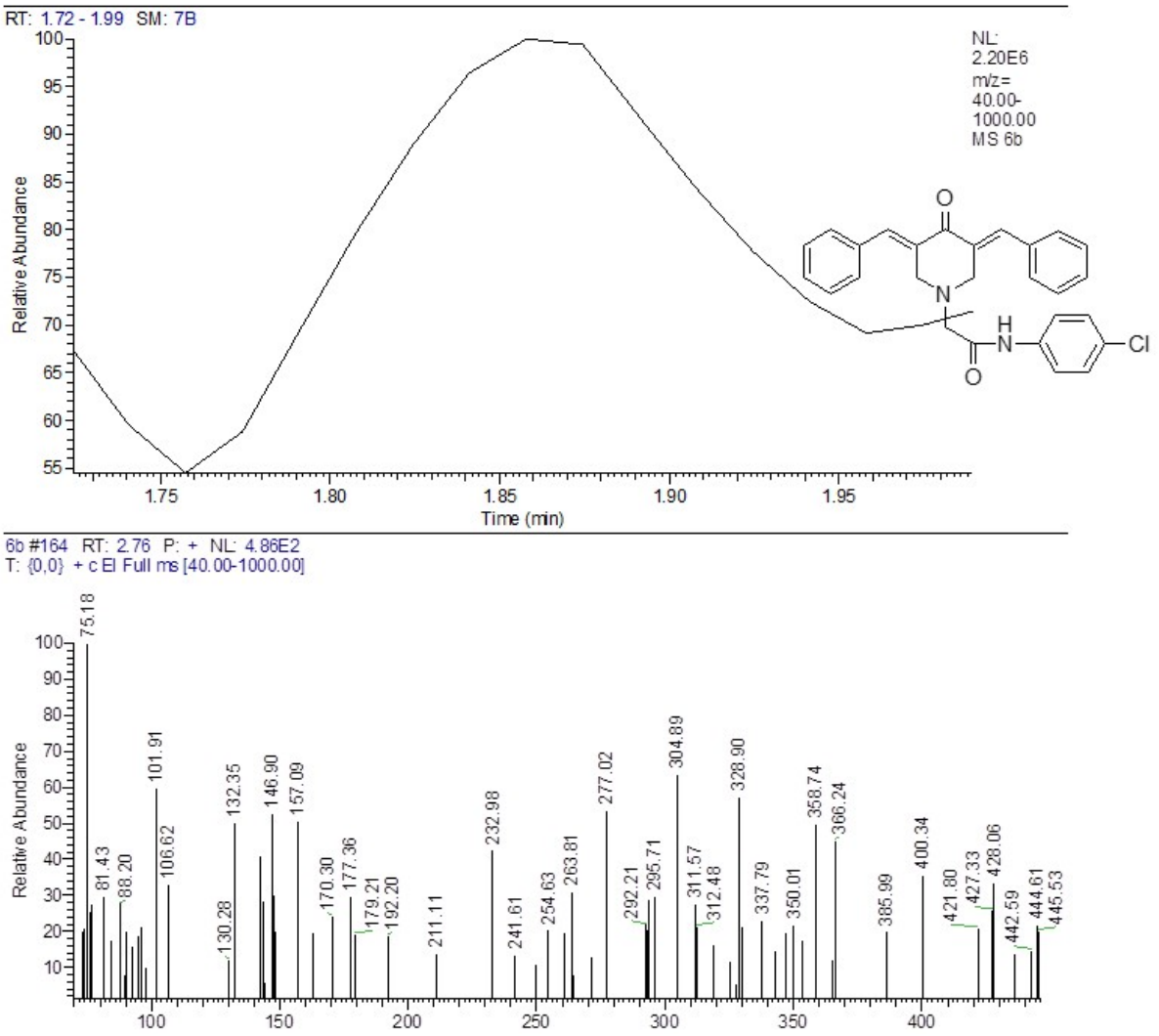

Figure S60. Mass spectrum of compound 4b

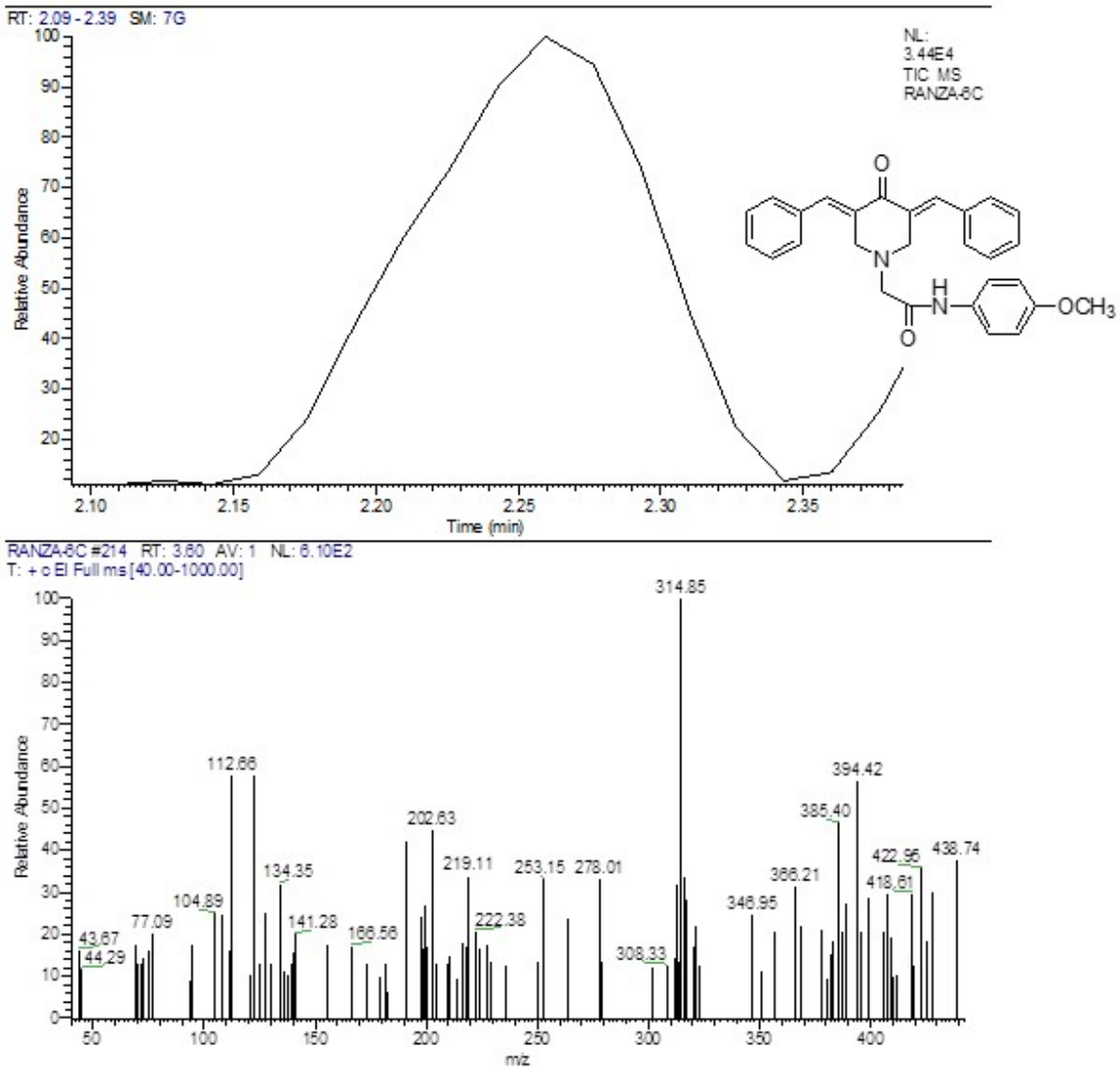

Figure S61. Mass spectrum of compound 4c

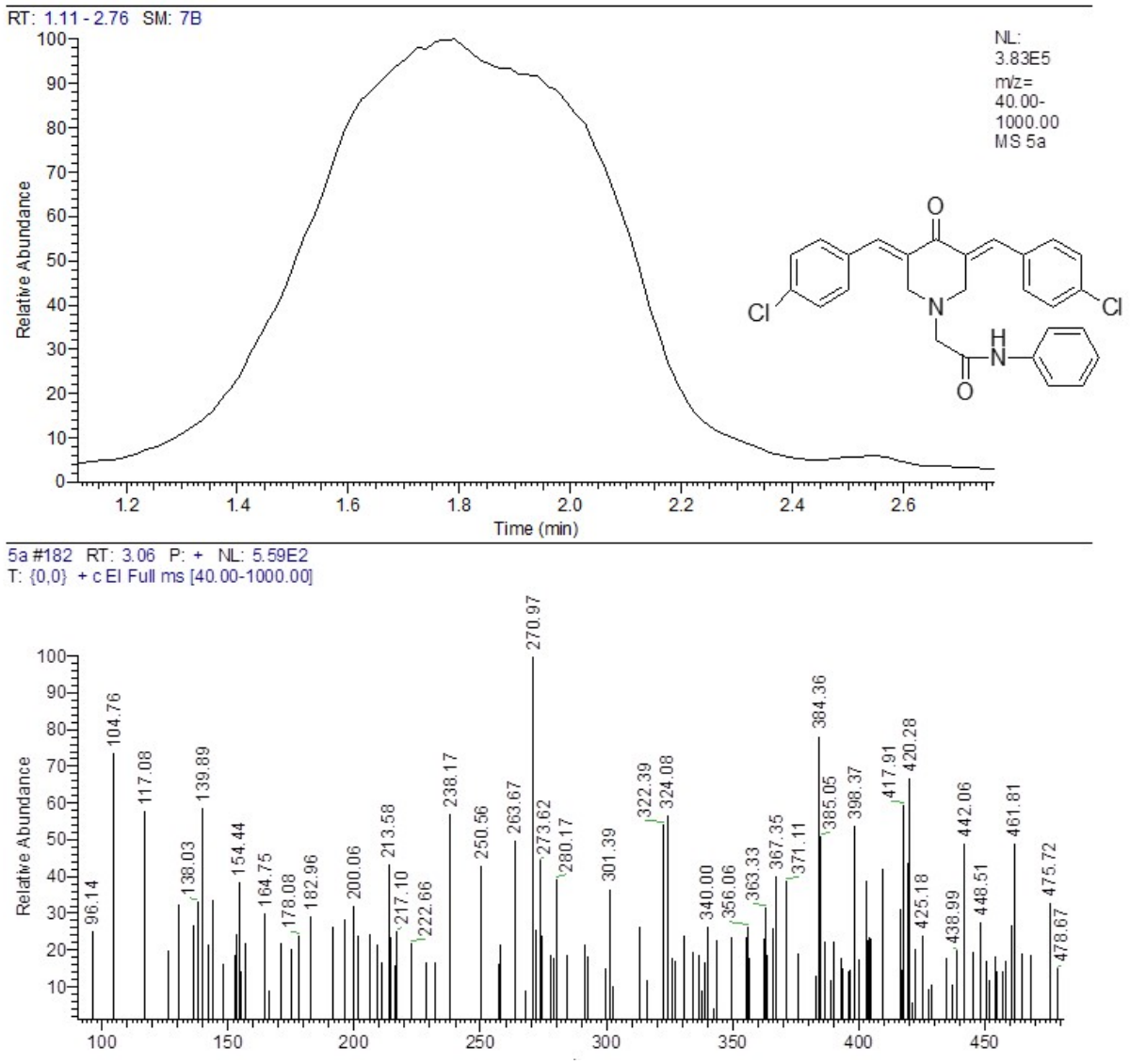

Figure S62. Mass spectrum of compound 4d

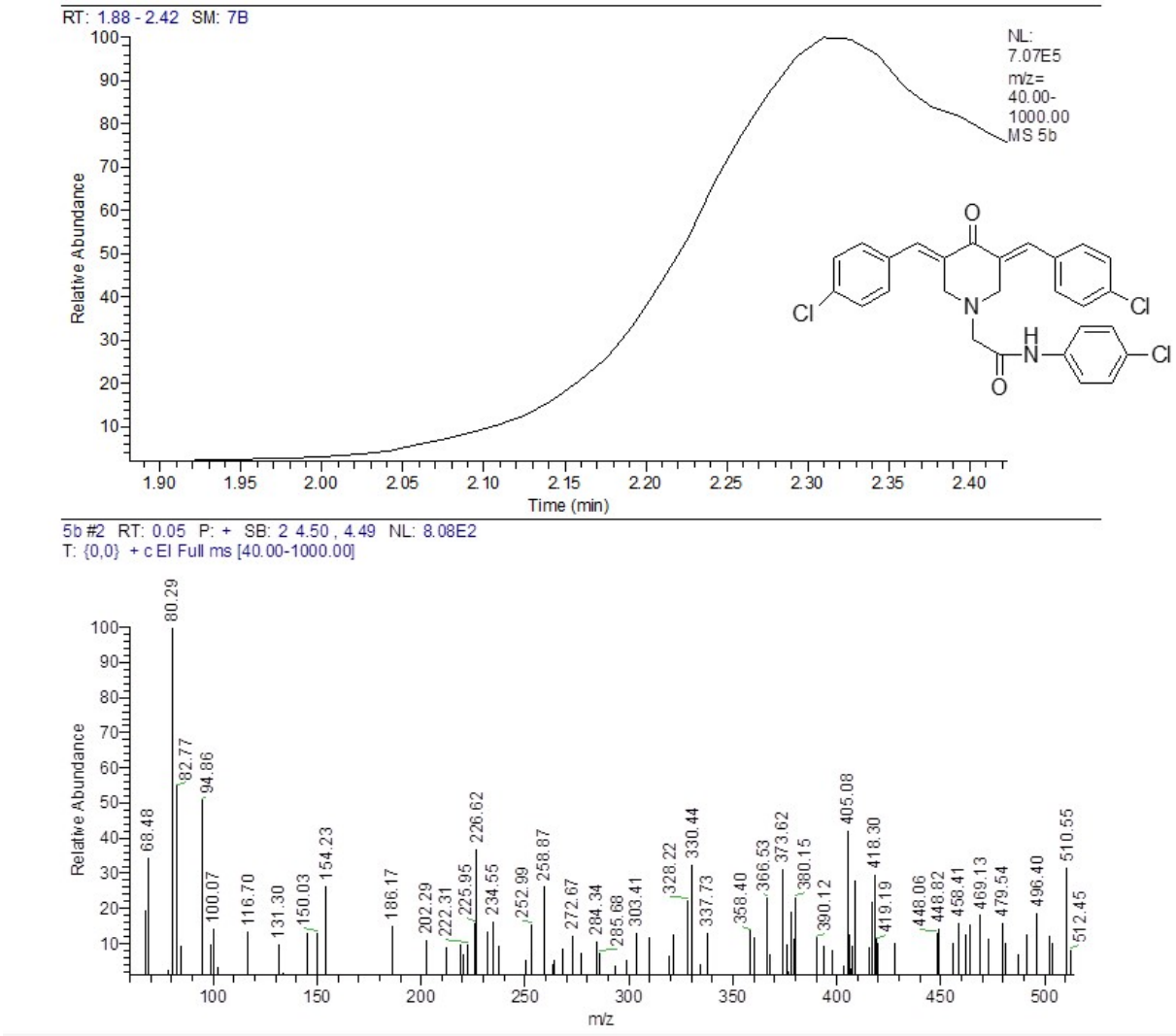

Figure S63. Mass spectrum of compound 4e

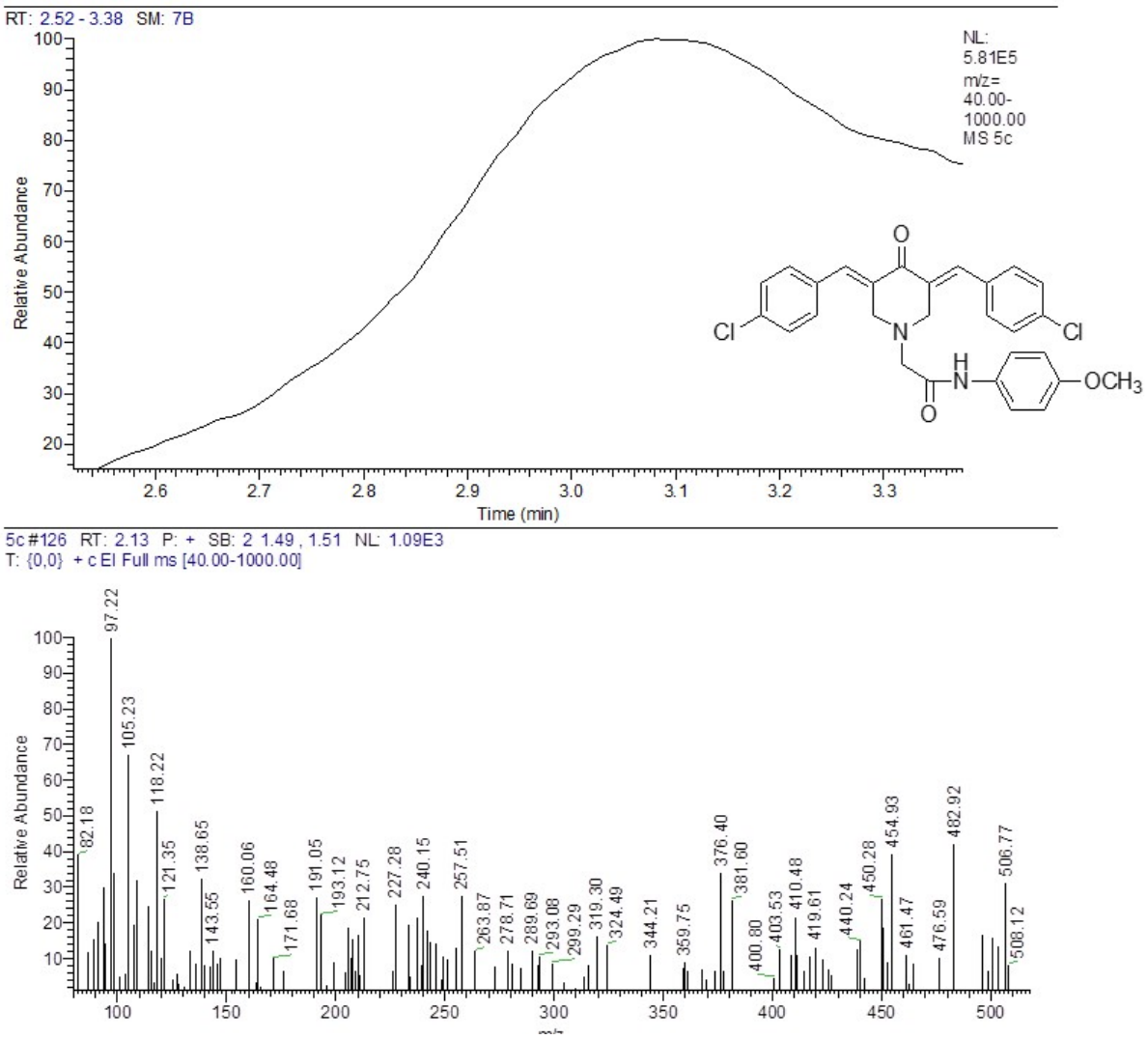

Figure S64. Mass spectrum of compound 4f

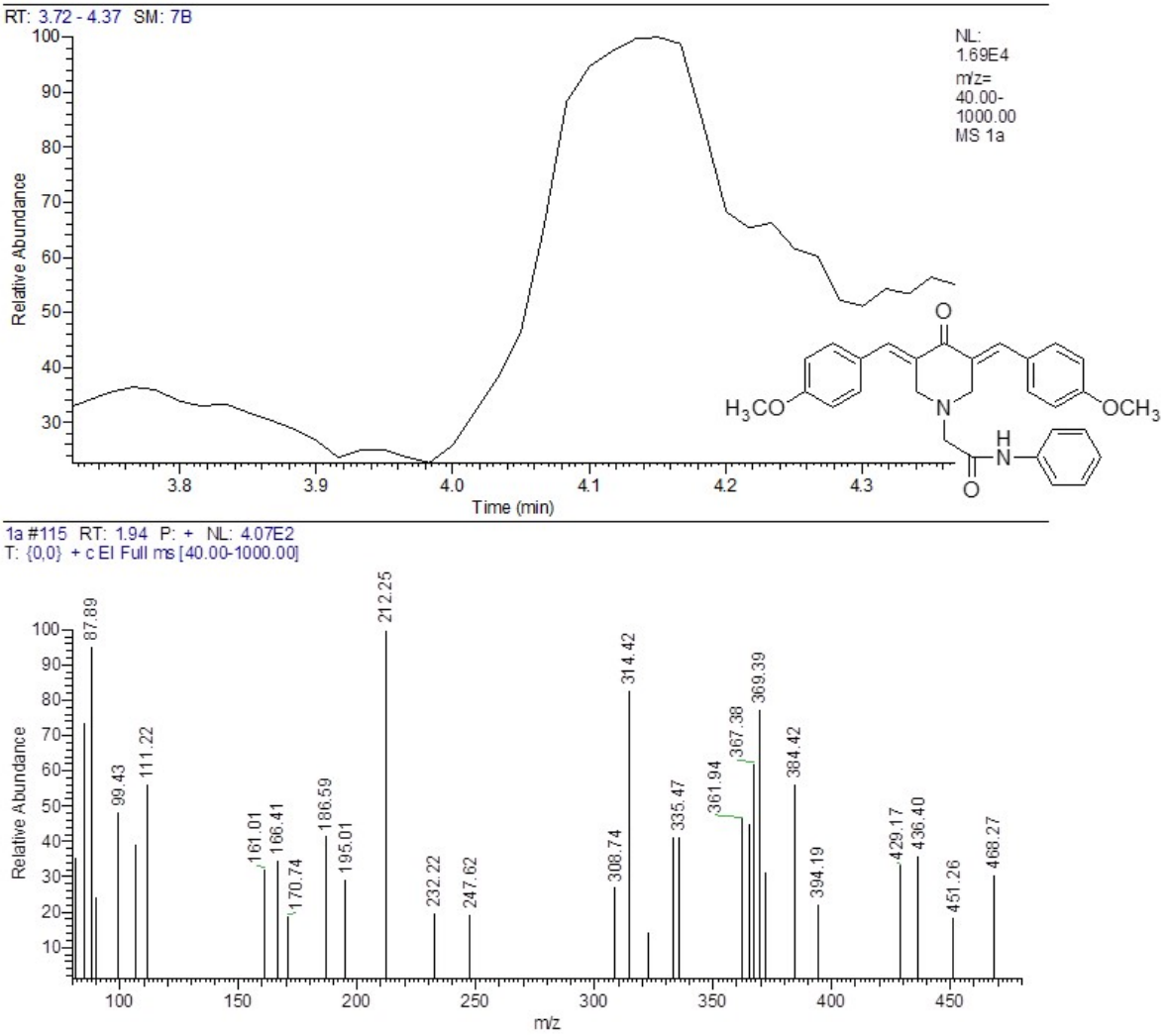

Figure S65. Mass spectrum of compound 4g

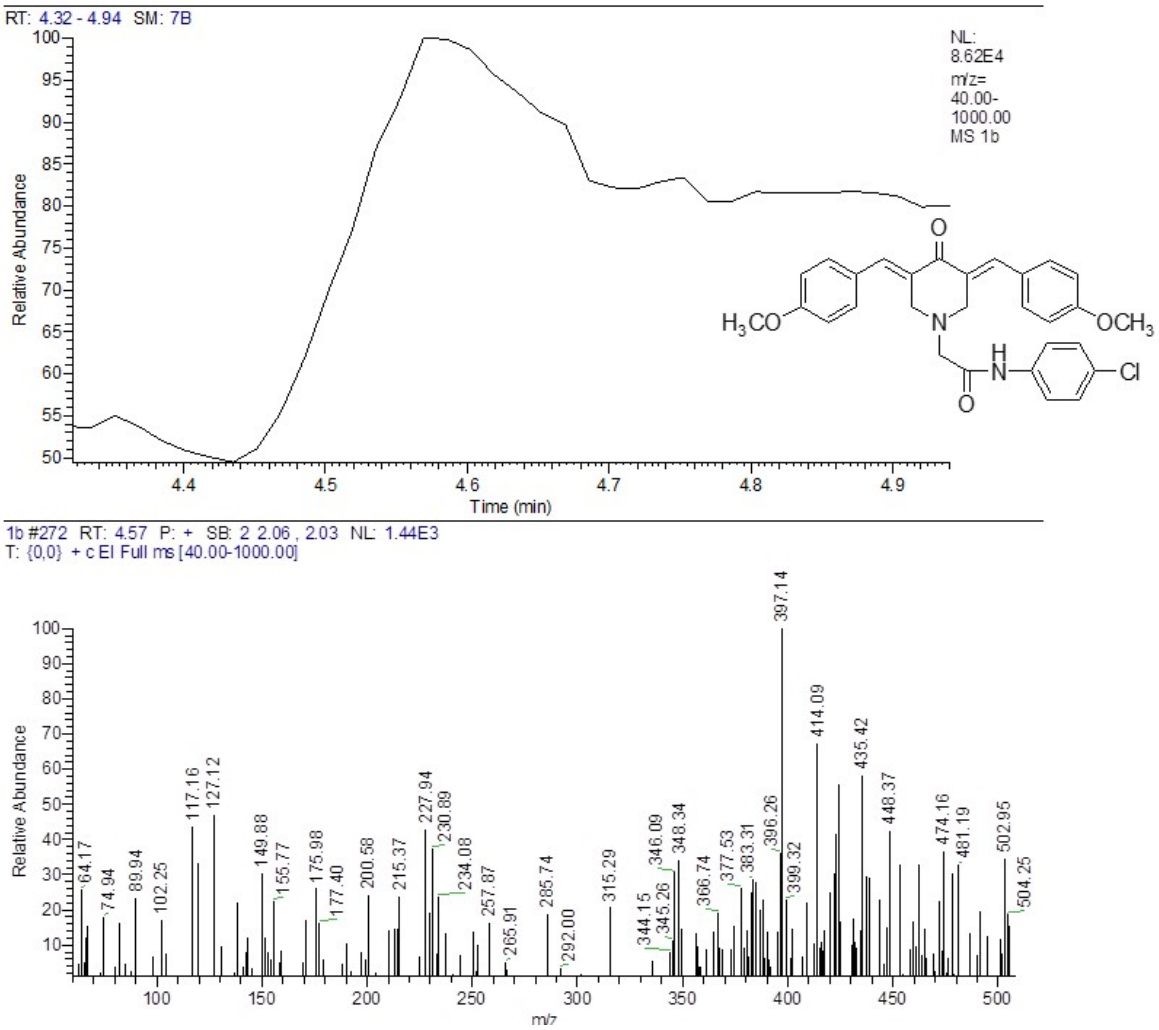

Figure S66. Mass spectrum of compound 4h

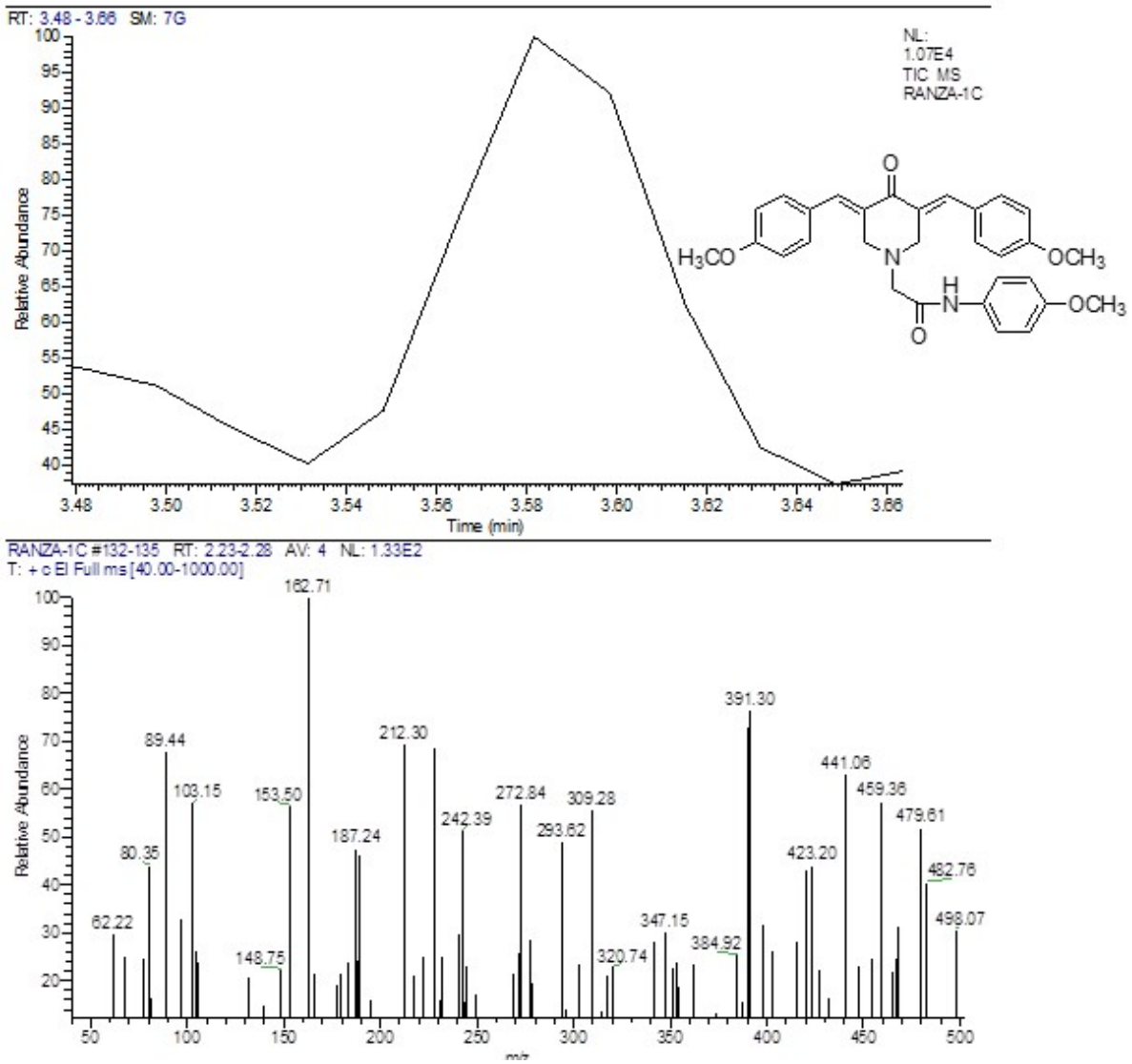

Figure S67. Mass spectrum of compound 4i

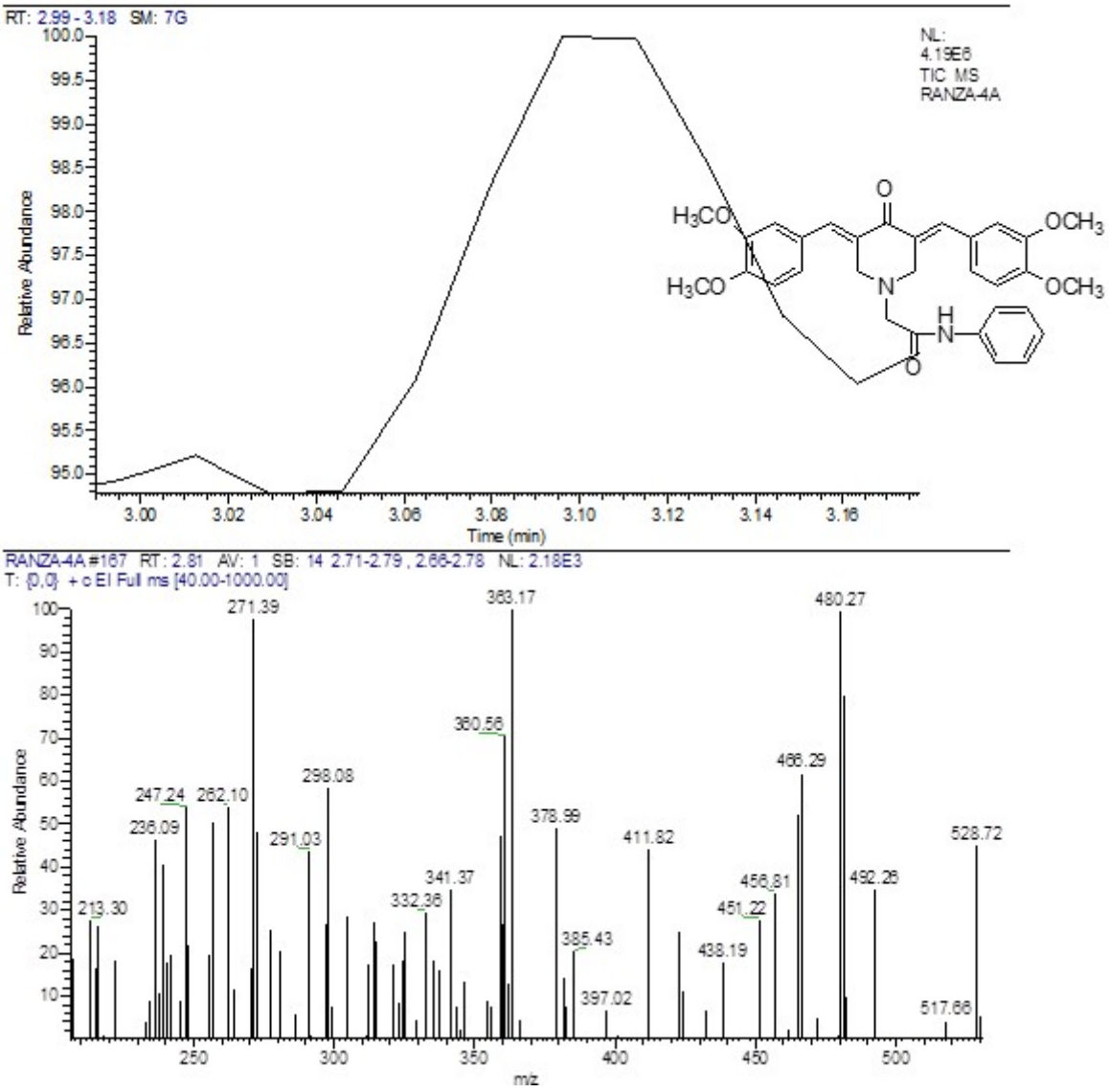

Figure S68. Mass spectrum of compound 4j

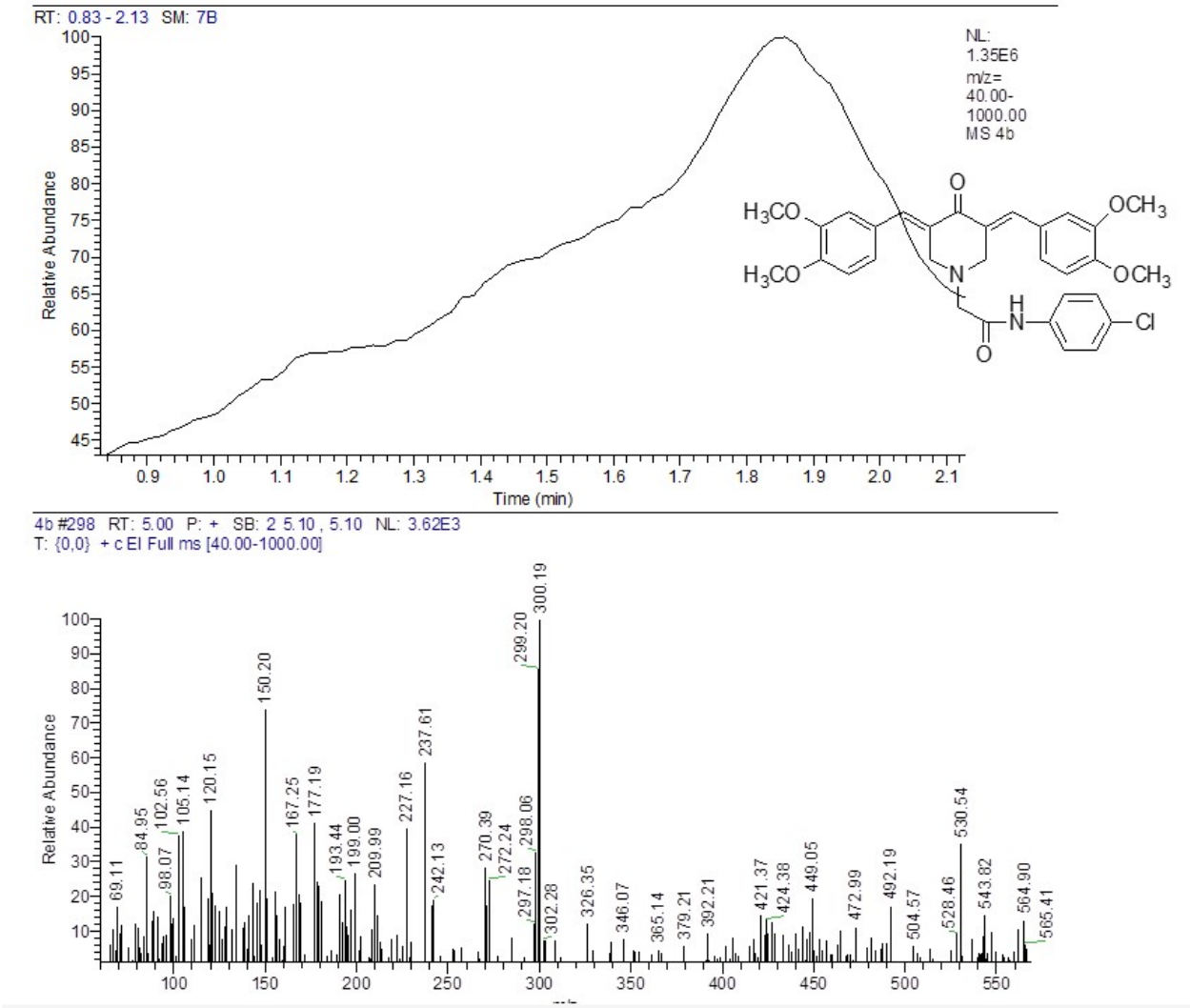

Figure S69. Mass spectrum of compound 4k

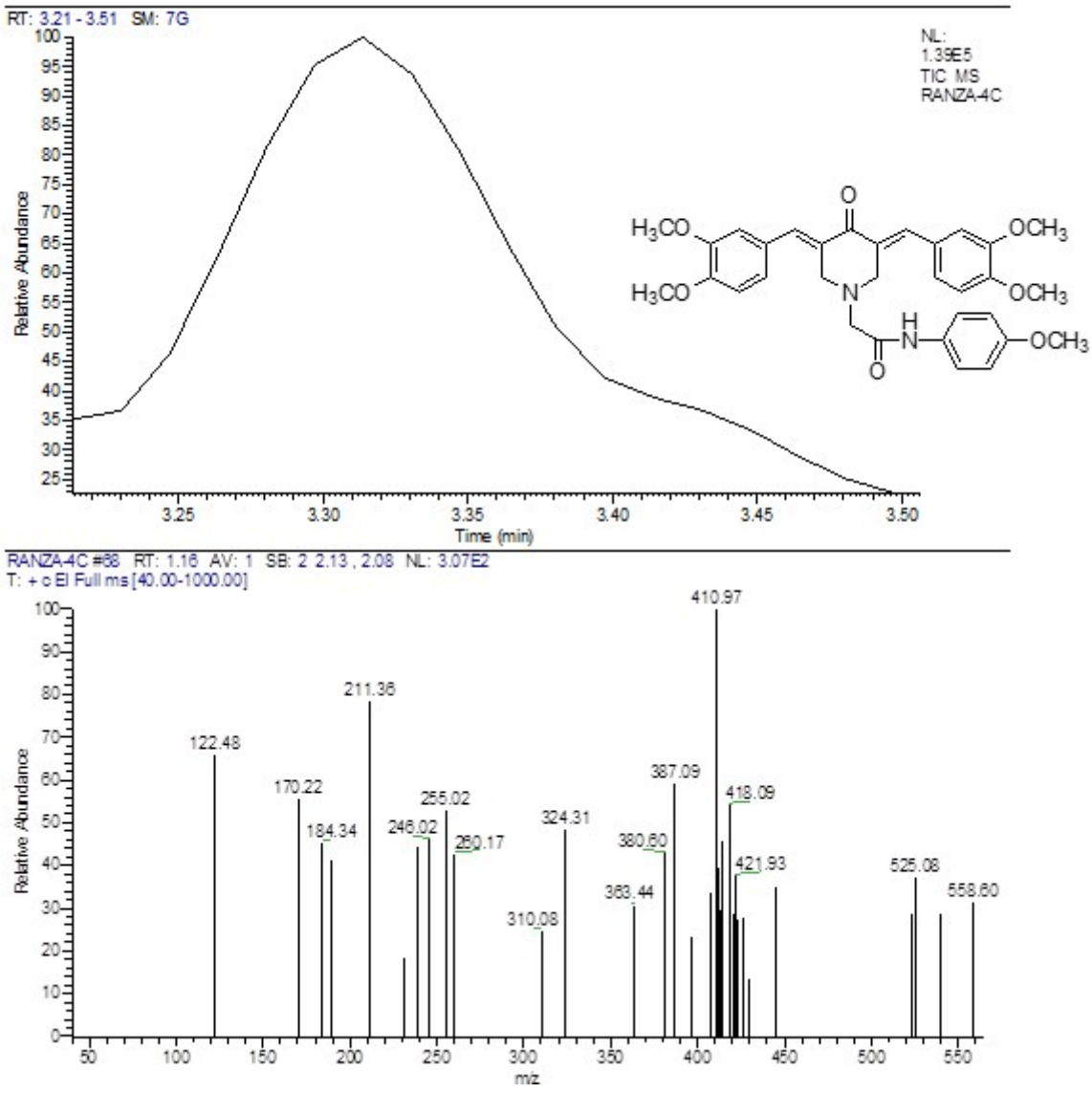

Figure S70. Mass spectrum of compound 4l

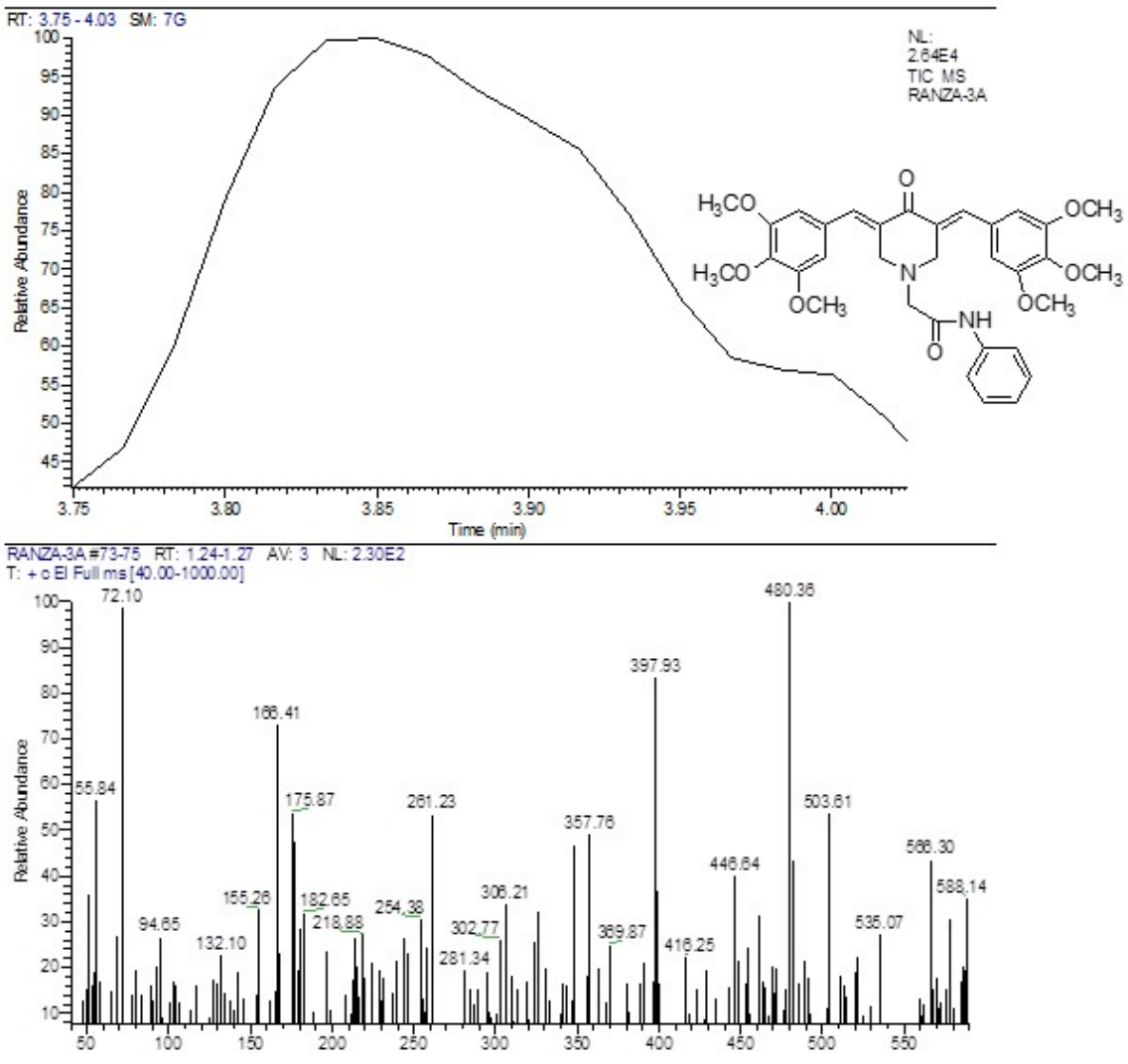

Figure S71. Mass spectrum of compound 4m

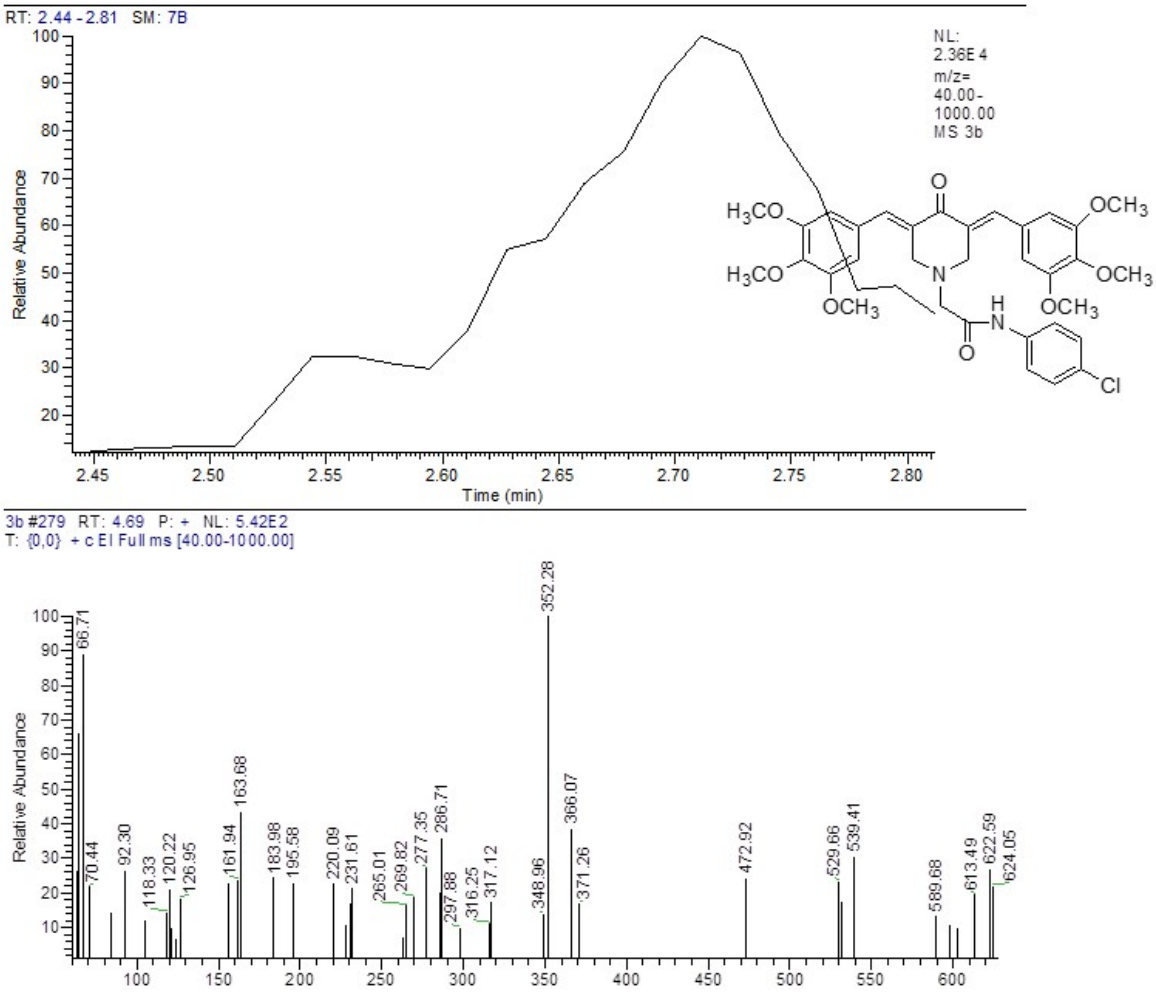

Figure S72. Mass spectrum of compound 4n

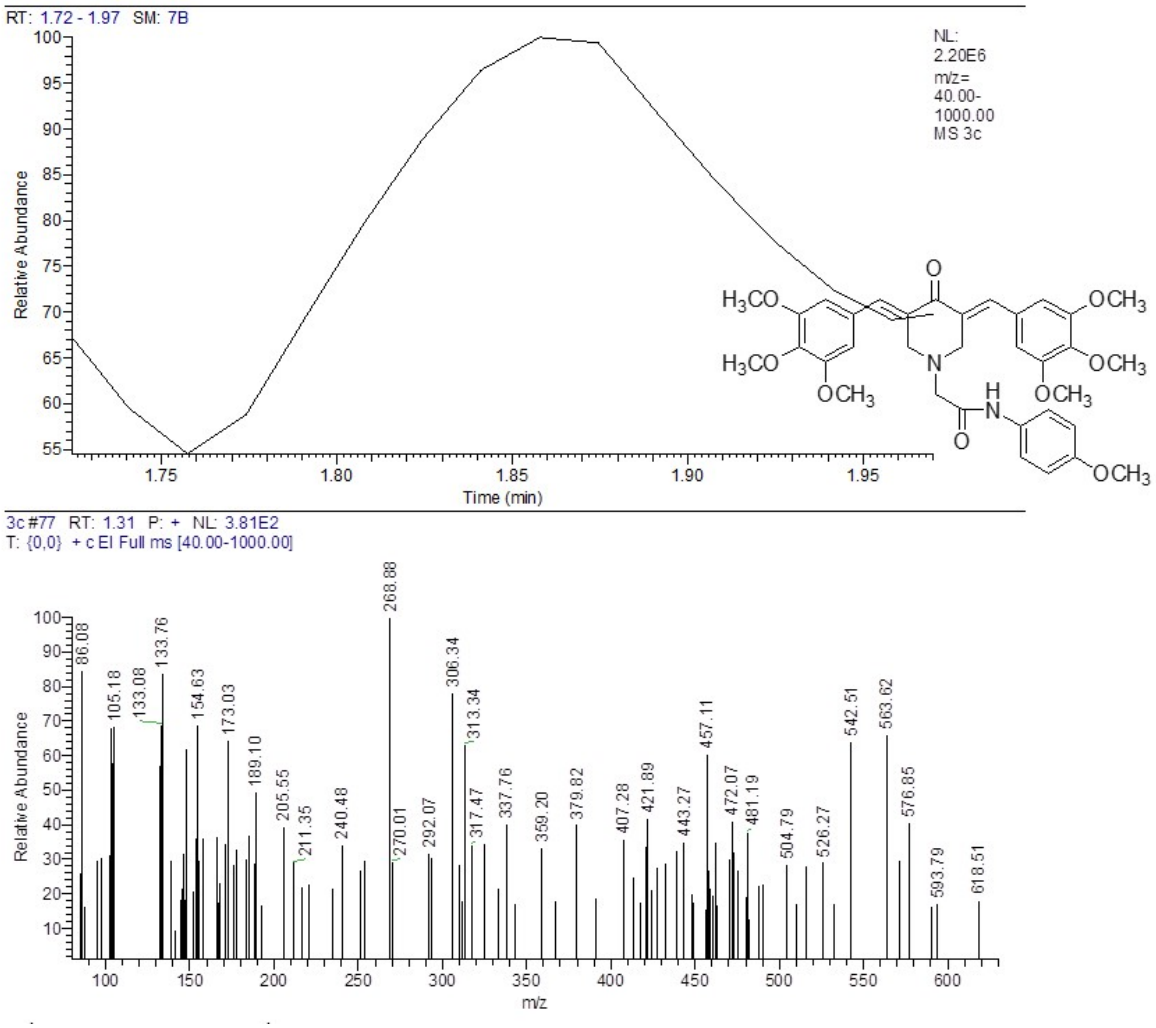

Figure S73. Mass spectrum of compound 4o

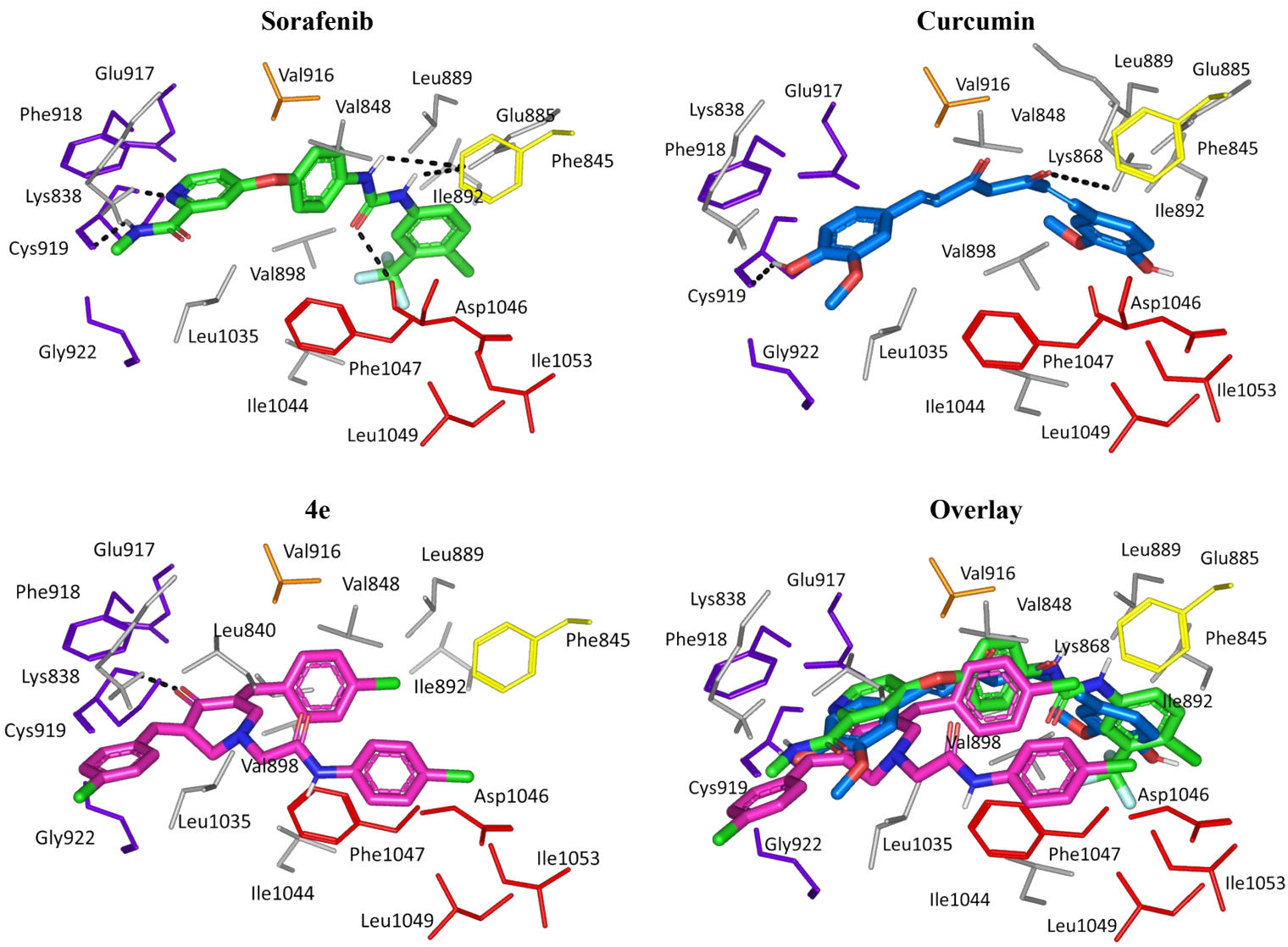

Figure S74. Docked binding modes and interactions for top-docked compound, sorafenib, and curcumin parent compound within VEGFR2 ATP-binding site and kinase site. (**A**) Binding modes and overlay of docked 4e (magenta sticks), co-crystallized ligand (sorafenib; green sticks), and curcumin (blue sticks) at VEGFR2 inactive state (PDB; 2OH4). Residues (lines) within a radius of 5 Å from the bounded ligands are displayed, labelled with sequence number, and coloured in regard to their position at the structural loops; A-loop (red), hinge region (purple), catalytic loop (blue), and glycine-rich loop (yellow). Black dashed lines represent the depicted polar ligand-VEGFR2 interactions.

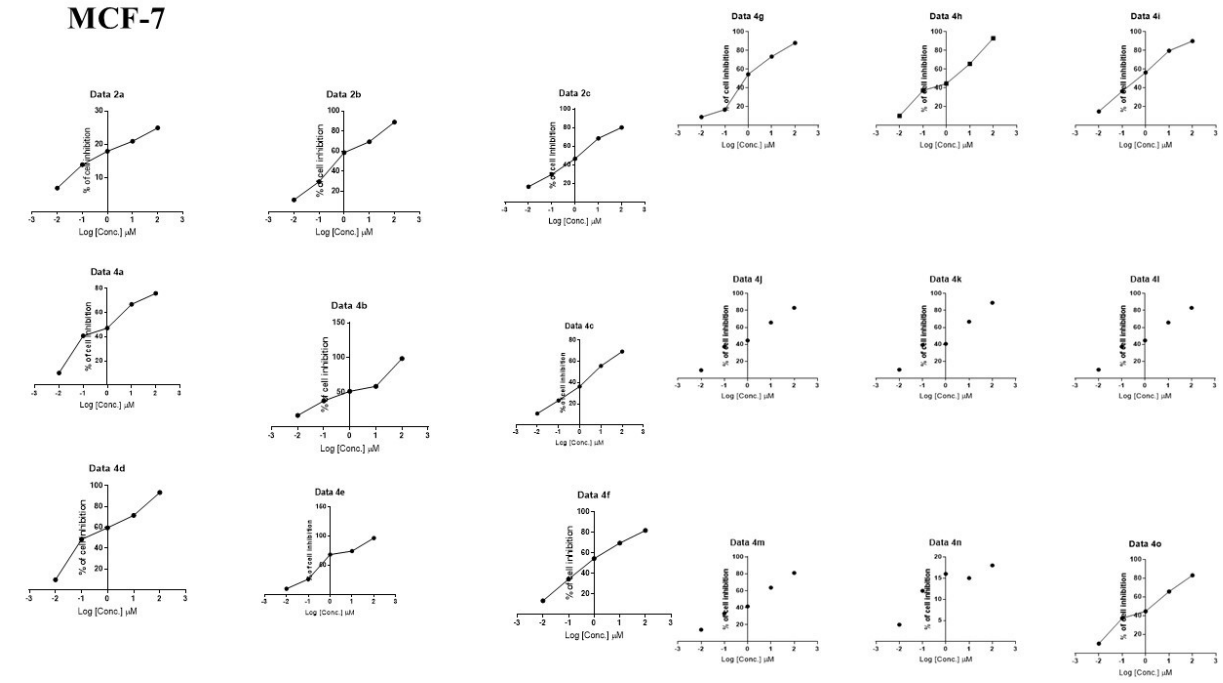

Figure S75. IC_{50} curves for all compounds on MCF-7 cell line.

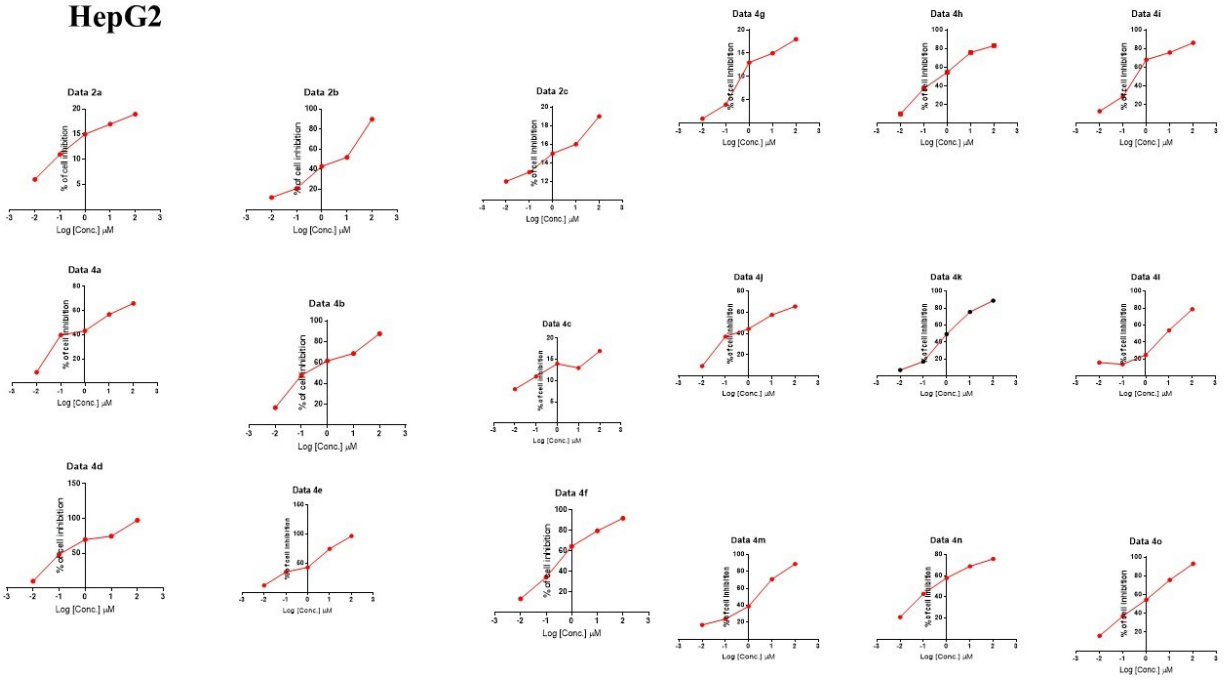

Figure S76. IC_{50} curves for all compounds on HepG2 cell line.

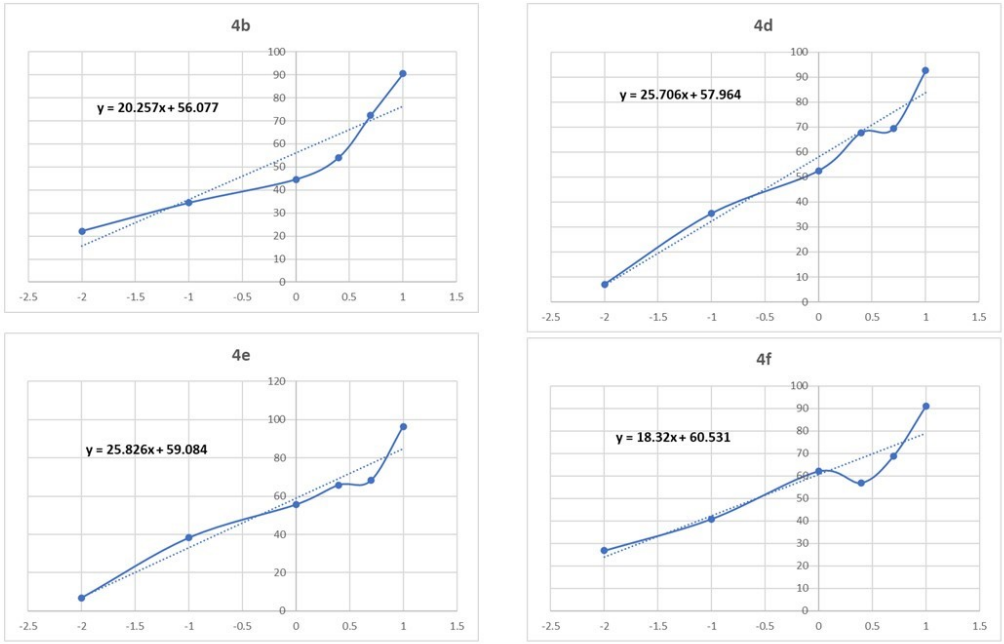

Figure S77. VEGFR2 Enzyme inhibition curves for compounds **4b** and **4d-f**.

VEGFR2

VEGFR2 Enzyme inhbition

ΔT=30 min

Compound [μM]		Cont.	10	5	2.5	1	0.1	0.01	
4b		0.651	0.012	0.19	0.289	0.358	0.446	0.493	
		0.642	0.084	0.17	0.297	0.341	0.416	0.48	
		0.628	0.086	0.17	0.296	0.365	0.398	0.523	IC50= 27.5 nM±1.1
Mean		0.640333	0.060667	0.176667	0.294	0.354667	0.42	0.498667	
SD		0.01159	0.042158	0.011547	0.004359	0.012342	0.024249	0.022053	
% of valibility		100	9.474232	27.5898	45.91359	55.38782	65.59084	77.87611	
% of inhibition		0	90.52577	72.4102	54.08641	44.61218	34.40916	22.12389	

Sorafenib=29.7 nM

ΔT=30 min

Compound [μM]		Cont.	10	5	2.5	1	0.1	0.01	
4d		0.651	0.037	0.199	0.201	0.301	0.399	0.599	
		0.642	0.038	0.189	0.203	0.299	0.413	0.591	
		0.628	0.068	0.201	0.216	0.312	0.429	0.596	IC50= 19.8 nM±0.7
Mean		0.640333	0.047667	0.196333	0.206667	0.304	0.413667	0.595333	
SD		0.01159	0.017616	0.006429	0.008145	0.007	0.015011	0.004041	
% of valibility		100	7.44404	30.66111	32.27486	47.47527	64.60177	92.97241	
% of inhibition		0	92.55596	69.33889	67.72514	52.52473	35.39823	7.02759	

ΔT=30 min

Compound [μM]		Cont.	10	5	2.5	1	0.1	0.01	
4e		0.651	0.015	0.202	0.215	0.248	0.401	0.559	
		0.642	0.024	0.21	0.217	0.304	0.399	0.6	
		0.628	0.029	0.199	0.225	0.301	0.386	0.63	IC50= 11.6 nM±0.63
Mean		0.640333	0.022667	0.203667	0.219	0.284333	0.395333	0.596333	
SD		0.01159	0.007095	0.005686	0.005292	0.031501	0.008145	0.035642	
% of valibility		100	3.539823	31.80635	34.20094	44.40396	61.73868	93.12858	
% of inhibition		0	96.46018	68.19365	65.79906	55.59604	38.26132	6.871421	

ΔT=30 min

Compound [μM]		Cont.	10	5	2.5	1	0.1	0.01	
4f		0.651	0.041	0.201	0.281	0.259	0.382	0.486	
		0.642	0.019	0.199	0.279	0.261	0.379	0.496	
		0.628	0.114	0.198	0.267	0.208	0.374	0.423	IC50= 21.9 nM±1.1
Mean		0.640333	0.058	0.199333	0.275667	0.242667	0.378333	0.468333	
SD		0.01159	0.049729	0.001528	0.007572	0.030039	0.004041	0.039577	
% of valibility		100	9.057782	31.12962	43.05049	37.89693	59.08381	73.13899	
% of inhibition		0	90.94222	68.87038	56.94951	62.10307	40.91619	26.86101	

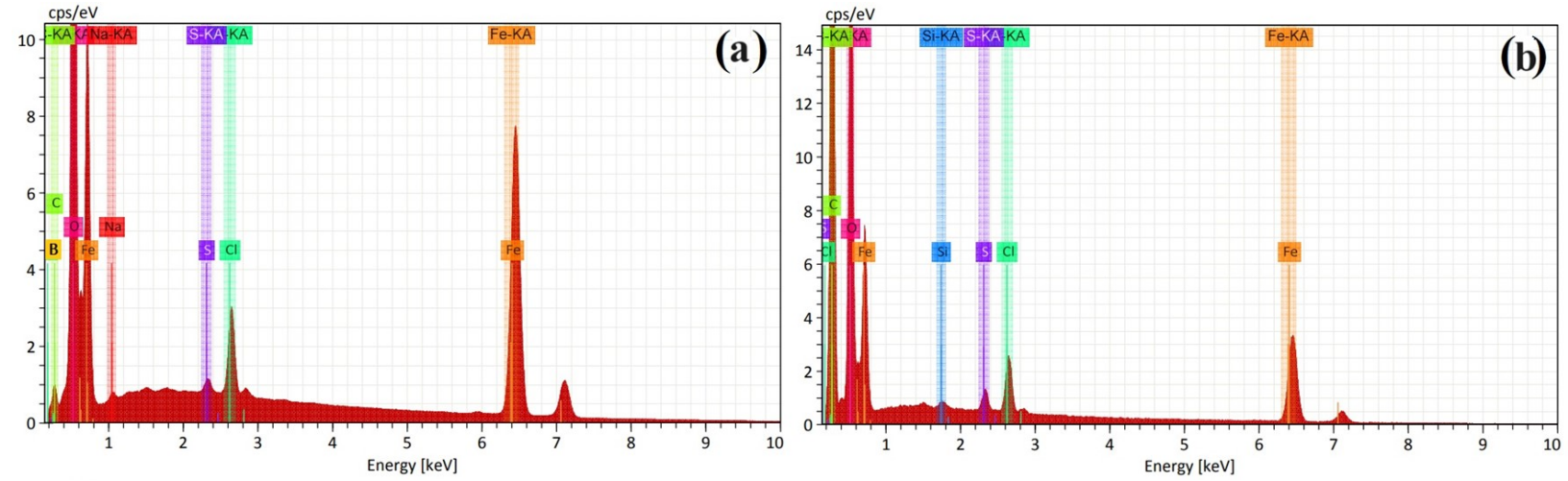

Figure S78. Elemental analysis of the synthesized iron oxide nanocomposite; where (a) EDX of Fe_2O_3 NPs-B, and (b) EDX of Fe_2O3 NPs-HA.